5-30-1991

Design and analysis of a folded meander dipole antenna using the MININEC program

Pedro A. Barros
Florida International University

DESIGN AND ANALYSIS OF
A FOLDED MEANDER DIPOLE ANTENNA
USING THE MININEC PROGRAM

BY

PEDRO A. BARROS

ABSTRACT OF THE THESIS

DESIGN AND ANALYSIS OF A FOLDED MEANDER DIPOLE
ANTENNA, USING THE MININEC PROGRAM.

by

Pedro A. Barros

Florida International University, 1991

Miami, Florida

Professor Tadeusz Babij, Major Professor

The Mini-Numerical Electromagnetic Code (MININEC) program, a
PC-Compatible version of the powerful NEC program, is used to
design a new type of reduced-size antenna. The validity of the
program to model simple well-known antennas, such as dipoles
and monopoles, is first shown. More complex geometries such as
folded dipoles, and meander dipole antennas are also analysed
using the program. The final design geometry of a meander folded
dipole is characterized with MININEC, yielding results that serve
as the basis for the practical construction of the antenna.
Finally, the laboratory work with a prototype antenna is described,
and practical results are presented.

FLORIDA INTERNATIONAL UNIVERSITY
Miami, Florida

DESIGN OF AND ANALYSIS OF A FOLDED MEANDER DIPOLE
ANTENNA USING THE MININEC PROGRAM

A Thesis submitted in partial satisfaction of the

the requirements for the degree of Master of Science

In Electrical Engineering

by

Pedro A. Barros

1991

To Professors: Tadeusz Babij, Wanaba Subbarao, and
                 Mark Hagmann.

This thesis, having been approved in respect to form and
mechanical execution is referred to you for judgement upon
its substantial merit.

_____
Dean Gordon Hopkins
College of Engineering
and Applied Science.

The Thesis of Pedro A. Barros is approved.

_____
Wanaba Subbarao

_____
Mark Hagmann

_____
Tadeusz Babij, Major Professor

Date of Examination: 5-30-1991

_____
Dean Richard Campbell
Division of Graduate Studies

Florida International University, 1991

CONTENTS

LIST OF FIGURES

LIST OF TABLES

1.0   INTRODUCTION

1.1 PREAMBLE:

This Thesis describes the design of a new type of antenna, using one of the most promising CAD tools for antenna design existing today: the MININEC program.

MININEC is a shortened version of the powerful Numerical Electromagnetic Code (NEC) program for antenna analysis and design used mainly with mainframe computers. MININEC has the great advantage, for engineers and engineering students, that it can be run in any IBM PC-Compatible microcomputer, with 512 Kbytes of memory. It represents a most useful tool for the analysis and design of thin-wire antennas of moderate complexity.

The antenna design presented here, stems from the author's special interest in electrically small and reduced-size antennas. There are indeed many practical applications for reduced-size antennas , from aerospace to military, to portable (and small) communications equipment, to make research in this field not only interesting, but necessary.

One of the most interesting reduced-size antennas investigated in recent years are meander antennas (3). These antennas are extensively described in the next chapters and analysed with MININEC. They provide a good reduction in size, and maintain most of the important radiation characteristics of conventional antennas. Furthermore, they are basically wire-antennas, which makes them very suitable for analysis with MININEC.

Before any practical design could be accomplished, it was necessary to start with applying the program to some simple and well - known antennas such as monopoles and dipoles, and then to proceed with the analysis of meander monopoles and dipoles. The purpose of this preliminary effort, that covers a good part of this paper, was threefold.

First, it was necessary to validate the results of MININEC, by comparing them with known reference data. Validation tests were accomplished on monopoles and dipole antennas, for this reason.

Second, it was important to gain enough experience with the operation of the program. Convergence tests were on different antenna geometries, to test the accuracy of the results and the inherent limitations of the program.
Third, since meander antennas are obviously the cornerstone of our design, it was important to run a complete analysis of these geometries, and of the folded dipole.

1.2 BACKGROUND - CAD ANTENNA DESIGN

Before the digital computer, the design of antennas was more a
cut-and-try operation than an accurate mathematical process. [1]
For complex-geometry antennas, this operation involved many hand-
calculations, iterations, simplification of antenna geometry and,
of course, long hours of practical laboratory work.

Along came the computer, and scientists and engineers rushed to
convert proven algorithms into computer programs or to develop
new algorithms suitable for use in computers as analysis or design
tools.

Today, the most powerful of these computer tools available for the
design and analysis of linear antennas is the Numerical Electromag-
netic Code (NEC). It is a highly user-oriented computer code offering
a comprehensive capability for analysis of the interaction of elec-
tromagnetic waves with conducting structures. The program is based
on the numerical solution of integral equations for the currents
induced on the structure by an exciting field. [11]

NEC combines an integral equation fot smooth surfaces with with one
for wires to provide convenient and accurate modeling for a wide
range of applications.

A NEC model model may include nonradiating networks and transmission
lines, perfect and imperfect conductors, lumped element loading, and
ground planes. The ground planes may be perfectly or imperfectly con-
ducting. Excitation may be via an applied voltage source or incident
plane wave.
The output may include induced currents and charges, near or far zone
electric or magnetic fields, and impedance or admittance. Many other
commonly used parameters such as gain and directivity, power budget,
and antenna to antenna coupling are also available. [11]

NEC was developed at the Lawrence Livermore National Laboratory
under the joint sponsorship of the U.S. Navy and Air Force. The NEC
user community comprises 17 government facilities, 11 domestic uni-
versities, over 20 domestic companies and at least 8 foreign organi-
zations. [1] [11]

NEC is a poweful tool for many engineering applications. It is ideal
for modeling co-site antenna environments in which the interaction
between antenna and environment cannot be ignored.

However, in many applications, the extensive full capability of NEC
is not really required (for example, in cases where the antenna and
its environment are not very complex, or the information sought re-
quires only a simplified model.)
In addition, NEC require the use of a a large main frame computer.
These computer systems are expensive and not readily available.

Even when such computer is available, heavy demand may result in slow turn-around, even for relatively simple NEC runs.

The obvious solution to this problems was the development of a "stripped-down" version of NEC that retains only the the basic solution and the most frequently-used options and that can be implemented in a simple micro-computer system. This program is written in Basic and has appropiately been named MININEC.

MININEC offers many of the required NEC options but makes use of the Basic language that is compatible with most microcomputers. MININEC is only suitable for for small problems on small computers compatible with the IBM format. However, with the use of a compiler the program can be used to analyse antenna problems of practical sizes.

3 METHODOLOGY

The performance of an antenna system is generally evaluated in terms of the following parameters: [2]

PARAMETERS	PERFORMANCE MEASURE
Impedance	Compatibility to RF equipment
Mismatch or VSWR	(Notably transmitters and receivers)
Bandwidth.	
Power (voltage) limit.	
Coupling	
Near Electric Field	RF radiation suceptibility and
Near Magnetic Field	hazard.
Far Field Patterns	
Gain	Link performance.
Beam-width	

Prediction of these perforfance parameters may be accomplished trough one or more of the following techniques:

TECHNIQUE	LIMITATION
Full scale measurement	The antenna design must be complete and the antenna constructed before any data may be collected. Mesurements are hampered by noise and interference in the environment.
Scale model measurement	Antenna design must be near completion in order to construct a meaningful model.

TECHNIQUE	LIMITATION
Scale model measurement (cont'd.)	Depending on antenna, it may require a large investment in resources to establish and maintain. Some phenomena do not scale linearly. Interference can also be a problem.
Computational extrapolation from empirical data.	This approach suffers from the same problems of any measurement scheme with the added necessity to maintain and retrieve from potentially large data bases.
Exact EM analysis	Exact analysis is limited to rather simple canonical geometries for which an exact solution may be possible. This amounts to a very small set of possible geometries.
Approximate EM solutions	Requires a thorough understanding of the constraints to avoid inappropriate use and invalid data. Solutions are approximate and must be interpreted in a way consistent with the constraints of the model. Usually this technique requires access to computer resources.

Some of the approximate methods of solution include finite difference techniques, quasi-optical techniques such as the geometric theory of diffraction, and method of moments technique. [2]

MININEC makes use of the technique known as the method of moments, to calculate the performance parameters of a thin wire antennas, following these steps:

1.- Formulate the thin wire model in terms of an appropriate set of integral-differential equations.

2.- Reduce the integral-differential equations to asystem of linear algebraic equations. This is accomplished in the method of moments by making certain simplifying assumptions, including the selection of a set of current expansion and testing functions. These assumptions will be treated in a later chapter.

3.- Specify the environment. That is, include the effects of a ground plane or free space, locate and account for all excitation sources and incorporate all loads into the solution.

4.- Solve the system of linear equations for the currents.

5.- Use the currents to compute the antenna performance parameters.

2.0   THE THEORY OF MININEC

2.1 INTRODUCTION

The MININEC program is based on the numerical solution of an integral
equation representation of the electric fields. There is nothing new
or unusual about this formulation. The real advantage is that the
solution technique results in a relatively compact computer code. The
discussion that follows is transcribed from [1].   It is inclu-
ded in this paper because it is considered important in understanding
the validity of the program as an antenna design tool.

2.2 THE ELECTRIC FIELD INTEGRAL EQUATION AND ITS SOLUTION

In solving wire antenna problems, it has become customary to make
several assumptions that are valid for thin wires. They are:
  1- That the wire radius is very small with respect to the length.
  2- The wire radius is very small with respect to the wavelength.

Because it is necessary to subdivide wires into short segments,
the radius is assumed small with respect to segment length as well,
so that the currents can be assumed to be axially directed (there
are no azimuthal current components).

Figure 2.1 gives the geometry of a typical arbitrarily oriented wire.
For simplicity, it is assumed that the wire is straight, but the
theory applies equally to bent configurations. Also shown is the wire
broken into segments or subsections.
  The vector and scalar potentials are given by: [2]

$$\overline{A} = \frac{\mu}{4\pi} \int_s I(s)\overline{s}(s)k(r)ds$$

(1.1)

(1.2)

$$\Phi = \frac{1}{4\pi_\iota} \int_s q(s)k(r)ds$$

Where the integration is along the length s of the wire and:

$$k(r) = \frac{1}{2\pi} \int_{-\pi}^{\pi} \frac{e^{-jkr}}{r} d\phi$$

where r is the distance from the source point of the current to the
observation point of the field, and the integration is over the angu-
lar variation around the wire.
  The linear charge density (via the continuity equation) is:

$$q(s) = -\frac{1}{j\omega}\frac{dI}{ds} \qquad\qquad (1.3)$$

The method of moments solution used in the MININEC system is based on relating the current distribution of the wire to the incident field on the surface of the wire. The integral equation relating the incident field E-inc. and the vector and scalar potentials is:

$$-\overline{E}_{inc} \cdot \overline{s} = -j\omega \overline{A} \cdot \overline{s} - \overline{s} \cdot \nabla \phi \qquad\qquad (1.4)$$

2.3 MATRIX EQUATION REPRESENTATION

Equation (1.4) is solved in MININEC by using the following procedure. The wires are divided into equal segments and, as shown in figure 2.1, the vectors r_n, n= 0,1,2,...N are defined with respect to the global coordinate origin, 0. The unit vector parallel to the wire axis for each segment shown are defined as:

$$\overline{s}_{n+1/2} = \frac{\overline{r}_{n+1} - \overline{r}_n}{|\overline{r}_{n+1} - \overline{r}_n|} \qquad\qquad (1.5)$$

Pulse testing and pulse expansion functions used in MININEC are defined as follows:

$$P_n(s) = 1 \ , \ \text{for} \ s_{n-1/2} < s < s_{n+1/2} \qquad\qquad (1.6a)$$

$$P_n(s) = 0 \ ; \ \text{otherwise} \qquad\qquad (1.6b)$$

Where the points S n+1/2 and S n-1/2 designate segment midpoints

$$s_{n+1/2} = \frac{s_{n+1} + s_n}{2} \qquad\qquad (1.7a)$$

$$s_{n-1/2} = \frac{s_n + s_{n-1}}{2} \qquad\qquad (1.7b)$$

6

A difference approximation is applied to equation (1.3) to compute the charge. Thus, as shown in figure 2.2, the charge can be represented as pulses displaced from the current by a half pulse width.

Substituting (1.11) into (1.10) produces a system of equations that can be expressed in matrix form. Each matrix element $Z_{m,n}$ associated with the nth. current pulse and the Sm observation point on the wire surface involves scalar and vector potentials terms with integrals of the form:

$$\psi_{m,u,v} = \int_{s_a}^{s_b} k(s_m - s')ds'$$

(1.12)

where

$$k(s_m - s') = \frac{1}{2\pi} \int_{-\pi}^{\pi} \frac{e^{-jkr_m}}{r_m} d\phi$$

(1.13)

and

$$r_m = \left[(s_m - s')^2 + 4a^2 \sin^2\left(\frac{\phi}{2}\right) \right]^{1/2}$$

(1.14)

Equation (1.12) does not lend itself to straightforward integration because of the singularity at r = 0. The 1/r can be substracted from the integrand and then added as a separate term, to yield:

$$k(s_m - s') = \frac{1}{2\pi} \int_{-\pi}^{\pi} \frac{d\phi}{r_m} + \frac{1}{2\pi} \int_{-\pi}^{\pi} \frac{e^{-jkr_m} - 1}{r_m} d\phi$$

(1.15)

The first term of (1.15) can be rewritten as an elliptic integral of the first kind:

$$\frac{\beta}{\pi a} F\left(\frac{\pi}{2}, \beta\right) = \frac{1}{2\pi} \int_{-\pi}^{\pi} \frac{d\phi}{r_m}$$

(1.16)

where:

$$\beta = \frac{2a}{\left[(s_m - s')^2 + 4a^2 \right]^{1/2}}$$

8

The following approximation can be used:

$$F\left(\frac{\pi}{2}, \beta\right) = \left[\sum_{i=0}^{4} a_i m^i\right] + \left[\sum_{i=0}^{4} b_i m^i\right] \ln(1/m)$$ (1.17)

where:

$$m = 1 - \beta^2 = \frac{(s_m - s')^2}{(s_m - s')^2 + 4a^2}$$

and

$a_0 = 1.38629\ 436112$ $b_0 = .5$
$a_1 = .09666\ 344259$ $b_1 = .12498\ 59397$
$a_2 = .03590\ 092383$ $b_2 = .06880\ 248576$
$a_3 = .03742\ 563713$ $b_3 = .03328\ 355346$
$a_4 = .01451\ 196212$ $b_4 = .00441\ 787012$

Thus as Sm approaches S'

$$\frac{\beta}{\pi a} F\left(\frac{\pi}{2}, \beta\right) \Rightarrow -\frac{1}{\pi a} \ln\left[\frac{|s_m - s'|}{8a}\right]$$ (1.18)

and this singularity is also substracted from k(Sm-S')
Thus

$$k(s_m - s') = -\frac{1}{\pi a} \ln\left[\frac{|s_m - s'|}{8a}\right]$$

$$+ \frac{\beta F\left(\frac{\pi}{2}, \beta\right) + \ln\left[\frac{|s_m - s'|}{8a}\right]}{\pi a} + \frac{1}{2\pi} \int_{-\pi}^{\pi} \frac{e^{-jk r_m} - 1}{r_m} d\phi$$ (1.19)

This equation is substituted into equation (1.12) and written as

$$\int_{s_a}^{s_b} k(s_m - s') ds' = I_1 + I_2 + I_3$$ (1.20)

9

Or in terms of the global coordinates,

$$\bar{r}_{n+1/2} = \frac{\bar{r}_{n+1} + \bar{r}_n}{2} \qquad (1.8a)$$

$$\bar{r}_{n-1/2} = \frac{\bar{r}_n + \bar{r}_{n-1}}{2} \qquad (1.8b)$$

It is assumed that the components of the vectors -E inc and A in equation (4) are sufficiently smooth over each segment that their respective values on each segment may be replaced by those taken at the point Sm on the wire. The pulse functions of (1.6) are then used as testing functions on (1.4) resulting in:

$$\boldsymbol{E}_{inc}(s_m) \cdot \left[\left(\frac{s_m - s_{m-1}}{2} \right) \hat{s}_{m-1/2} + \left(\frac{s_{m+1} - s_m}{2} \right) \hat{s}_{m+1/2} \right] =$$

$$j\omega \bar{A}(s_m) \cdot \left[\left(\frac{s_m - s_{m-1}}{2} \right) \hat{s}_{m-1/2} + \left(\frac{s_{m+1} - s_m}{2} \right) \hat{s}_{m+1/2} \right] \qquad (1.9)$$

$$+ \phi(s_{m+1/2}) - \phi(s_{m-1/2})$$

The vector quantities in brackets are simply:

$$(\bar{r}_{m+1/2} - \bar{r}_{m-1/2})$$

So that (9) can be written as:

$$\boldsymbol{E}_{inc}(s_m) \cdot (\bar{r}_{m+1/2} - \bar{r}_{m-1/2}) = j\omega \bar{A}(s_m) \cdot (\bar{r}_{m+1/2} - \bar{r}_{m-1/2}) \qquad (1.10)$$

$$+ \phi(s_{m+1/2}) - \phi(s_{m-1/2})$$

The currents are expanded in pulses centered at the junctions of adjacent segments as illustrated in figure 2.1. Note that pulses are omitted from the wire ends. This is equivalent to placing a half pulse of zero amplitude at each end. This imposes a boundary condition for a zero current at unattached wire ends. The current expansion can be written as:

$$I(s) = \sum_{n=1}^{N} I_n P_n(s) \qquad (1.11)$$

7

I_1, I_2 and I_3 are defined as:

$$I_1 = -\frac{1}{\pi a} \int_{s_a}^{s_v} \ln\left[\frac{|s_m - s'|}{8a}\right] ds' = \frac{8}{\pi} u(1 - \ln|u|)\Big|_{u_1}^{u_2} \qquad (1.21)$$

where

$$u_1 = \frac{s_u - s_m}{8a}$$

and

$$u_2 = \frac{s_v - s_m}{8a}$$

Similarly,

$$I_2 = \int_{s_a}^{s_v} \frac{\beta F\left(\frac{\pi}{2}, \beta\right) + \ln\left[\frac{|s_m - s'|}{8a}\right]}{\pi a} ds' \qquad (1.22)$$

This integral has a well behaved integrand and can be integrated numerically. The integration is broken up into two integrals over the ranges (Su,Sm) and (Sm,Sv) for best accuracy. Gaussian quadrature is used for the numerical integration. The number of points in the integration is automatically selected by consideration of the source to observation distance. The final integral is:

$$I_3 = \frac{1}{2\pi} \int_{s_a}^{s_v} \int_{-\pi}^{\pi} \frac{e^{-jkr_m} - 1}{r_m} d\phi \qquad (1.23)$$

This integrand is nonsingular and can also be integrated numerically, To obviate the need for double integration, it is convenient to approximate the integral by replacing r_m of equation(1.14) by a reduced kernel approximation. Thus,

$$I_3 = \int_{s_a}^{s_v} \frac{e^{-jkr_a} - 1}{r_a} ds' \qquad (1.24)$$

where,

$$r_a = \sqrt{(s_m - s') + a^2}$$

This integral can be integrated numerically by the same procedure as for I_2.

Thus, equation (1.12) with its singularity problem is evaluated by adding equation I_1 of equation (1.21), I_2 of equation (1.22), and I_3 of equation (1.24)

By substitution, the matrix equation to be solved is:

$$[V_m] = [Z_{mn}][I_n]$$

(1.25)

where

$$Z_{mn} = -\frac{1}{4\pi j\omega\epsilon}[k^2(\bar{r}_{m+1/2} - \bar{r}_{m-1/2}) \cdot (\xi_{n+1/2}\psi_{m,n,n+1/2} + \xi_{n-1/2}\psi_{m,n-1/2,n})$$

$$-\frac{\psi_{m+1/2,n,n+1}}{s_{n+1} - s_n} + \frac{\psi_{m+1/2,n-1,n}}{s_n - s_{n-1}}$$

$$+\frac{\psi_{m-1/2,n,n+1}}{s_{n+1} - s_n} - \frac{\psi_{m-1/2,n-1,n}}{s_n - s_{n-1}}]$$

(1.26)

and

$$V_m = E_{inc}(s_m) \cdot (\bar{r}_{m+1/2} - \bar{r}_{m-1/2})$$

(1.27)

[Zmn] is a square matrix and [In] and [Vm] are column matrices with m=1,2,3...N and n=1,2,3...N for N total unknowns (i.e. N is the total number of current pulses) The extension of these equations to two or more coupled wires follows the same line of development and is covered in reference 2.

The column vector [Vm] represents an applied voltage that superimposes a tangencial electric field along the wire for a distance of one segment length centered at the location of the current pulses. Hence, for a transmitting antenna, all elements of [Vm] are set to zero except for the element(s) of the segment(s) located at the desired feed point(s). For an incident plane wave, all elements of [Vm] must be assigned a value depending on the strength, polarization (or orientation) and angle of incidence of the plane wave. The applied voltage source (transmit case), however is the only ready-made or pro-grammed option in the current calculation algorithm.

As stated before, the [Zm,n] matrix in equation (1.25) is filled by the evaluation of an elliptic integral and use of the Gaussian quadrature for numerical integration. The solution to (1.25) can be accomplished by using any one of a number of of standard matrix solution techniques The MININEC version used in the antenna design, described in this paper, uses a triangular decomposition (LU decomposition) with the Gaussian elimination procedure and partial pivoting.
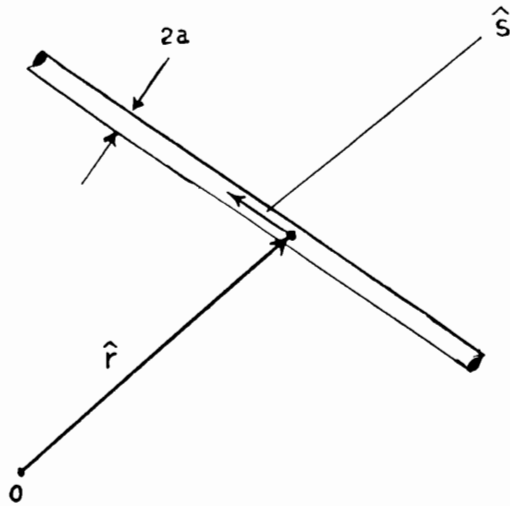
(a) ARBITRARILY ORIENTED WIRE.
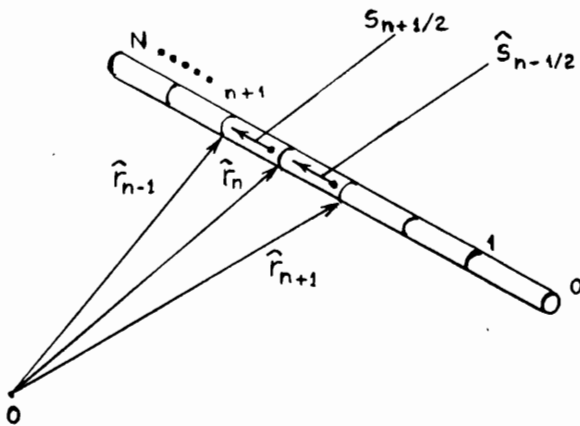
(b) SEGMENTATION SCHEME FOR THE SAME WIRE.

FIGURE 2.1: GEOMETRY OF AN ARBITRARILY ORIENTED WIRE
(FROM [1])
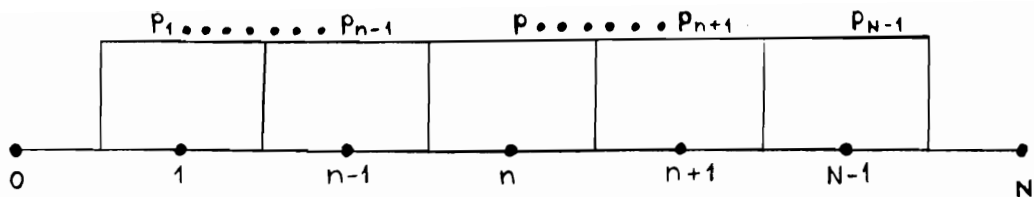
(a) UNWEIGHTED CURRENT PULSES
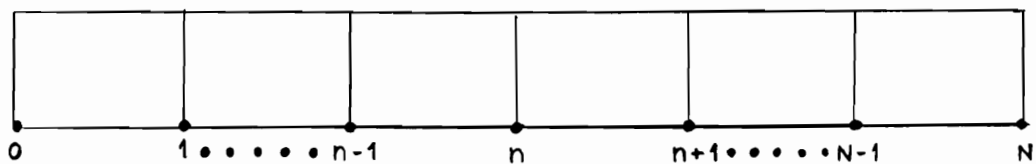
(b) UNWEIGHTED CHARGE REPRESENTATION.

FIGURE 2.2: WIRE SEGMENTATION WITH PULSES FOR CURRENT AND CHARGES
(FROM [1])

3.0 VALIDATION

3.1 GENERAL

Validation of the MININEC system is based on the comparison of the results of the program, when applied to a known geometry, with practical or theoretical data for that geometry.

There are extensive discussions in references 1 and 2 on this subject. In particular, convergence tests are done for three cases: an electrically short dipole (much shorter than the first resonance length), a dipole near resonance, and a dipole near antiresonance.

The segmentation scheme for each specific geometry seems to be important in obtaining accurate results. In general, it can be said that there is an optimum number of segments for each geometry. The exact number can only be determined on the basis of experience in using the program. Figures 3.1 and 3.2 show the convergence of MININEC data as the segment number is increased, on a center-fed half wave dipole in free space, when compared with at theoretical value published by R. W.P. KING. [5]

It can be seen that the optimum number of segments for this antenna would be around 32 segments. However, the program run time increases with the number of segments. (greater complexity of the solution). Probably, a smaller segment number would also be adequate, since the results do not differ more than 5% for a number greater than 8 segments. In fact, the reactive curve does not converge any further for more than 12 segments.

Another important conclusion that can be drawn from these convergence tests is the fact that, in general, segment (or wire) radius is inversely proportional to the accuracy of the result. For small radii (r << 0.01 wire length) the accuracy of the result will not vary much, but it will tend to converge to the theoretical value. However, for design purposes, the radius of the wire should reflect the "true" radius utilized in the finished antenna. This will norma--lly be a one or two millimeters at the most.

.2 QUARTER WAVE MONOPOLE ON CONDUCTING GROUND

As a further validation test, the impedance of a quarter-wave monopole on conducting ground was calculated for several frequencies, corresponding to a length-to-wavelength ratio from 0 to 0.75 (well past antiresonance).

PERCENT DIFFERENCE vs. NUMBER OF SEGMENTS

RWP KING ADMITTANCE: $Y = G + jB = 9.611 - j4.752$ mMHOS

$f = 299.8$ MHz

$a = .001588$ m

$k_o h = p1/2$

$h = .25$ m

B

G

P
E
R
C
E
N
T

32

24

16

8

0

-8

0   4   8   12   16   20   24   28   32   36   40

NUMBER OF SEGMENTS
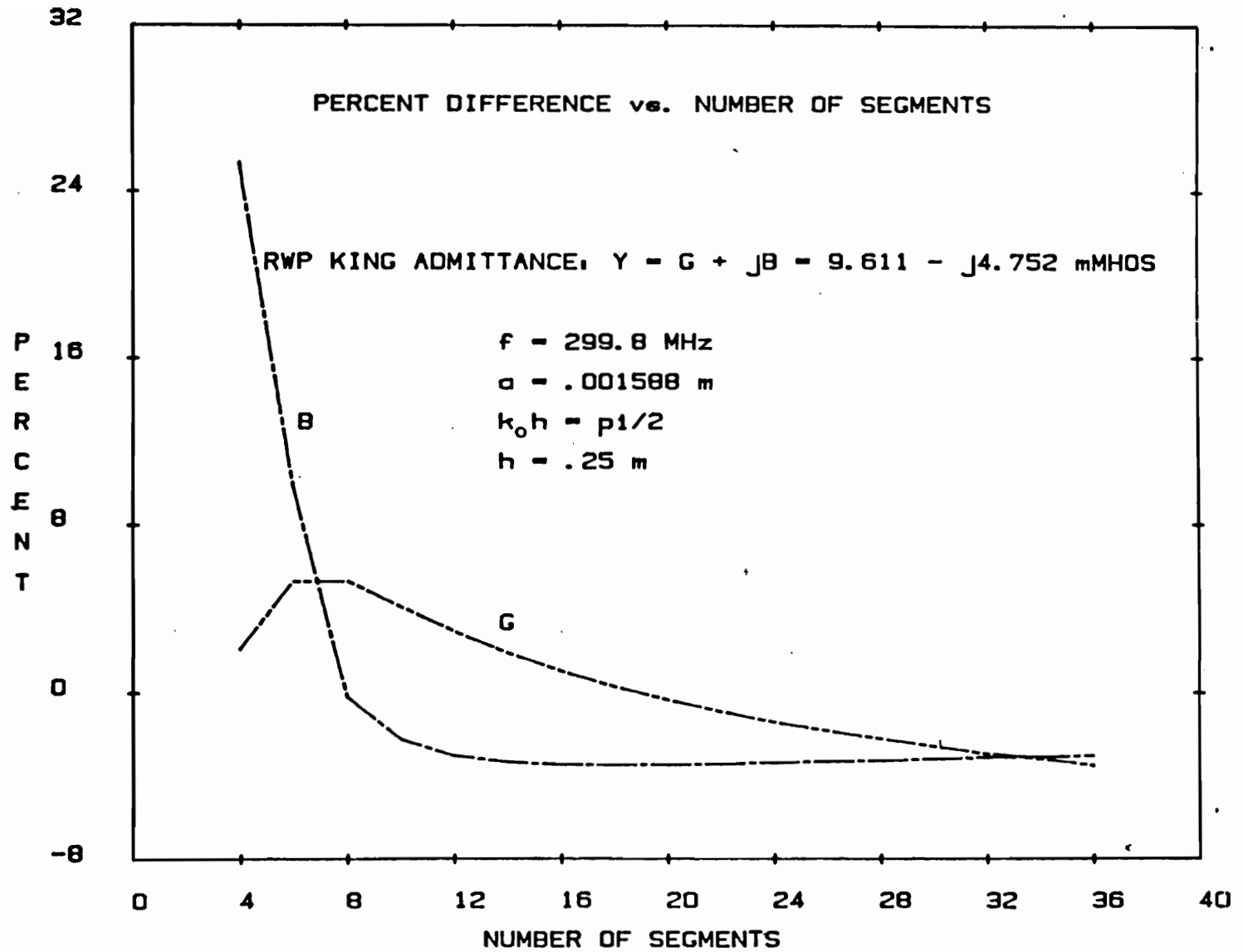
FIGURE 3.1:   HALF-WAVE DIPOLE CONVERGENCE TEST (FROM [1])

ADMITTANCE (Y= G + jB) vs. NUMBER OF SEGMENTS

RWP KING ADMITTANCE: Y = 9.611 - j4.752 mMHOS

f = 299.8 MHz
a = .001588 m
$k_0 h$ = pi/2
h = .25 m
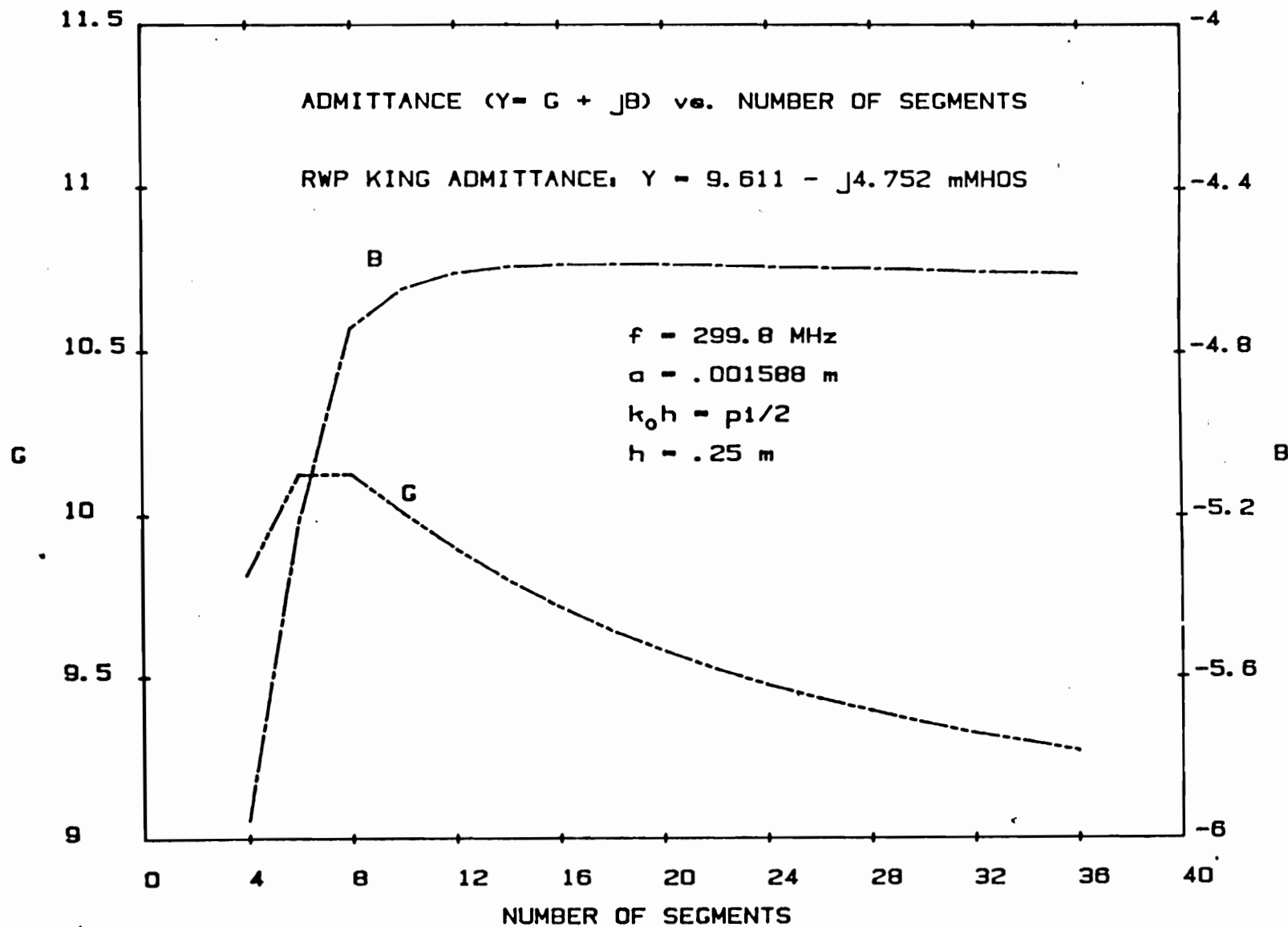
FIGURE 3.2: HALF-WAVE DIPOLE CONVERGENCE TEST (FROM [1])

The geometry was chosen to have a wire length of 100 times the wire radius, and having 16 segments. The antenna had a length of 0.25 mts. which means resonance occurs at 300 MHz.
The MININEC version used was that from [2] : The MININEC System by Artech House.

Both the Real and Imaginary part of the impedance were calculated and compared to theoretical values obtained from [4] (Kraus)
A frequency sweep was accomplished to obtain the curve.

Figures 3.3 and 3.4 show the curves of real and imaginary parts of the quarter wavelength monopole on a perfectly conducting ground It can be seen that both curves show excellent coincidence with theoretical values for length/wavelength ratios close to 0.25 (resonance for a monopole). The values differ more for antiresonance but they do not exceed 10% of difference in the worst case.

The next step was to compute the input impedance of the described monopole for different segment densities. The segmentations scheme started as low as 2 segments for this single-wire antenna and was increased to a maximum of 50 segments.

The following Table 3.1 shows the results of this test.

TABLE 3.1:   SEGMENTATION DENSITY CONVERSION

SEGMENT No.	INPUT IMPEDANCE (Ohms)
2	36.95 + j 23.87
4	39.95 + j 19.40
10	41.60 + j 20.42
20	42.3 + j 21.63
30	42.6 + j 22.20
40	42.8 + j 22.53
50	42.93 + j 22.69

This results were compared with the practical results from [5], obtained by R.W.P King, for a monopole with a wire radius-to-wavelength ratio of 0.001 and a length-to-wavelength ratio of 0.25. This impedance is:

$$Z_{ref} = 43.7 + j\ 22.84$$

FIGURE 3.3: INPUT RESISTANCE OF A QUARTER-WAVELENGTH MONOPOLE.

□ THEORETICAL (KRAUS) [4]   + MININEC (16 Seg.)
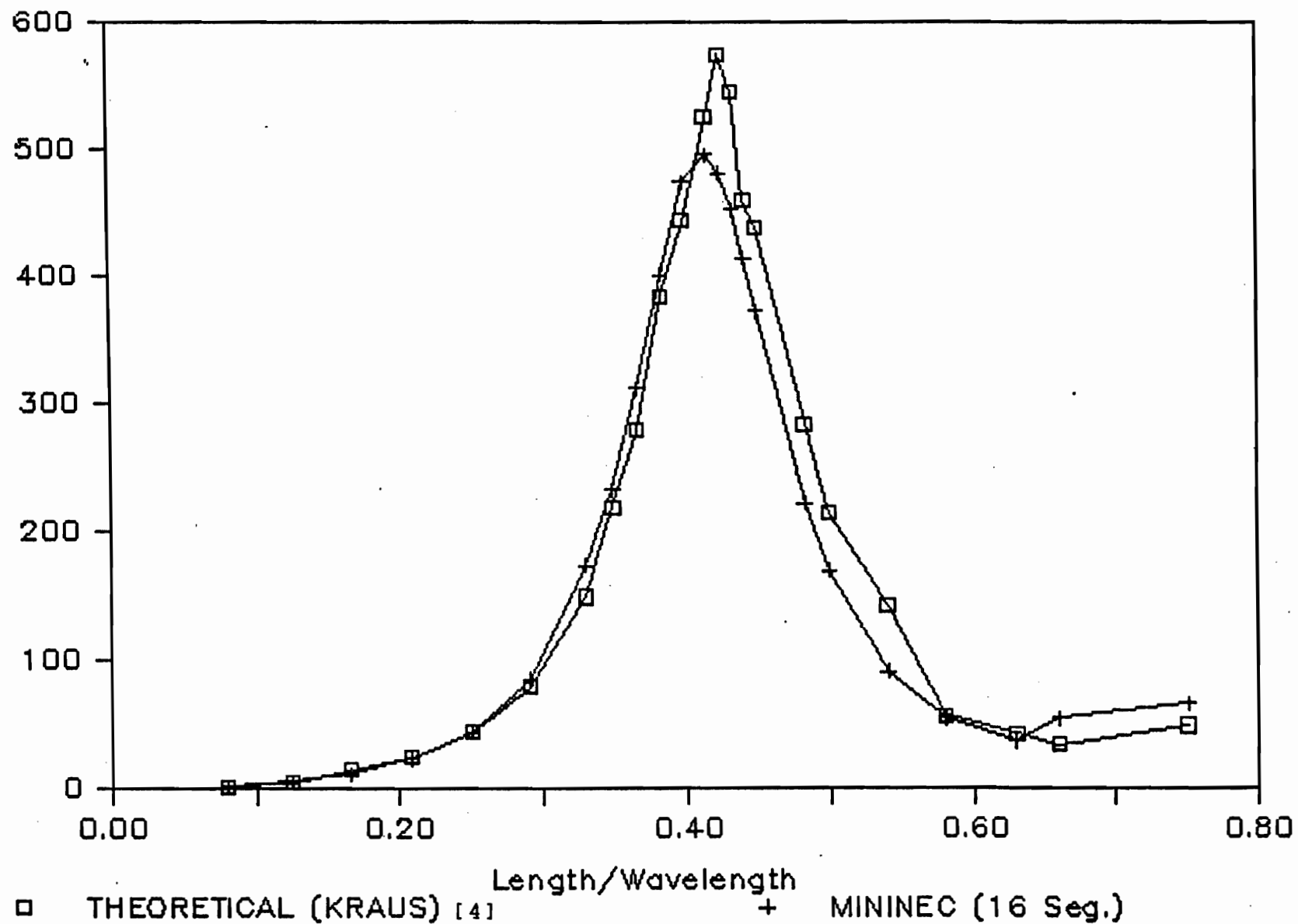
FIGURE 3.4: INPUT REACTANCE OF A QUARTER WAVELENGTH MONOPOLE.

□   THEORETICAL (KRAUS) [4]   +   MININEC (16 Seg.)
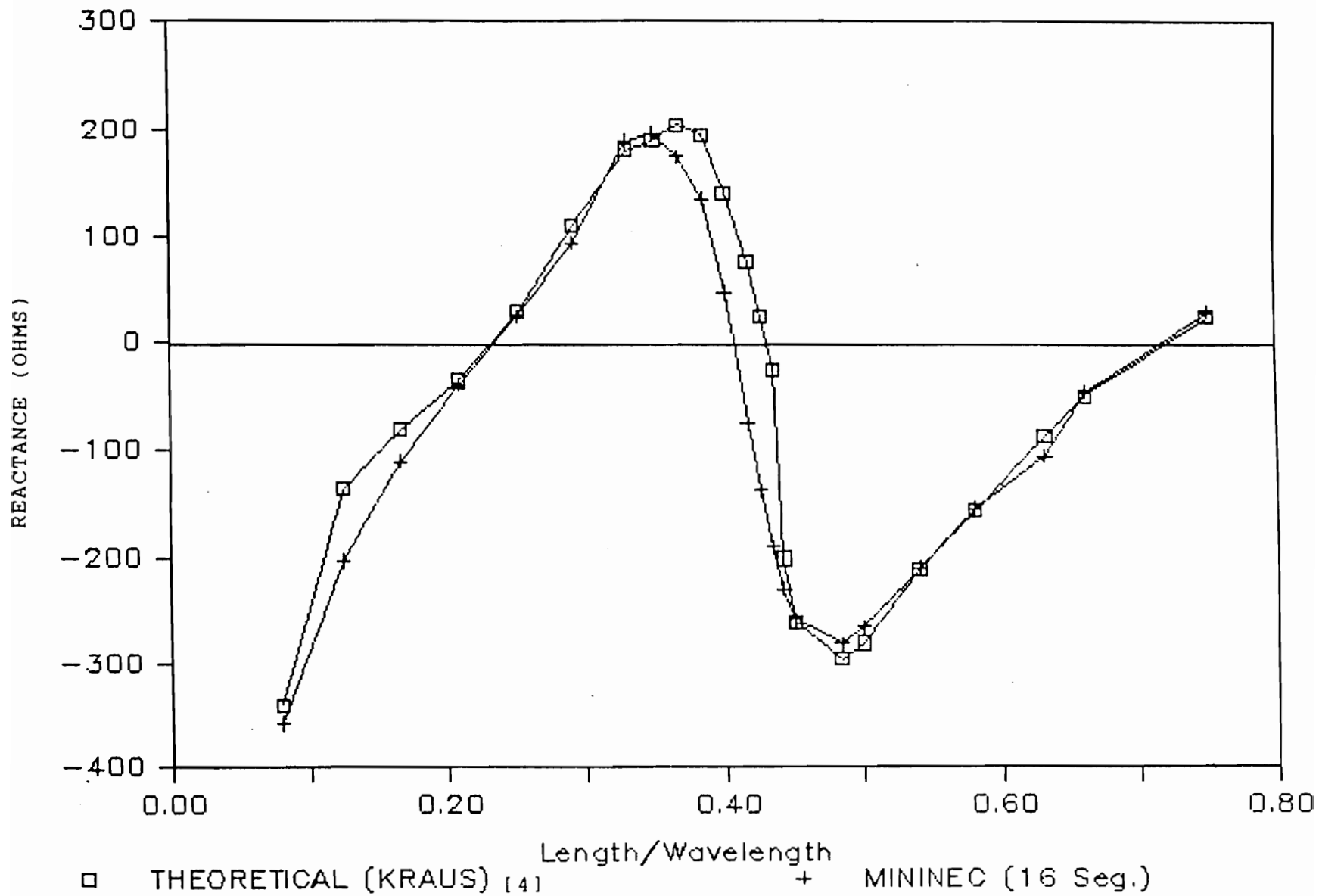
FIGURE 3.5(a): MONOPOLE INPUT RESISTANCE.
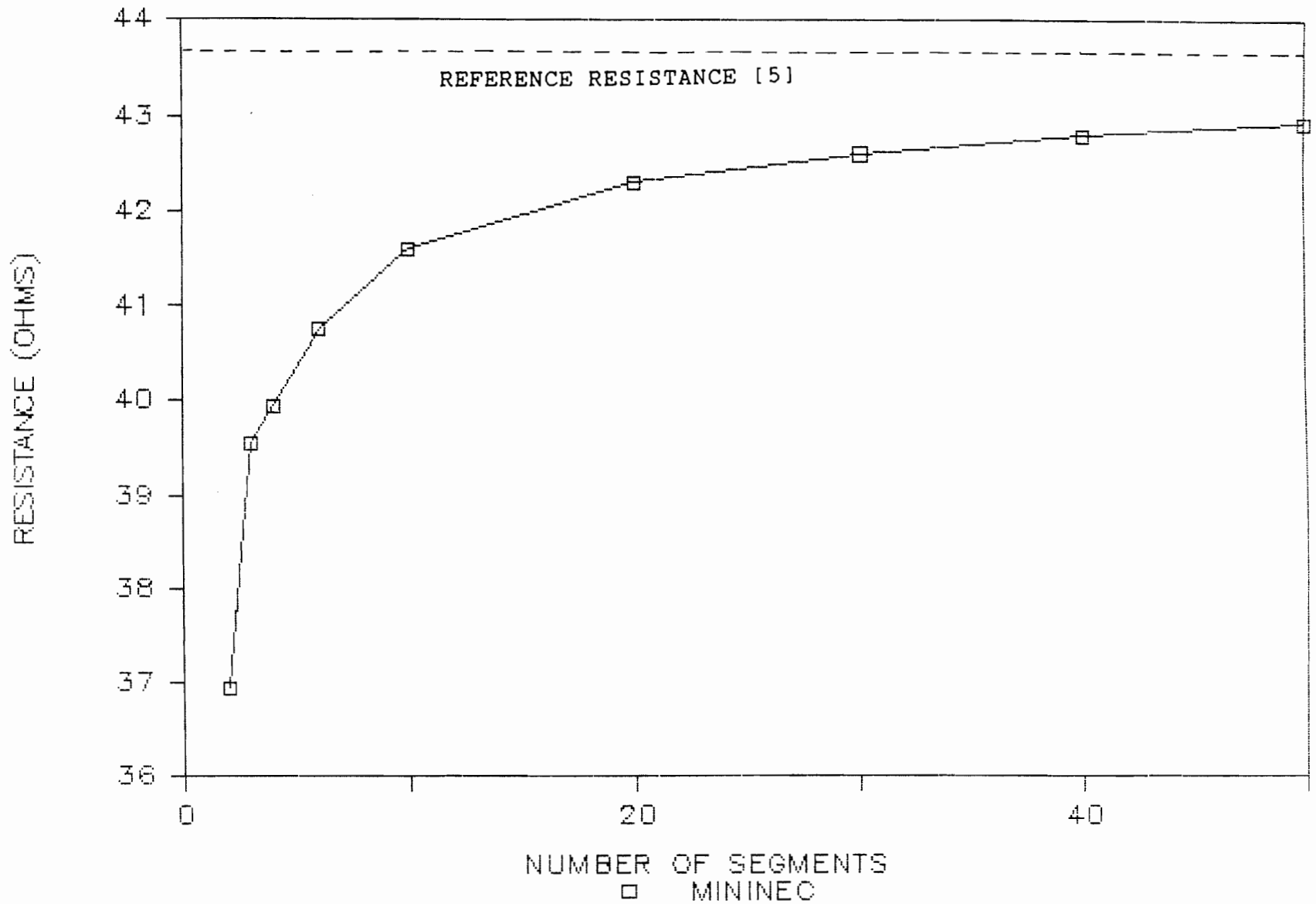
FIGURE 3.5(b): MONOPOLE INPUT REACTANCE.

REFERENCE REACTANCE (R.W.P KING)   [5]

REACTANCE (OHMS)

NUMBER OF SEGMENTS

□   MININEC
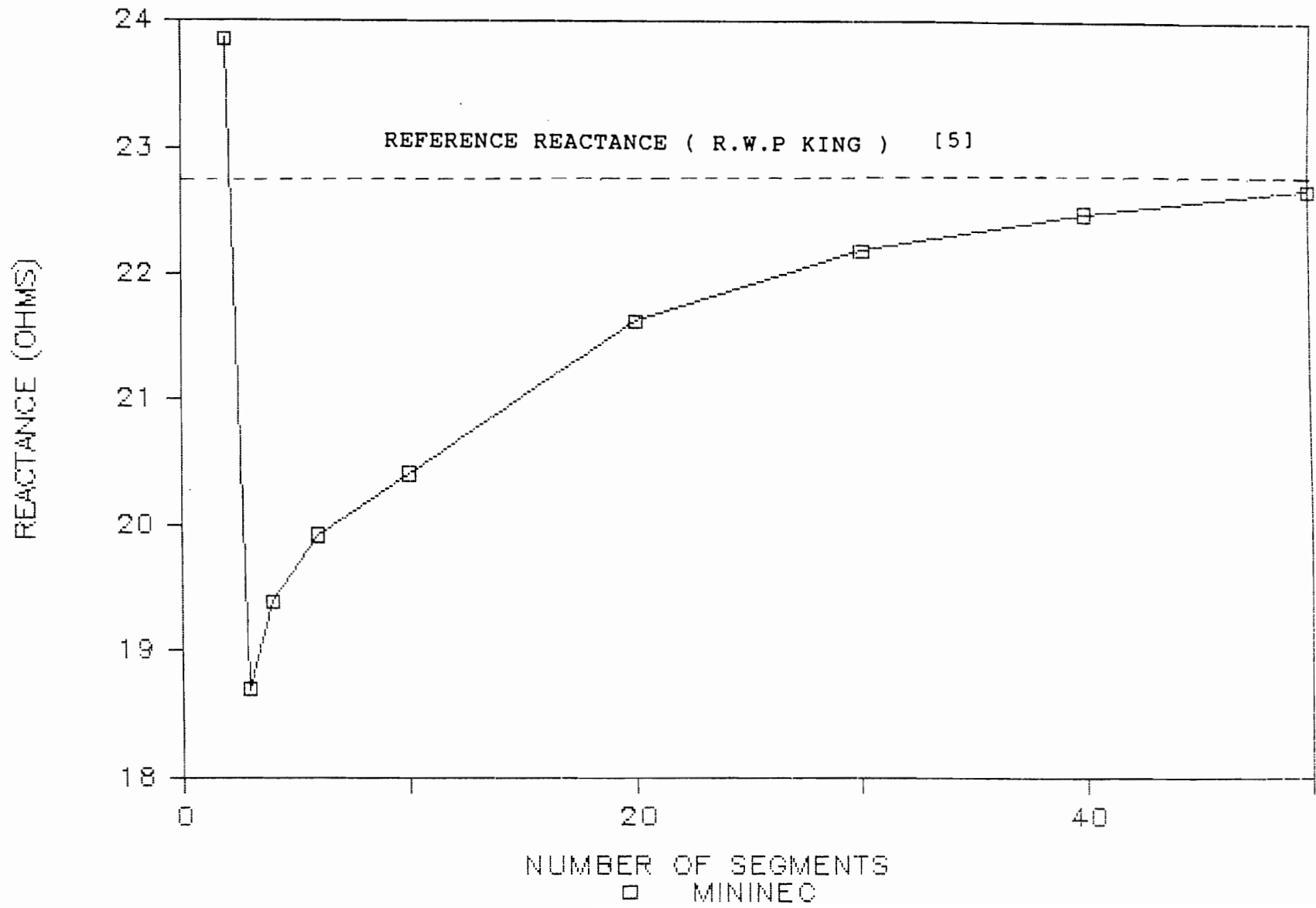
The convergence of the impedance as the number of segments is increased is shown graphically in Figure 3.5.
Note that for a monopole with only 2 segments, the value of the reactance does not follow the convergence curve, whereas the resistance does follow the trend. This singularity is due to the fact that a very low segmentation density in MININEC, usually will yield erronous or inaccurate results. This will be shown in more detail in the next section, where more complicated geometries are analysed.

3.3 MEANDER ANTENNAS

3.3.1 GENERAL:

As a final proof of the validity of the program, it was necessary to analyse more complicated geometries. Meander antenna geometries were chosen because they obviously have a close relationship to the antenna design presented in this paper.

Meander antennas were first investigated by J. Rashed and Chen-To Tai in 1982 [3]. These antennas are a new type of reduced-length antennas. Previous works on the subject of reducing the size of a monopole while preserving the resonant frequency ended up in drawbacks such as bandwidth deterioration, pattern distorsion and reduced antenna efficiency.

Meander antennas are constructed from a continously folded wire intended to reduce the resonant length. Since the wire is folded three times over its course on each half section, the total length of the monopole is only one-third of the length of a monopole made from the same wire. Refer to to figure 3.6.

The following parameters are defined for meander antennas:

- Reduction factor B (<1): If a conventional monopole of length L and a meander monopole of length l, have the same resonant frequency, then the resonant factor is designated as:

$$B = l/L$$

Equivalently, the resonant frequency of a meander monopole, fmo, is B times the resonant frequency fo, of a monopole with same length.

- Number of meander sections per wavelength, N:
  This number serves to describe the geometry. A full meander section corresponds to N=4 while the geometry of figure 3.6 corresponds to N=2. For a quarter-wavelength vertical monopole, this will normally coincide   with the number of horizontal wires in the geometry.

Experiments of reference [3] have shown that the reduction factor is of the order of 0.6 rather than one third. This factor depends primarily on the number of sections per wavelength N and the width of the rectangular loops w. Also, experimental results show that antenna efficiency is comparable to that of an unfolded monopole.

Some measurements have been made with the separation of the wires, w, as a variable. These experiments show that when w increases, the reduction factor B decreases, but the resonant resistance drops drasticallly, these effects are also accompanied by a narrower bandwidth. Furthermore, for an increasing w, cross polarization appears in the plane xz. These aspects are further discussed in the next chapter.

3.3.2 MEANDER MONOPOLE ON CONDUCTING GROUND.

The impedance of the monopole shown on Figure 3.6, having an N=6, was compared with the results obtained by Rashed & Tai [3]. the total length of the wire is 13.5 cmts. and has a value of N=6.

Furthermore, impedance computations were carried out for several segmentation schemes. It was established that for a total number of segments of less than 30 for this geometry, the program did not yield accurate results. Also for a segment number above 50, numerical errors ocurred. For segment numbers between 30 and 50, the impedance converges very well to the experimental value.
The following table illustrates the results:

TABLE 3.2: MEANDER MONOPOLE IMPEDANCE VERSUS NUMBER OF SEGMENTS

NUMBER OF SEGMENTS	COMPUTED IMPEDANCE
24	114.8 + j5,469.8
35	19.2 + j11.4
42	19.6 + j15.2
49	19.8 + j17.4
51	Error occurs.

REFERENCE INPUT RESISTANCE (Measured) : 20.5 Ohms.

It can be seen that the real portion of the computed impedance converges very well to the measured value of the input resistance, at resonance.
The computations were all done for the same experimental resonance frequency of 1050 MHz.
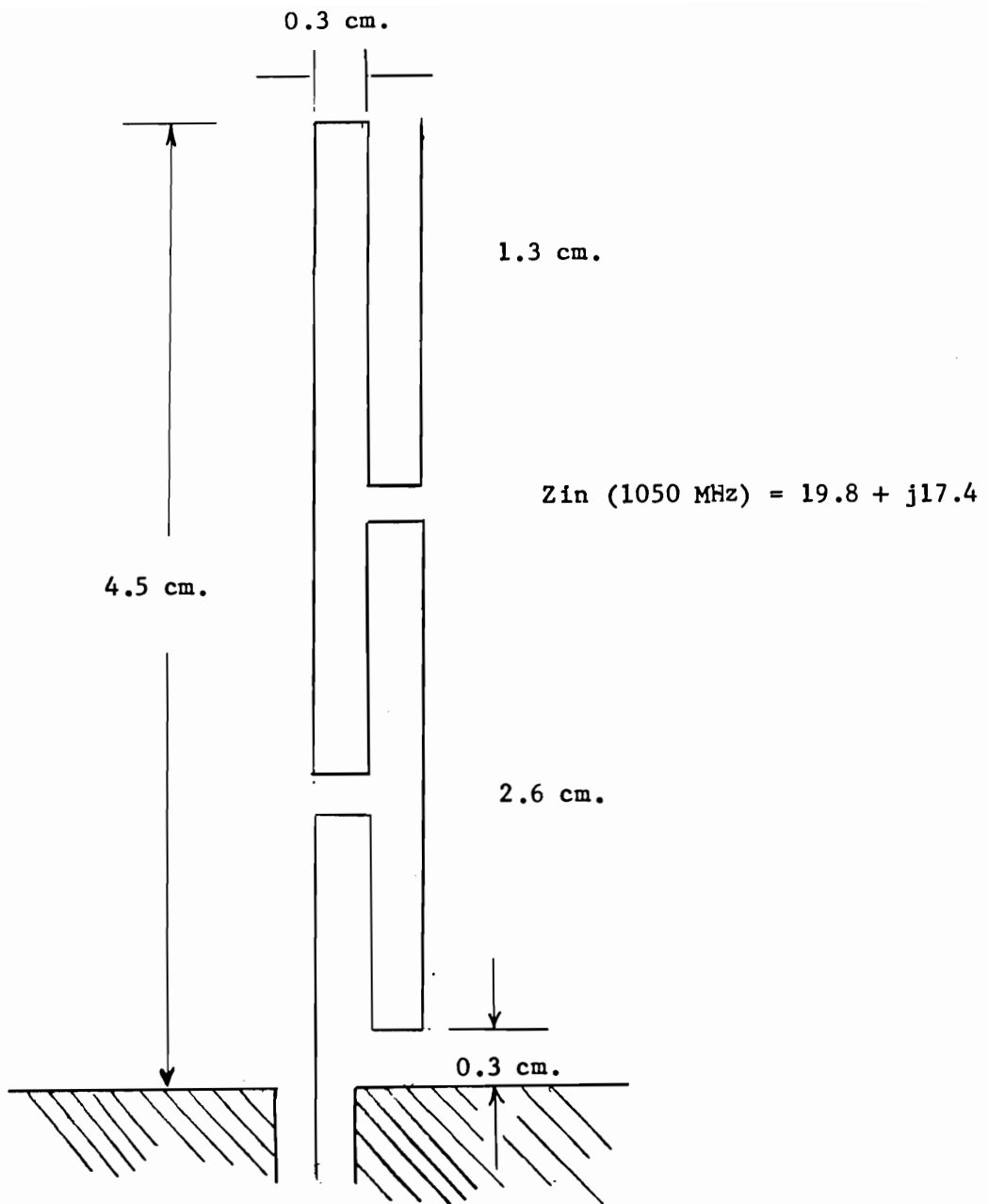
FIGURE 3.6: MEANDER MONOPOLE ANTENNA WITH N = 6.

Labels in figure:

0.3 cm.

1.3 cm.

Zin (1050 MHz) = 19.8 + j17.4

4.5 cm.

2.6 cm.

0.3 cm.

3.3 CONCLUSIONS

By the previous validation tests, it has been shown that MININEC, provides a reliable computer-based tool for analysis and synthesis of thin wire antennas. Since the antenna design described in the following chapters was based on the results obtained with this software, it was of primary importance to establish the validity of the program as a design tool. Furthermore, some of the program's limitations and characteristics were explored, that enabled the user to treat the results with enough confidence.

In particular, the segmentation density used for a specific geometry plays an important role in obtaining accurate results. The convergence testsfor various antennas reveals the accuracy that can be expected and provides a rational criterion for selection of segmentation density. Numerical problems may occur in the solution of a geometry when quantities become too small for the inherent accuracy of a computer. An example is the erronous results that can occur for very short segments (in terms of wavelength).
A practical limit for a semgent length seems to be about 10E-4 wavelength, for a single precision 16-bit computer.

4.0   PRELIMINARY DATA ANALYSIS

4.1   GENERAL:

This chapter will describe the preliminary analysis of known antennas, that led to the design of a folded meander dipole antenna covered in this paper. This antenna makes use of the reduction property of meander antennas, but has two important advantages over the simple monopole geometries of [3]

- a- Folded dipole geometries can be designed to have a wide range of impedances, with careful choise of wire diameters and separation between the two branches of the dipole.

- b- The size-reduction factor has been found to be typically less than 0.5. That is, this antenna has less than half the size of a folded dipole that has the same resonant frequency.

Preliminary analysis of simpler geometries such as meander dipoles and folded dipole antennas were accomplished as a means of obtaining sufficient reference data to accurately accomplish the subject design. These analysis, using MININEC are described in this chapter, as they provide in themselves sufficient explanation for some of the properties encountered in the final configuration.

Two known types of geometries were analysed using MININEC: meander monopoles antennas of reference (3) and the well-known folded dipole antenna. The analysis served the purpose of gathering some data on the behaviour and characteristics of these antennas, as well as to compare the results of MININEC with known theoretical or experimental data.

4.2   MEANDER ANTENNAS

4.2.1 BACKGROUND

The basics principles of meander antennas were covered in chapter 3. This section will describe with more detail some of the characteristics of these antennas, as obtained by modelling a basic meander monopole geometry, using MININEC.
As was previously said, meander antennas are made of a continously folded wire intended to reduce the resonant length of an antenna. Some of the main characteristics of the monopole meander antennas are summed :

1- The reduction factor, defined as the ratio of the heigth h of a meander monopole , to the length L of a conventional monopole having the same resonant frequency , is of the order 0.60 to 0.7. That is, the meander monopole is 30% to 40% smaller than a conventional monopole.

2- The input impedance is typically less than that of a conventional monopole. It varies according to the number N of meander sections per wavelength. This means that antenna has to be matched to the transmission line.

3- Antenna efficiency, by contrast to other size-reducing schemes, is similar to that of a conventional antenna.

Other important characteristics were obtained my running MININEC with a simple meander monopole on conducting ground and N=2. Some of the possible meander-monopole geometries with varying N (number of meander sections per wavelength) are shown in figure 4.1

4.2.2 EFFECT OF w ON ANTENNA CHARACTERISTICS

The effect of w, the wire separation on meander antennas was analysed. The model used was a meander monopole on perfectly conducting ground, with a total wire length of 13.5 cm., a heigth of aproximately 4.5 cm., and N=2. .The wire radius was 0.4 mm.

The results are shown in table 4.1 below. It can be seen that , as w increases, the resonant resistance drops drastically, and the reduction factor r decreases.

TABLE 4.1: EFFECT OF WIRE SEPARATION w ON CHARACTERISTICS OF MEANDER MONOPOLE N = 2, TOTAL WIRE LENGTH = 13.5 cm.

w (cm.)	Resonant Resistance	Freq. (MHz)	r
0.25	11.72 Ohms	970	0.59
0.5	7.82 Ohms	820	0.5
1.0	4.99 Ohms	680	0.43
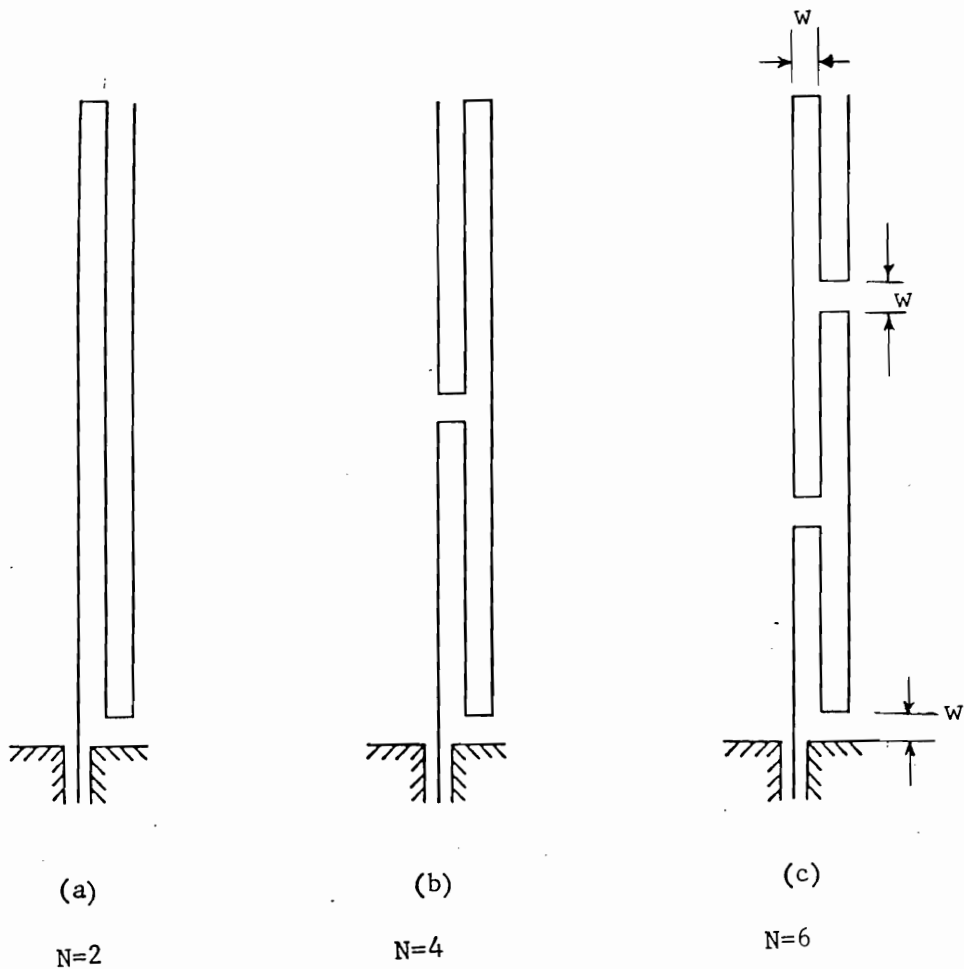
FIGURE 4.1: SPECIAL CASES OF MEANDER MONOPOLES.

(N is defined as the number of Meander
sections per wavelength. For example,
the monopole with N=4 is composed of
a full Meander section.)

EFFECT ON ANTENNA BANDWIDTH

For each of the above antennas, with different wire separation w, the impedance was calculated for different frequencies. The bandwidth in each case was obtained using the following method:

1-Impedance values are normalized to the resonant resistance value, so that when plotted in a Smith Chart, they pass the center of the chart.

2- A circle corresponding to a VSWR = 2.0 is used to find the upper & lower frequencies.

The results are shown in table 4.2. Also the bandwidth as a percentage of the resonant frequency is shown for each case. This number is sometimes referred as the antenna "Q" factor.

It can be seen that, as w increases, the bandwidth tends to decrease accordingly. It is worth noting that the bandwidth of a meander monopole is considerably less than that of a conventional monopole. A reference monopole with the same resonant frequency would have a bandwith of about 10% its resonant frequency.

Figure 4.2 shows the Smith-chart plot of the meander monopole antenna impedances and their corresponding bandwidths.
Figure 4.3 is the Smith-Chart for a conventional quarter-wavelength monopole.

TABLE 4.2: BANDWIDTH OF MEANDER MONOPOLES WITH N=2

Antenna #	w (cm)	Res. Freq. (MHz)	Q (%)
1	0.25	970	3.6
2	0.5	820	2.1
3	1.0	680	1.5
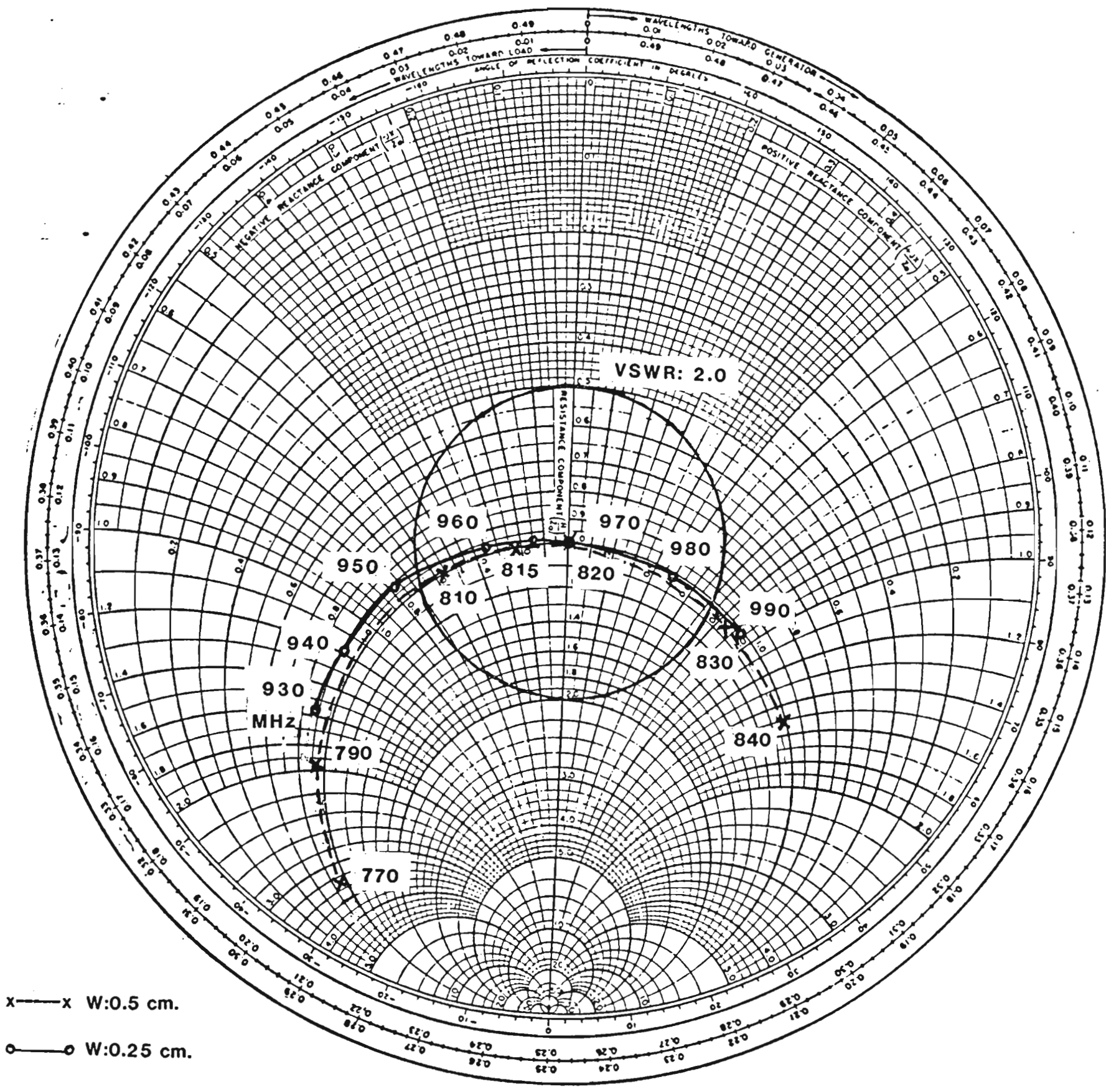
FIGURE 4.2 IMPEDANCE CURVE FOR MEANDER MONOPOLES WITH W:0.25 AND 0.5 cm.
CURVES ARE NORMALIZED TO THE RESONANT RESISTANCE VALUE.

VSWR: 2.0

280   286

270   290

260   300

310

330
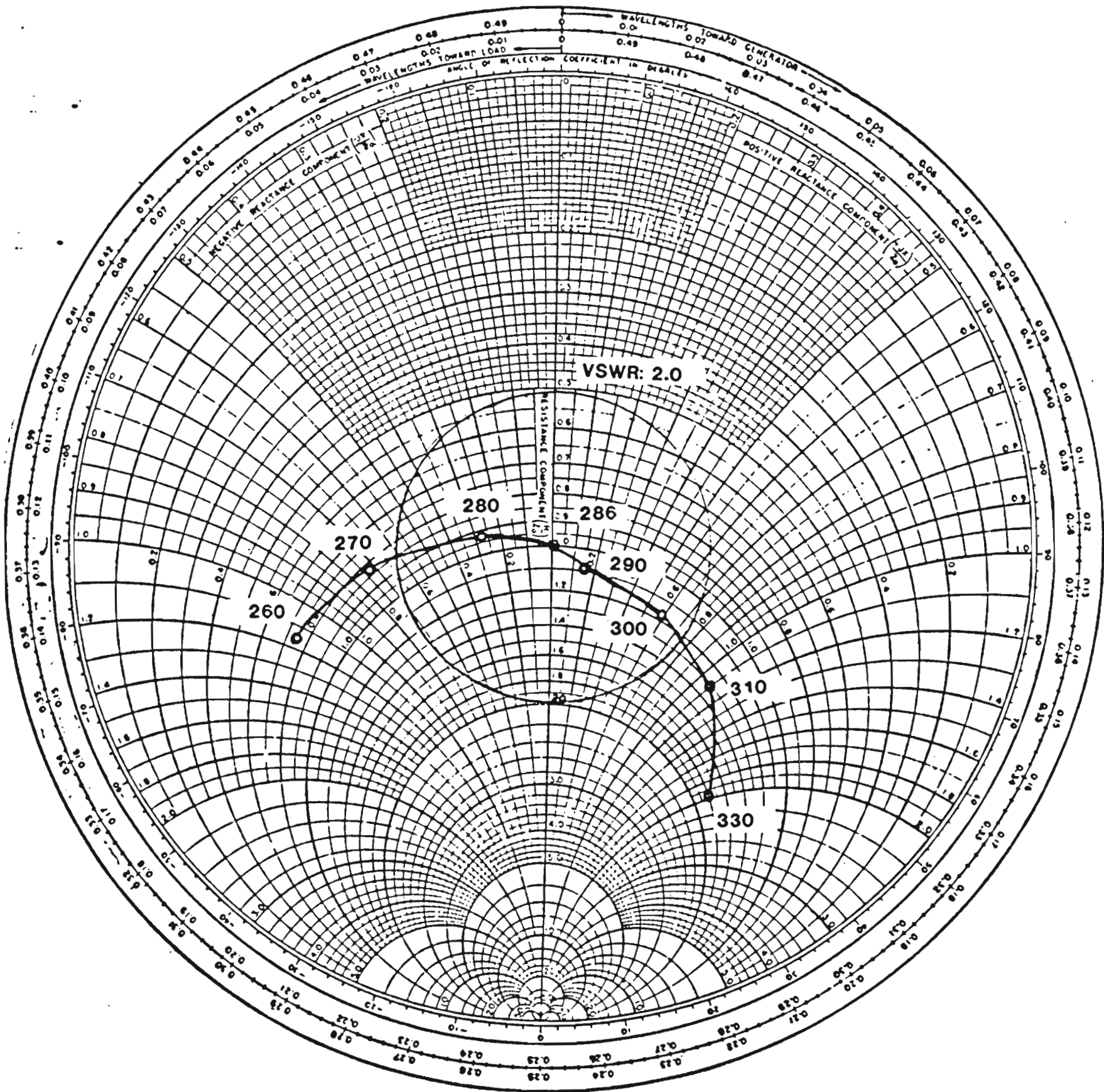
FIGURE 4.3:   IMPEDANCE OF A CONVENTIONAL MONOPOLE
OF LENGTH = 50 cm.
Resonant Frequency is 286 MHz.

31

4.2.3 EFFECT OF N IN ANTENNA CHARACTERISTICS:

The effect of N, or the number of meander sections per wavelength was analysed using MININEC. It was found that for a small constant w, an increasing N means an increase in the reduction factor typically ranging from 0.6 for N=2 to 0.7 for N=10. However, one can decrease the reduction factor r even further, by increasing w, as shown previously.

In general, the lower the N, the better the size reduction property. But meanwhile, the resonant resistance and the bandwidth decrease as r decreases. For the lowest value of N, i.e. N=2 the reduction factor is 0.6 which corresponds to about 40 percent reduction in size. In this case, the resonant resistance is about 11 ohms, much lower than a conventional monopole.

The results are shown in table 4.3:

TABLE 4.3: EFFECT OF N ON ANTENNA CHARACTERISTICS
              TOTAL WIRE LENGTH = 13.5 CM.
              W = 0.25 CM.

N	fo(MHz)	Resonant R (Ohms)	Reduction Factor r
2	970	11.7	0.59
6	1051	20.1	0.71
10	1113	21.9	0.74

Again, here we have a compromise between size-reduction and input resistance. In the case of the highest-resistance meander monopole (N=10), it would be possible to further increase the value of this resistance by increasing wire separation, to obtain a value of about 24 ohms. If this monopole were to be fed by a conventional 50-ohm coaxial line ,the antenna VSWR at resonance would be close to 2.0.

This is a very acceptable value of VSWR, and the experimental monopoles of reference (3), yield an efficiency comparable to that of a conventional monopole. However, is this loss of matching and level of complexity in the geometry, worth a mere 30% in size reduction ? The answer, of course lies in the antenna application.

In the case of a monopole with an N=2, the reduction factor, again, can be reduced to less than 0.6. The low resonant resistance value can be matched to a conventional transmission line with a sleeve, without significant loss in efficiency.
This, of course represents a more viable solution, if the goal is to reduce the size of a monopole to roughly half its size.

4.2.4   CURRENT DISTRIBUTION

The current distribution of a meander-monopole with N=2 was obtained, as well as that of a conventional monopole. Figure 4.4 shows both current distributions. The sample monopoles had their length of 13.5 cm. divided into 38 segments, were mounted on a perfectly conducting infinite ground plane and were fed at the base by a one-volt source.

The curves show the current magnitude and phase variation versus segment number, with the voltage source being connected to segment number 1.

Note that in general, the current values for the meander monopole are greater, reflecting the lower input resistance. Also, the meander monopole has its maximum current magnitude shifted from the excitation point, unlike the case of a conventional monopole. Otherwise, the distribution follows the decreasing pattern of the conventional monopole, with the current at the end of the wire being equal to zero.

The phase in the current distribution curve for a meander monopole is seen to be relatively constant, having a variation not exceeding 2 degrees through the length of the antenna.
This contrasts with the conventional monopole that has a constantly decreasing phase. However, the overall phase variation through the length of the wire seems to be too small to be considered signi-ficant.
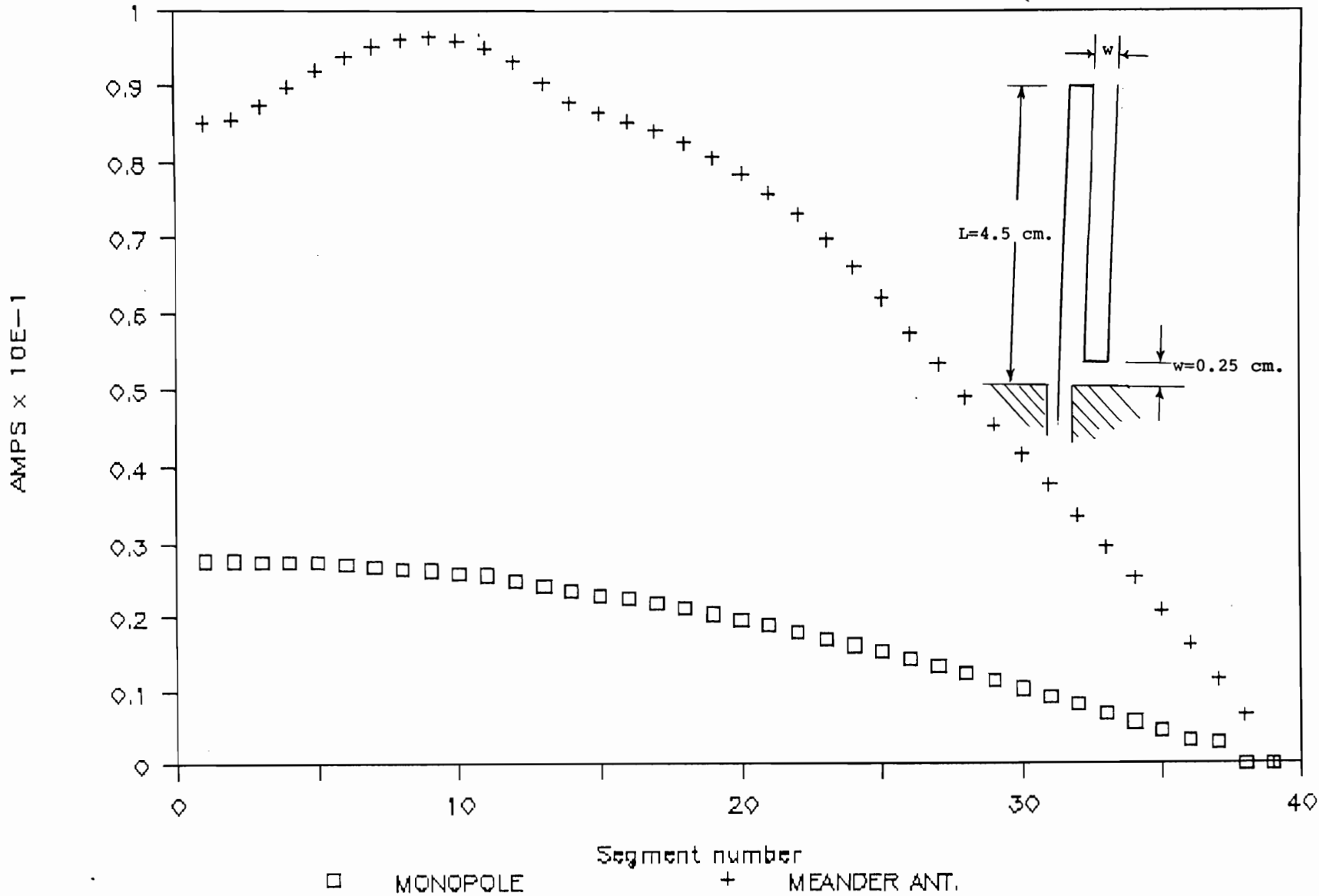
FIGURE 4.4(a): CURRENT DISTRIBUTION (MAGNITUDE)
MEANDER AND CONVENTIONAL MONOPOLE.
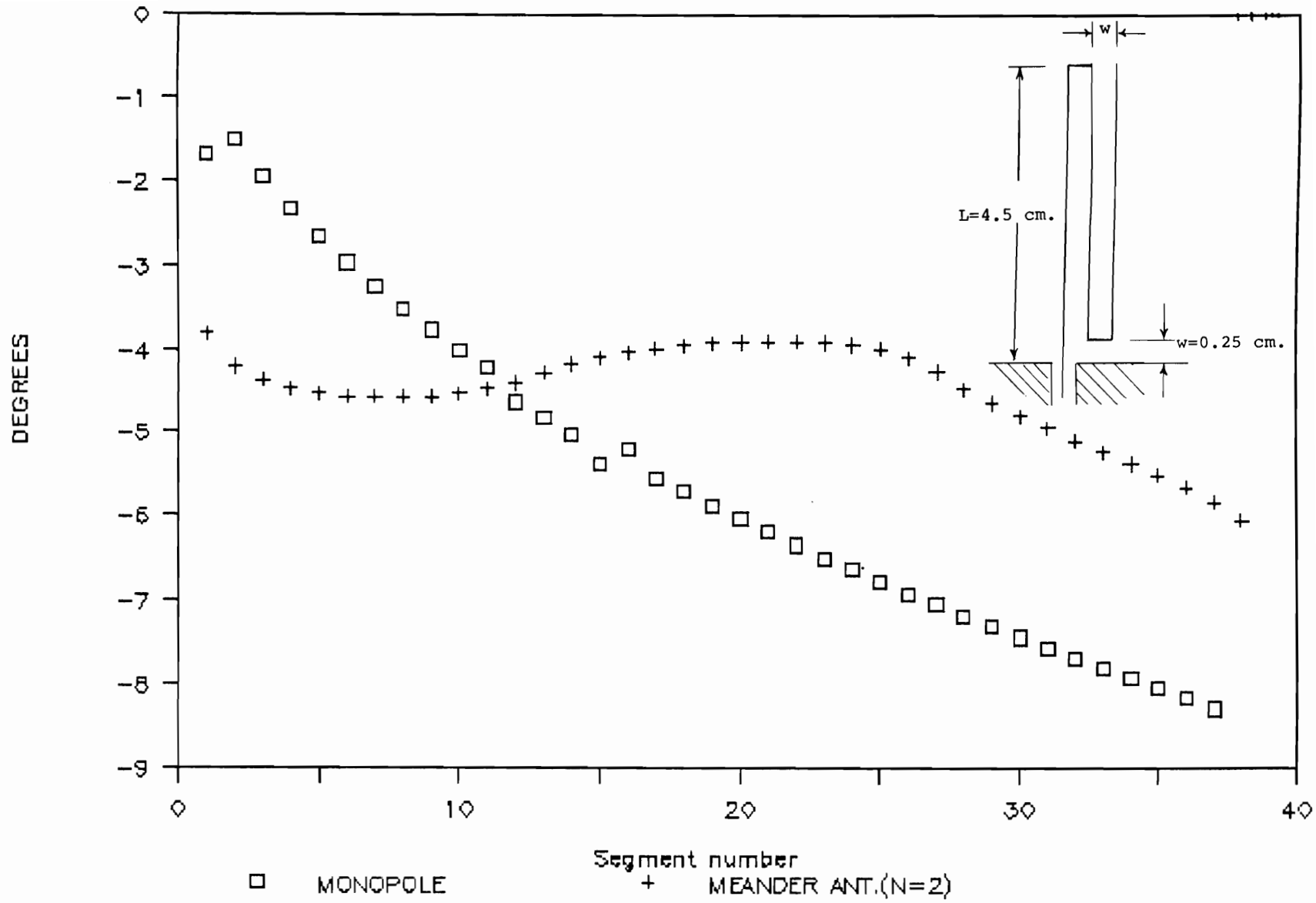
FIGURE 4.4(b): CURRENT DISTRIBUTION (PHASE)
MEANDER AND CONVENTIONAL MONOPOLE.

It is generally assumed that the current distribution of an infinitesimally thin antenna (length-to-radius equals infinity) is sinusoidal, and that the phase is constant over a half-wavelength interval, changing abruptly by 180 degrees between these intervals.

In the magnitude curve for the monopole, we can clearly see this trend, although only a quarter of the sinusoidal cycle can be seen, due to the antenna length. The phase for both the meander antenna and the monopole are almost constant, varying only a few degrees in both cases, reflecting the finite-diameter condition of the wires. The effect of finite-diameter wire and the ratio diameter-to-antenna length is discussed in more detail in the following section.

4.3   CYLINDRICAL ANTENNAS AND THE DIPOLE.

4.3.1   CYLINDICAL ANTENNAS:

The concept of cylindrical antennas is not opposed to that of thin-wire antennas. Rather, it is a name given generally to wire monopoles or dipoles that have a length-to-wire radius ratio that is a finite quantity. A special case, of course is when the antenna is made of hollow pipe. The name "cylindrical" is used to reflect the fact that most theoretical work on dipoles is based on the assumption that the wire radius is very (infinetesimally) small compared to the antenna length. This assumption, although useful, is not accurate for real-life models, Wire antennas having a finite length-to-diameter ratio have characteristics varying from the theoretical model, in accordance to the diameter of the conductor they are made of.

The impedance characteristics of cylindrical dipoles have been ex-tensively investigated [5] [6] [7]. Theoretical work has mainly been confined to thin antennas, with length-to-diameter ratio greater than 15. In most cases, the effect of the junction connecting the radiating elements and the transmission line is usually not consi-dered. Among various theories, the induced-emf method of computing the impedance of a cylindrical antenna based upon a sinusoidal current distribution is still found to be very useful. The formula derived from this method is extremely simple. It is, however, valid only when the half length of a center driven antenna is not much longer than a quarter wavelength. In practice, this is the most use-ful range.

To elliminate unnecessary computations, the formula has been reduced to the following form:

$$Z_1 = R(kl) - j[120(\ln\frac{l}{a} - 1)\cot kl - X(kl)] \qquad (4.1)$$

where:

      Z1 = input impedance of a center-driven cylindrical antenna of total length 2l and radius a.

      kl = 2π (1/λ) ; electrical length, corresponding to 1, measured in radians.

The functions R(kl) and X(kl) are shown in table 4.4 below, for the range kl< π/2

TABLE 4.4: FUNCTIONS R(kl) AND X(kl) CONTAINED IN THE FORMULA OF A CENTER DRIVEN DIPOLE [6]

kl	R(kl)	X(kl)	kl	R(kl)	X(kl)
0	0	0	0.9	18.16	15.01
0.1	0.1506	1.010	1.0	23.07	17.59
0.2	0.7980	2.302	1.1	28.83	20.54
0.3	1.821	3.818	1.2	35.60	23.93
0.4	3.264	5.584	1.3	43.55	27.88
0.5	5.171	7.141	1.4	52.92	32.20
0.6	7.563	8.829	1.5	64.01	38.00
0.7	10.48	10.63	π / 2	73.12	42.46
0.8	13.99	12.73			

Note that for a kl equal to half wavelength, the impedance obtained
is the known value for a half-wave dipole.
For antennas of half-length grater than half-wavelength, a number
of refined theories provide formulas for the computation of the
impedance function.
It should be emphasized that that all these theories are formulated
by using an idealized model in which the terminal conditions are
not considered.

PRACTICAL EFFECT OF TERMINAL CONDITIONS

In practice, the antenna is always fed by a transmission line.
The effective terminal impedance of the line (often referred to
as the antenna impedance) then depends not only upon the length and
the diameter of the antennas, but also upon the terminal conditions.

In the typical case of a monopole on conducting ground, the impe-
dance would also be a function of the size of the ground plane.

For a given terminal condition, the variation of the impedance of
a cylindrical antenna as a function of the length and the diameter
of the antenna is best shown in the work of Brown and Woodward.(6)
The data cover a wide range of values of the length-to-diameter
ratio. Two useful sets of curves are reproduced in figures 4.5 (a)
and (b).
The impedance refers to a cylindrical monopole driven at the base
by a coaxial line though a large circular ground plane placed in
the surface of the earth.
The arrangement is similar to that of the small quarter-wave mono-
poles mounted in the metallic roof of police-cars and ambulances.

In the figures, the length and the diameter of the antenna are
measured in degrees, i.e. a length of one wavelength is equivalent
to 360 degrees. If the effects due to the terminal condition and
finite-size ground plane are neglected, the impedance would corres-
pond to one-half of the impedance of a center-driven antenna.

In using these data for design purposes, one must take into consi-
deration the actual terminal conditions as compared to the condition
specified by these two authors.

In general, MININEC will yield curves similar to the ones shown
for values of length-to-diameter ratio relatively high. Ratios
greater than 50, in particular, seem to satisfy the MININEC basic
principle that the diameter be very small compared to the wavelength
of the antenna.

The curves of Figures 3.3 and 3.4 were obtained for a length-to-
diameter ratio of about 100, using MININEC, and were used as a
preliminary validation of the program for a simple monopole geometry.
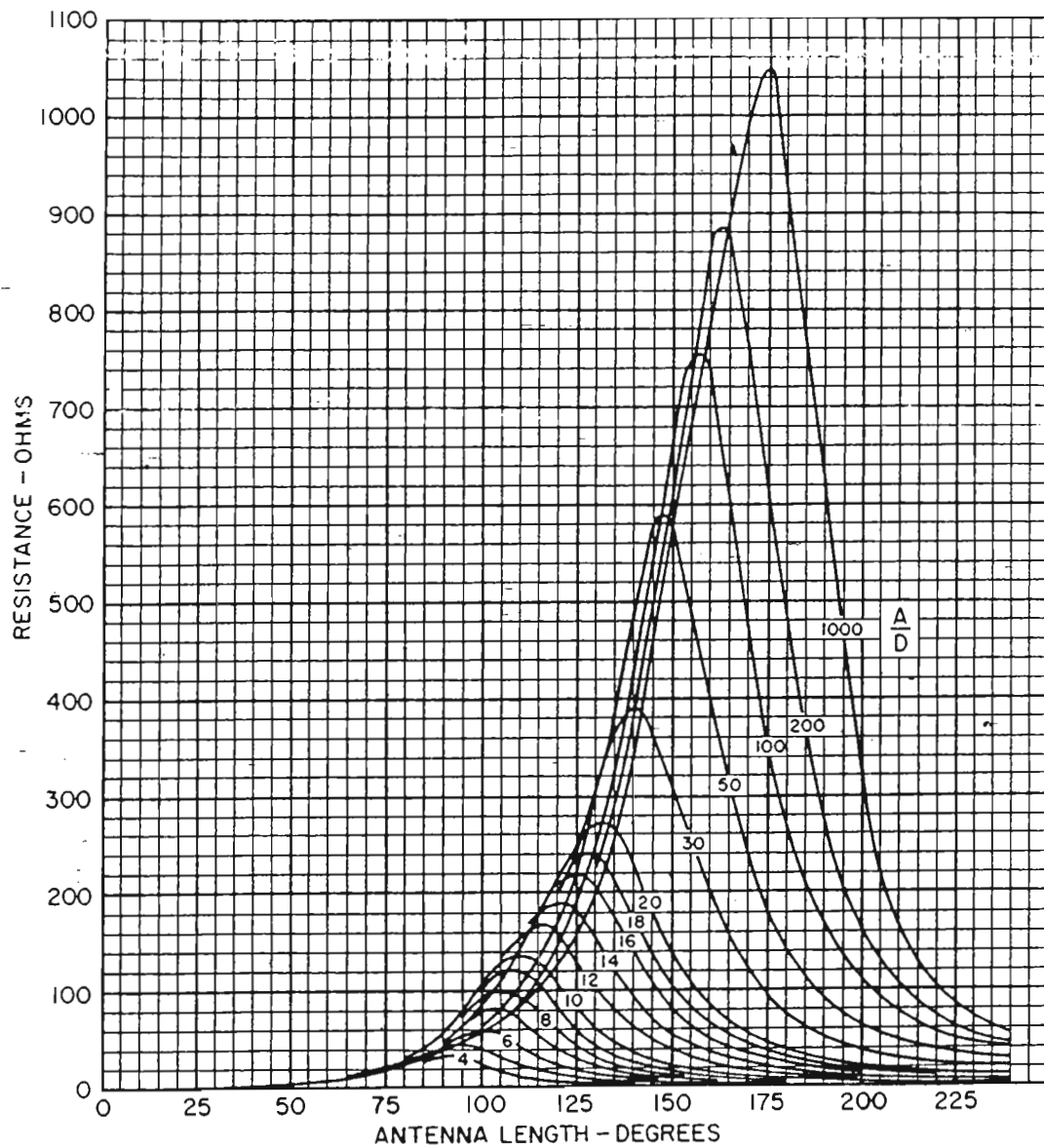
FIGURE 4.5(a) : INPUT RESISTANCE OF MONOPOLE OVER CONDUCTING
GROUND, FOR DIFFERENT DIAMETER TO LENGTH RATIOS (A/D)
VERSUS ELECTRICAL LENGTH. [9]
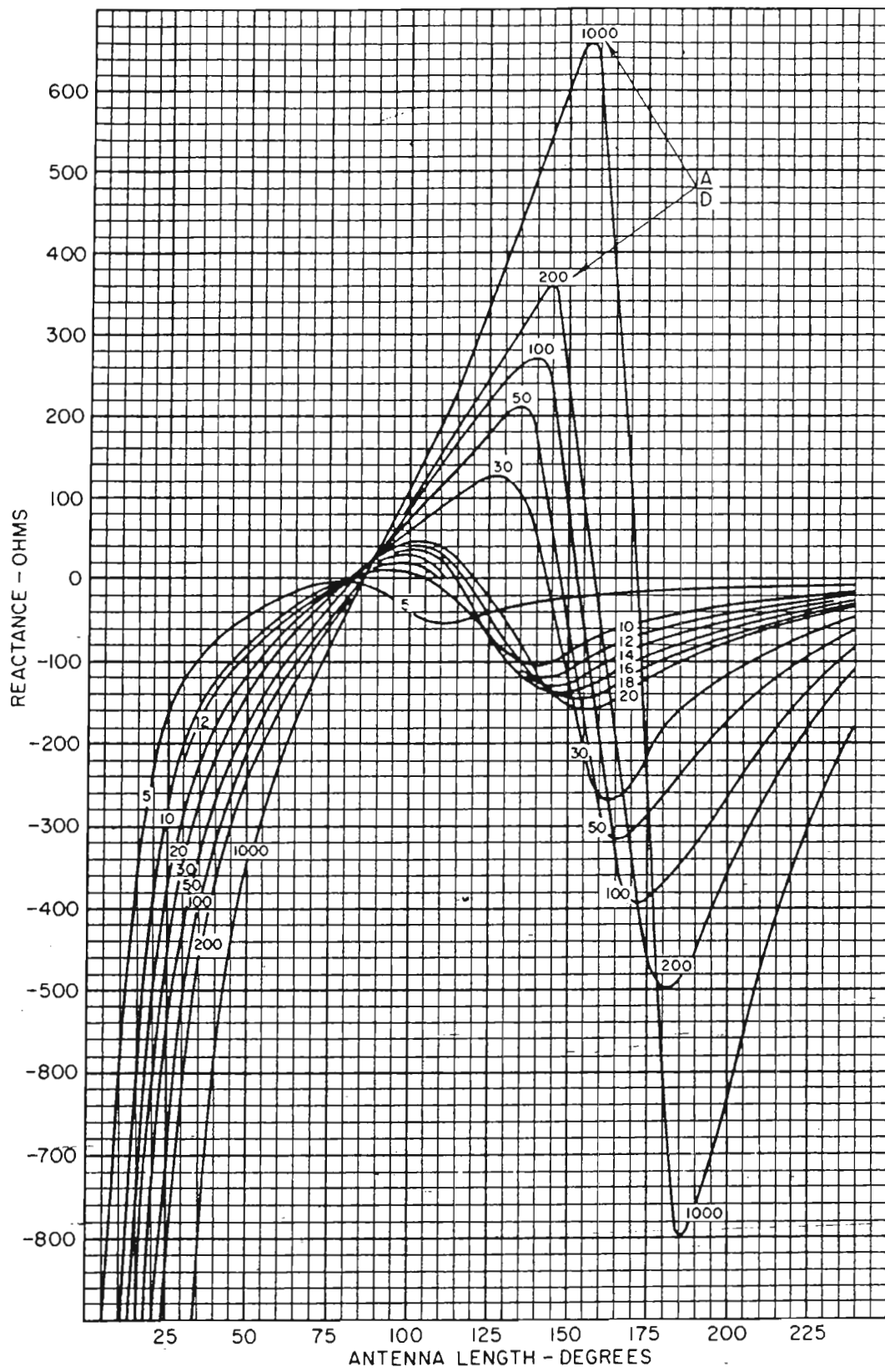
FIGURE 4.5(b) : INPUT REACTANCE OF MONOPOLE OVER CONDUCTING GROUND
FOR DIFFERENT DIAMETER TO LENGTH RATIOS (A/D)
VERSUS ELECTRICAL LENGTH [9]

40

4.3.2 THE DIPOLE:

The dipole antena is one of the simplest and most
extensively used antennas. There exists enough literature explaining
the theoretical aspects of dipole antennas, to try to cover them
here. However, it is important to mention some practical conside-
rations of dipole antennas that have direct relation to the design
at hand.

LENGTH OF A RESONANT DIPOLE ANTENNA

The resonant length of a dipole antenna at a given
frequency is defined as the length at which the impedance of the
antenna is purely resistive. This is analogous to a tuned circuit;
at the resonant frequency the input impedance of the circuit is a
resistance. Unlike the case of an open-circuited transmission line
the resonant lengths of a dipole antenna do not occur at at exact
multiples of a half-wavelength. For example, a dipole of exactly
a half-wavelength long has an input impedance of: [5]

$$Z_{in} = R_{in} + j\, X_{in} = 73 + j\, 42.5 \quad \text{Ohms.} \tag{4.2}$$

Practically, if we reduce the length slightly, the half-wave dipole
can be made to resonate with Xin=0. The amount of shortening required
to achieve this depends on the diameter of the antenna. As the
antenna becomes thinner the shortening factor tends to one, that is,
no change in length is required. For a typical dipole having a wire
radius-to-length ratio of about 100, the shortening factor is close
to 0.96. This means that the real resonant length for this case,
would be 0.96 of a half-wavelength. [5]

It should be noted that, as the length is reduced to achieve reso-
nance, the input resistance also decreases.
For practical purposes, however, a factor of 0.96 to 0.98 can be
used for most thin wire dipoles. The input resistance will be in
the order of 60 to 65 Ohms.

Figure 4.6 shows the factor by which the length of the dipole in
free space should be multiplied to to obtain the physical length of
a half-wave dipole, as a function of the ratio of half-wavelength to
conductor diameter.
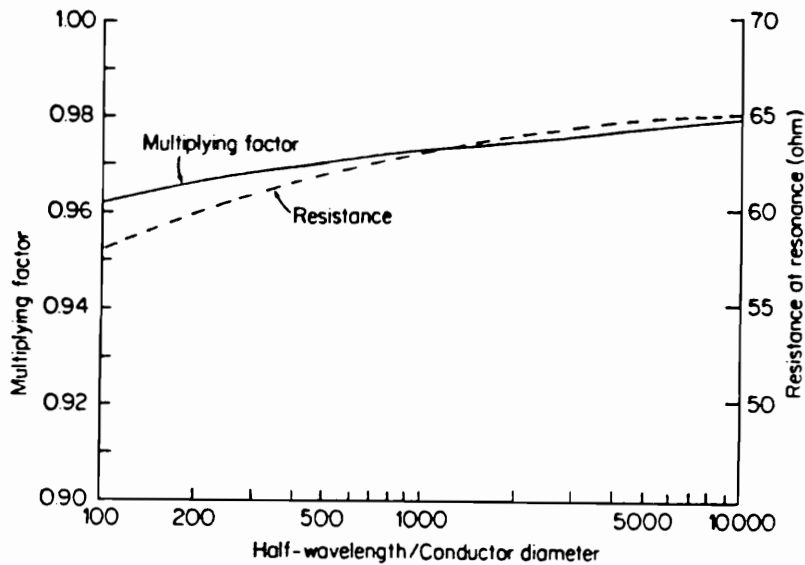
FIGURE 4.6: RESONANT RESISTANCE OF HALF-WAVELENGTH DIPOLE AND LENGTH FACTOR VERSUS HALF-WAVELENGTH TO WIRE-DIAMETER RATIO [10]

BANDWIDTH OF A DIPOLE:

The IEEE Standard Dictionary of Electrical and Electronic terms defines the bandwidth of an antenna as "the range of frequencies within which the performance of the antenna, with respect to some characteristics, conforms to a specified standard."[9] The characteristics referred to can be pattern or impedance. For the latter, which is usually more sensitive to frequency, a useful standard is that the voltage standing wave ratio be less than 2.0. If the antenna impedance is Za and the characteristic impedance of the transmission line feeding the antenna is Zo then the voltage reflection coefficient p is:

$$p = (Za - Zo) / (Za + Zo) \qquad (4.3)$$

The VSWR is related to p by:

$$VSWR = S = (1 + |p|) / (1 - |p|) \qquad (4.4)$$

From transmission line theory, the percentage of reflected power is equal to :

$$P. \text{ reflected} = |p| * |p| * 100 \qquad (4.5)$$

And the percentage of transmitted power is equal to:

$$P. \text{ xmitted} = (1 - |p| * |p|) * 100 \qquad (4.6)$$

A VSWR of 2.0 corresponds therefore to a reflected power of 11.1 %

Consider a dipole antenna of resonant length connected to a trans-
mission line that has a characteristic impedance equal to the input
impedance of the antenna at resonant frequency. The resistance change
in the region around resonance is relatively small compared to the
change around in reactance. Consequently, the principal cause of the
antenna change in VSWR is the reactive component of the antenna
impedance when the frequency is varied. An antenna that has a relati-
vely slow rate of change in diameter will therefore have a wider
bandwidth. Figure 3.5 (b) shows that an antenna with a larger dia-
meter-to-length ratio will have a wider bandwidth compared to an
antenna with a smaller diameter-to-length ratio.

The following figure shows the Voltage Standing Wave Ratio (VSWR)
as a function of frequency on a 72 ohm transmission line feeding
two dipoles of length 0.5 meter having two values of wire radius a.

Note that for the dipole of radius a= 0.005 m. the resonant frequency
is 285 MHz and the bandwidth is about 16%.
For the thinner dipole with radius a= 0.0001, the resonant frequency
is 294 MHz and the bandwidth is about 8%
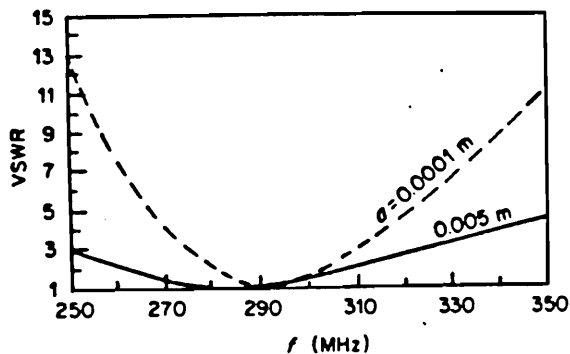
FIGURE 4.7   :   VSWR versus frequency on a 72 ohm transmission line
                 feeding two dipoles of 0.5 m. length having two
                 values of wire radius a. [9]

4.4 THE FOLDED DIPOLE:

4.4.1 THEORETICAL ANALYSIS:

This section will describe the theoretical principles underlying the characteristics of a folded dipole. The theoretical analysis is important in understanding some of the features of our final design.

A folded dipole is formed by joining two cylindrical dipoles at the ends and driving them by a pair of transmission lines at the center of one arm as shown in figure 4.8. The diameters of the two arms can be either identical or different. A simple analysis based upon a quasi static approach of the operation of a folded dipole has been given by Uda and Mushiake [8].
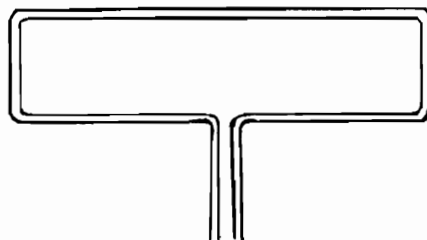
FIGURE 4.8   Folded Dipole.

According to their method, the excitation of a folded dipole can be considred as as a superposition of of two modes of operation, as shown in figure 4.9. As can be seen, there is a symmetrical mode, characterized by two equal driving voltages, and an asymmetrical mode, characterized by equal and opposite currents on the the two arms of the folded dipole.

The impedance of the symmetrical mode can be calculated by making use of the equivalent radius of two conductors.

As far as the impedance characteristics and radiation pattern are concerned, a thin cylindrical antenna with a non-circular cross-section behaves like a circular cylindrical antenna with an

44

$$V_1 = (1+a)\,V$$

$$I_i = I_r + I_f$$

$$Z_i = \frac{(1+a)\,V}{I_r + I_f}$$
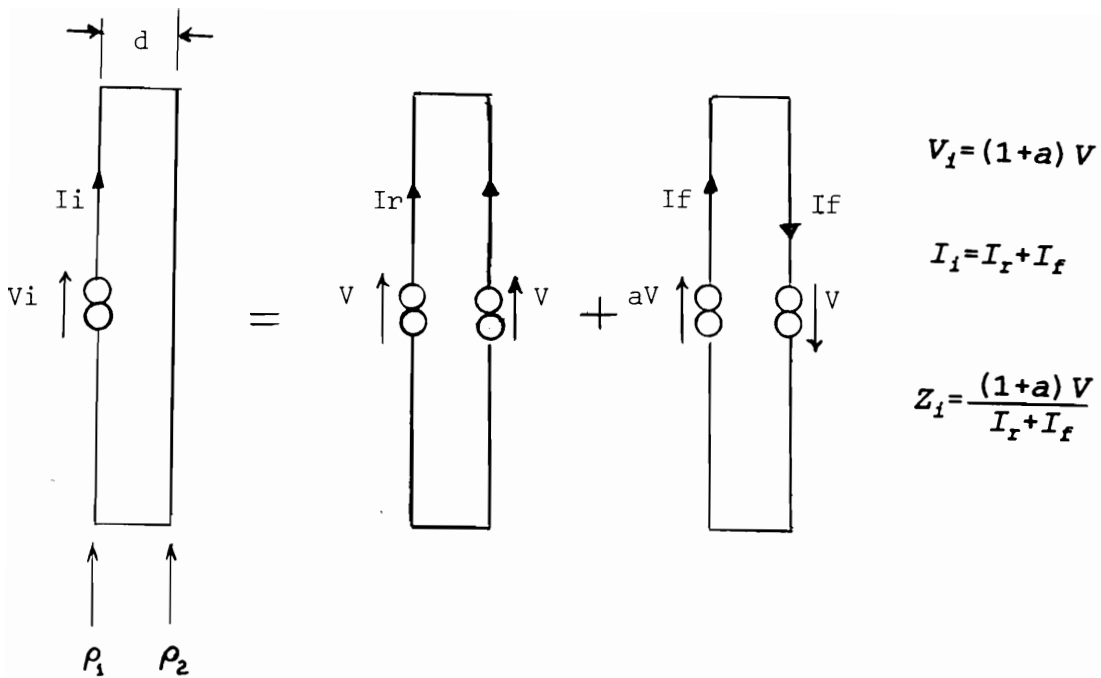
a) Decomposition of the folded dipole into two fundamental modes.
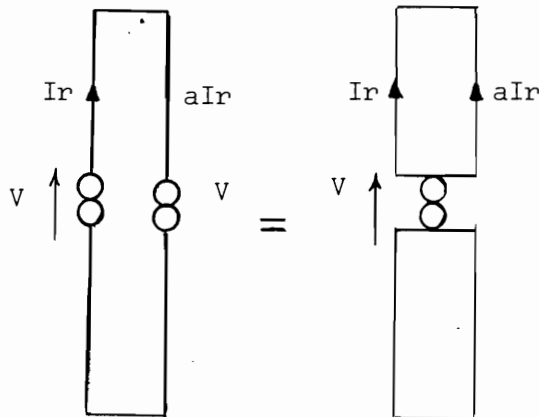
b) Equivalent representation of the symmerical mode in computing Zr.

FIGURE 4.9: EQUIVALENT REPRESENTATION OF THE FOLDED DIPOLE [6]

equivalent radius. In stating this characteristics, the terminal effect, is of course, not considered. The equivalent radius of many simply shaped cross sections can be found by the method of conformal mapping [9]. For an elliptical cross-section the following simple relation exists :

$$Aeq = 1/2 \ (a + b) \qquad\qquad (4.7)$$

where: a = major axis of ellipse.
        b = minor axis of ellipse.

For a rectangular cross section, the result is plotted in figure 4.10
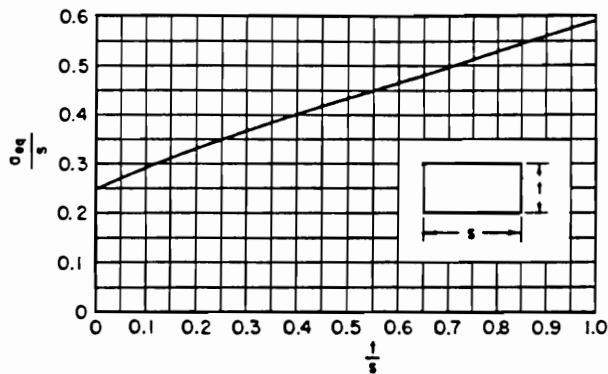
FIGURE 4.10: EQUIVALENT RADIUS OF A RECTANGLE AS A FUNCTION OF THE RATIO OF THICKNESS t TO WIDTH S [6]

The equivalent radius of parallel cylinders of radius ρ_1, ρ_2 and separated by a distance d between the centers is given by:

$$\ln\rho_e = \frac{1}{(\rho_1 + \rho_2)^2} \ (\rho_1^2 \ln_1 + \rho_2^2 \ln\rho_2 + 2\rho_1\rho_2 \ln d) \qquad\qquad (4.8)$$

This of course, represents the case of a folded dipole, where the radii of the two conductors composing the arms of the dipole are both finite quantities.

46

The symmetrical component of a folded dipole, can therefore be represented by a cylindical dipole (see fig. 4.9 - b) with an equivalent radius ρ_e given by:

$$\ln\rho_e = \ln\rho_1 + \frac{1}{(1+\mu)^2} (\mu^2\ln\mu + 2\mu\ln\nu)$$

(4.9)

where the parameters are:

$$a = \frac{\cosh^{-1}\dfrac{\gamma^2 - \mu^2 + 1}{2\gamma}}{\cosh^{-1}\dfrac{\gamma^2 + \mu^2 - 1}{2\gamma\mu}}$$

(4.10)

$$\mu = \rho_2/\rho_1$$

(4.11)

$$\gamma = d/\rho_1$$

(4.12)

The impedance of the asymmetrical mode, characterized by equal and opposite currents on the two arms is the same as the shorted section of a transmission line of length equal to 1; that is:

$$Z_f = \frac{(1+a)}{2I_f} = jZ_o\tan kl$$

(4.13)

where Zo is the characteristic impedance of the two-wire line. Expressed in terms of Zr and Zf, the impedance of a folded dipole is given by:

$$Z = \frac{V_i}{I_i} = \frac{(1+a)V}{I_r + I_f} = \frac{2(1+a)^2 Z_r Z_f}{(1+a)^2 Z_r + 2Z_f}$$

(4.14)

An equivalent circuit of a folded dipole, based upon the previous formula is shown in figure 4.11.

$2Z_r$ $(1 + a):1$ Z_r
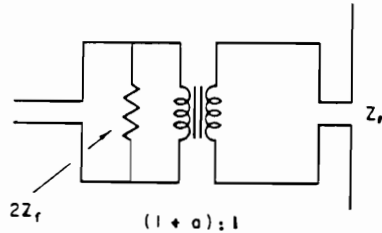
FIGURE 4.11: EQUIVALENT CIRCUIT OF A FOLDED DIPOLE [6]

4.4.2 IMPEDANCE TRANSFORMATION AS A FUNCTION OF CONDUCTOR SIZES:

The step-up impedance ratio shown in figure 4.11 as a function of μ and γ has been calculated, by using the formula for the parameter a, given in the previous section. (4.10)
When ρ_1 and ρ_2 are small compared with d, the wire separation, the value of a is given to a good approximation by:

$$a = \ln (d/\rho_1) / \ln (d/\rho_2) \qquad (4.15)$$

The step-up transformation ratio is an important property of folded dipoles, and in fact is what makes this antenna atractive : the possibility of obtaining almost any desired impedance, by a careful choise of the wire radii and the separation d betw en the arms.

The formulas described in this section have been tabulated for use by antenna designers. Figures 4.12 and 4,13 give two representations of the transformation ratio $(1 + a)^2$ in a logarithmic scale as a function of the ratio between wire radii. Note that in figure 4.12 for identical wire radius on both arms, the step-up ratio is 4.0 for all wire separations. This reflects the known value of a folded dipole: 300 ohms or about four times the impedance of an open dipole.

48
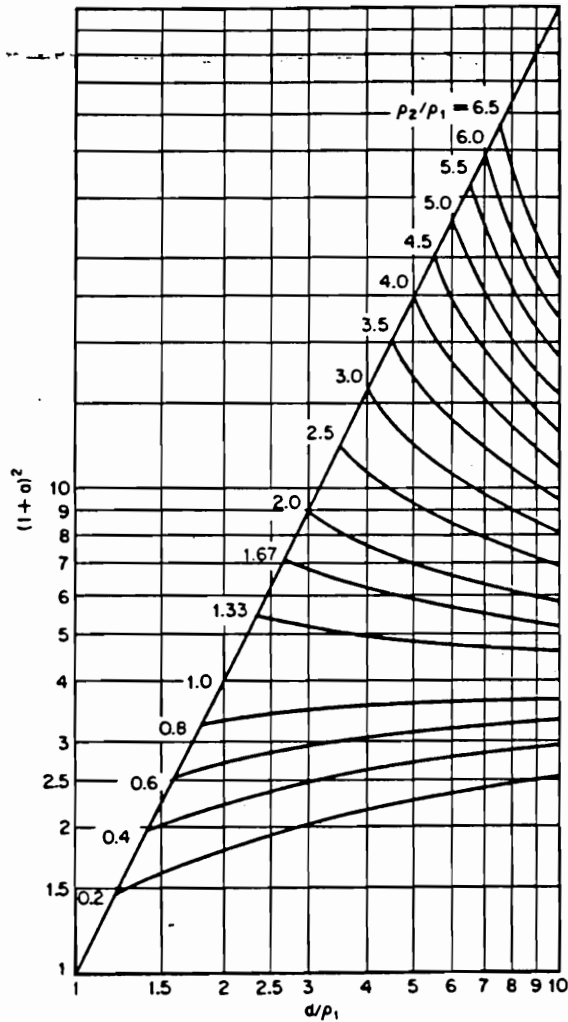
FIGURE 4.13: IMPEDANCE TRANSFORMATION RATIO VERSUS DIAMETER RATIO
            AND d/ρ_1 . [6]
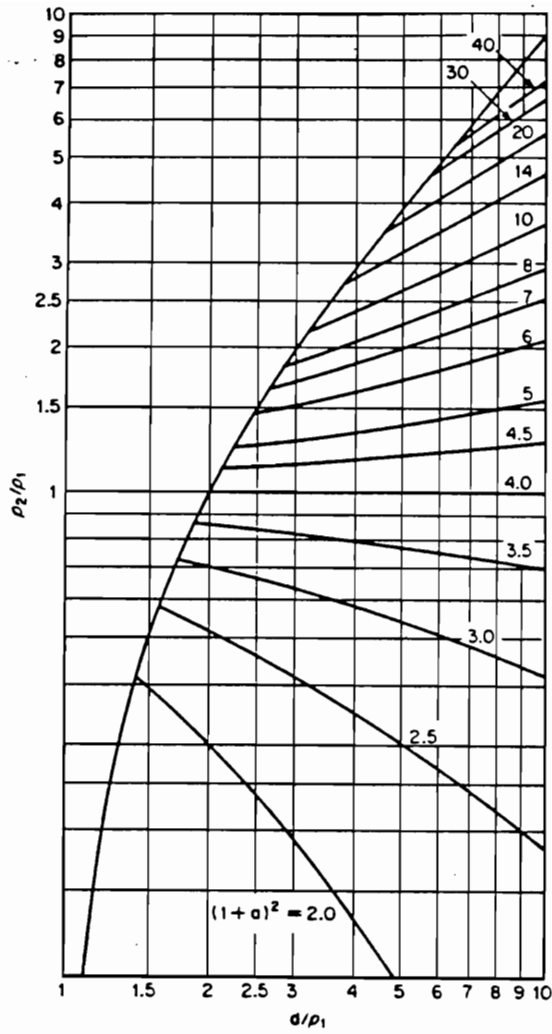
FIGURE 4.12: DIAMETER RATIO VERSUS IMPEDANCE TRANSFORMATION RATIO
AND d/ρ_1 . [6]

A step-up ratio of 4.0 means that the antenna will have four times the impedance of an open half-wavelength dipole. We know this resistance to be about 72 ohms at resonance. Therefore, our folded dipole, constructed of two arms of similar diameter, should have a resonant resistance of 4 * 72 = 288 ohms. As will be seen in the next section, this theoretical value is obtained with MININEC for all values of the wire separation d.

In practical thin-wire antenna geometries, the separation d between the conductors will be much larger than the wire diameter. The curves of figs. 4.12 and 4.13 are useful for design of thin wire folded dipoles for a relatively large radius/separation ratio. In effect, only for ratios close to the maximum absissa value of 10.0, would these curves be useful.

In general, figures 4.12 and 4.13 show that folded dipoles give the designer a great flexibility, since almost any desired value of impedance can be obtained, from a few ohms to several thousand ohms, with adequate choise of wire radii and separation.

4.4.3 MODELLING A FOLDED DIPOLE WITH MININEC

It was necessary to model a conventional folded monopole using MININEC, to ascertain the validity of the program for this particular antenna. The data obtained was then compared to the theoretical model described in the previous section. This was considered as a requirement prior to the development of a valid model for the reduced-size folded dipole of chapter 5.0.

Specifically, the resonant resistance, bandwidth and radiation pattern of a folded dipole were obtained with MININEC. Then, the most important feature of the impedance step-up ratio was analysed as obtained with the program.

First, the folded dipole of figure 4.14 was analysed. The wire separation is 1.0 cm. and the wire radius (equal for both arms) was 0.1 cm.
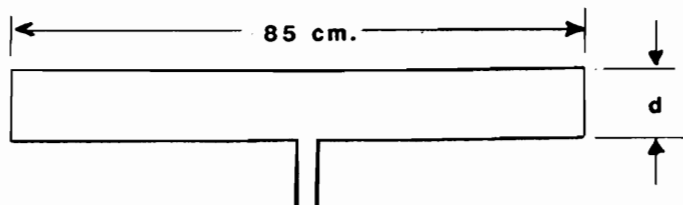
FIGURE 4.14: GEOMETRY OF FOLDED DIPOLE.

The segmentation density was chosen to be 34 segments. This segmentation meets the criteria for segment length described in chapter 3.0 and provides adequate accuracy of the results.
The radiation resistance was found to be exactly 288.3 ohms for a resonant resistance of 170.2 MHz. This correlates very well with the theoretical resistance presented in the previous section.

EFFECT OF WIRE SEPARATION IN RADIATION RESISTANCE:

The separation of the two arms was changed for three cases. The results are shown in table 4.5 below.

TABLE 4.5: EFFECT OF WIRE SEPARATION ON FOLDED DIPOLE RESONANT RESISTANCE.

d (cm.)	Resonant Res. (Ohms)	Fo (MHz)
1.0	288.3	170.2
3.0	288.5	166.5
6.0	287.8	160.1

The radiation resistance remains practically the same as the wire separation d is increased. This confirms the theoretical behaviour of folded dipoles.

On the other hand, it can be seen that the resonant frequency decreases as the wire separation is increased. In general, it can be said that for values of d that are very small compared to half the wavelength, the resonant frequency is that of a half-wavelength dipole. It has already been shown in previous sections, how the resonant length of a dipole is somewhat shorter than half wavelength by a typical factor of 2 to 10%. For the case where the folded dipole of length 85 cm. has a wire separation d = 1.0 cm. the resonant length is about 0.97 times the half-wavelength.
For the case where d = 6.0 cm. the resonant length is almost 0.90 times half the wavelength. That is 10% shorter than half-wavelength.

The fact that an increase in wire separation changes the resonant frequency, is of course to be expected. When d is changed, so is the total length of the wire composing the antenna. The overall geometry is changed, and the distribution of electric and magnetic fields are also changed.

EFFECT OF WIRE SEPARATION IN ANTENNA BANDWIDTH

For the three values of d described previously, a frequency sweep was done with MININEC, and a set of impedances was obtained in each case.

In order to determine the antenna bandwidth, a method similar to the one employed for meander antennas in section 4.2 was used. The impedances were now normalized to a transmission-line value of 300 ohms. This was chosen since the 300 ohm parallel-wire line is a common, commercially available transmission line, that is the most often-used means of feeding folded dipole receiving antennas.

The normalized impedances were entered in a Smith-Chart and a VSWR circle of 2.0 was used to determine the bandwidth.

The results are shown in the following table:

TABLE 4.6: BANDWIDTH OF A FOLDED DIPOLE AS WIRE SEPARATION d IS INCREASED

d (cm.)	Fo (MHz.)	Bandwidth (MHz)	Bandwidth (% of Fo)
1.0	170.2	12.0	7.0
3.0	166.5	19.0	11.0
6.0	160.1	28.0	18.0

As the results show, the bandwidth is increased as the wire separation is increased. In this case, our study was concentrated on cases where the separation d is less than one-tenth of the length of the dipole. This is generally the case for folded dipoles, as it is desirable for structural reasons when the antenna is composed of a folded wire.

The impedance values obtained with MININEC, for folded dipoles
with d = 1.0 and d = 6.0 cm. are shown in tables 4.7 and 4.8.
These correspond to the Smith-charts of figures 4.15 and 4.16.

Note that the impedance behaves very much like that of a conven-
tinal dipole: it is capacitive for frequencies below resonance,
and becomes inductive past resonance.

Only the impedance obtained with MININEC is given in these tables.
It has already been said that these impedances were normalized
to 300 ohms to be entered in the Smith-Charts.
Also, note the value of the impedance near resonance at 170 MHz.

The values have been rounded to the nearest integer, for simplicity.

TABLE 4.7: IMPEDANCE OF A FOLDED DIPOLE WITH d = 1.0 cm.

Freq. (MHz)	Impedance (ohms)
150	109 - j 432
155	146 - j 360
160	190 - j 265
165	239 - j 148
168	269 - j 69
170	288.3 - j 12
172	306 + j 45
175	331 + j 136
180	362 + j 288
185	377 + j 435
190	375 + j 564
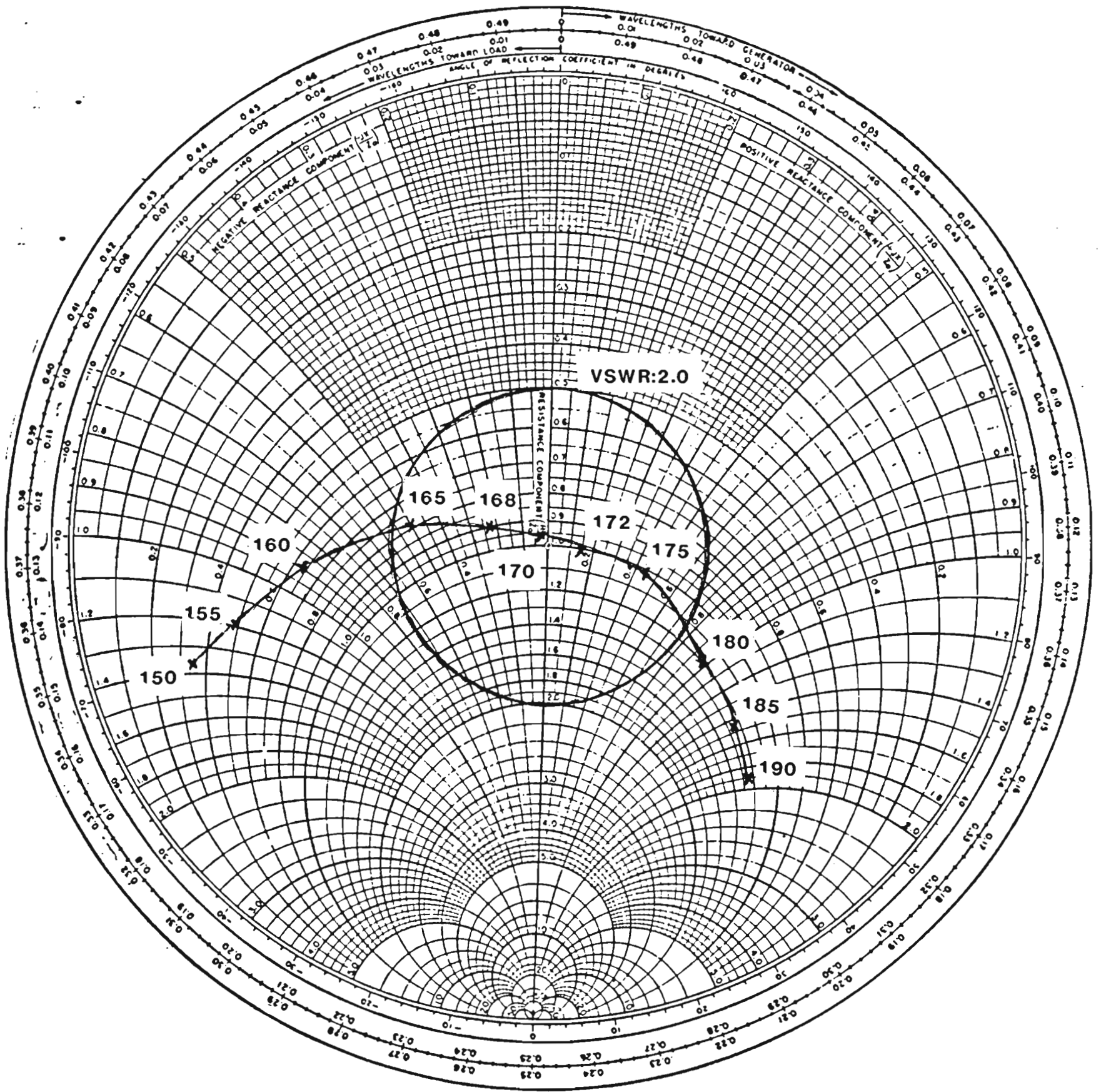
FIGURE 4.15 **IMPEDANCE OF A FOLDED DIPOLE** d: 1.0 cm.

NORMALIZED TO 300 OHMS
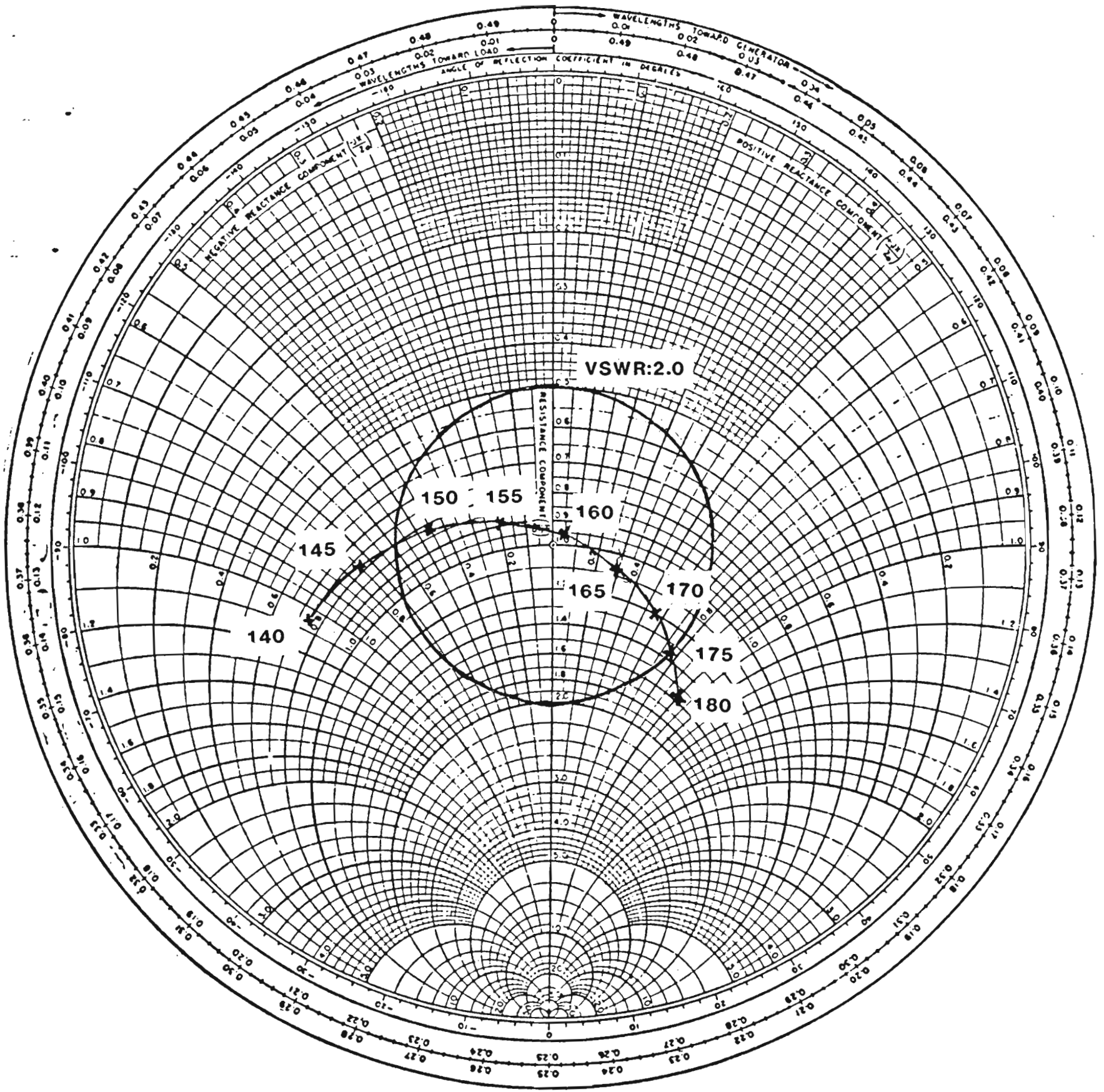
FIGURE 4.16   IMPEDANCE OF A FOLDED DIPOLE   d: 6.0 cm.

NORMALIZED TO 300 OHMS

TABLE 4.8: IMPEDANCE OF A FOLDED DIPOLE WITH d = 6.0 cm.

Freq. (MHz)	Impedance (Ohms)
140	225 - j 316
145	233 - j 221
150	246 - j 136
155	265 - j 56
160	289 + j 18
165	321 + j 91
170	361 + j 162
175	412 + j 233
180	477 + j 302

The radiation pattern of the folded dipole with d = 6.0 cm. has been plotted by MININEC. It should be explained that the antenna geometry that served as the basis for this pattern, had both arms parallel to the Z axis (vertical axis, in MININEC). The radiation pattern shown in figure 4.17 is that corresponding to the vertical pattern. Note that the gain is close to 2 dBi and that the pattern corresponds to the well-known shape for a folded dipole.

4.4.4. STEP-UP IMPEDANCE TRANSFORMATION RATIO

The problem of a stepped-up wire radius has been analysed with MININEC has been studied by the authors of MININEC (2). However, the model used was one of a single wire, with different wire radius steps. Furthermore, their model was only for an increase in wire radius with respect to the excitation point. The case of stepped-up radius in more complicated geometries was not analysed, nor was the the case of a step-down in wire radius.

Their results are quite encouraging, since MININEC follows very closely the theoretical and practical data it was compared to. The current distribution of a straight-wire antenna in free space is compared to results obtained with NEC and theoretical data .

In addition, the authors recommend that further analysis be conducted for more complex geometries, and for the case of a step-down in wire radius.

For the case of a folded monopole, it was necessary to establish the fact that MININEC would reflect the properties described in previous section, for the impedance transformation ratio.

The antenna described in figure 4.14 was modified to change the diameter of the second arm. This is the arm opposite the one that is being excited.

First, the folded dipole with d = 1.0 cm. was modified for several radius changes in the second arm, then the impedance transformation ratio was calculated and compared to that of figure 4.12.

The reason for choosing the value of d = 1.0 cm. was that the curves of figure 4.12 and 4.13 are drawn for a maximum value of d equal to ten times the radius of the excitation arm of the dipole. Our dipole of figure 4.14 has a wire radius of 0.1 cm., therefore our P_1/d ratio would be equal to 10 in this case.

The results of this analysis are shown in the table below. It can be seen that for stepped-down radius, the results differ significantly from the theoretical values of the impedance transformation ratio.

For values steps in radius greater than 3.0 the results also show a marked divergence from the reference data. The reason behind these discrepancies can probably be found in the low value of d when compared to the wire radius. In effect, the stepped-up radius (greater than 0.3 cm in the worst cases) is a significant percentage of the wire separation.

FIGURE 4.17:   VERTICAL RADIATION PATTERN
FOLDED DIPOLE
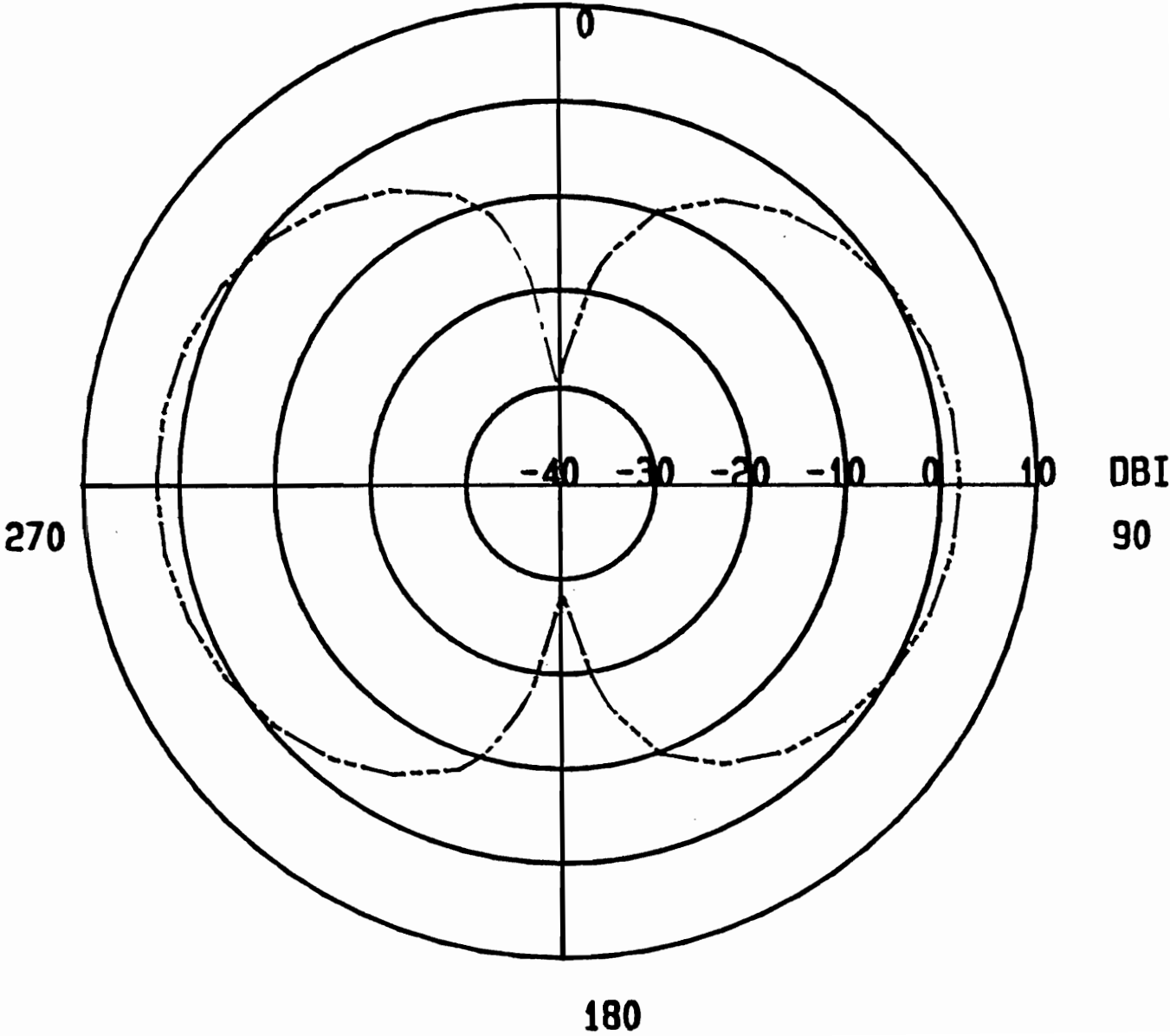
TABLE 4.9: IMPEDANCE TRANSFORMATION RATIO OF A FOLDED DIPOLE
WITH d = 1.0 cm.

ρ_2/ρ_1	Impedance (Ohms)	Fo (MHz)	$(a + 1)^2$ From [6]	$(a + 1)^2$ MININEC
0.5	565 - j 9.0	171	3.2	7.7
1.0	288 - j 9.1	170	4.0	4.0
1.5	280 - j 2.0	170	4.8	3.9
2.0	339 - j 5.6	170	5.8	4.7
2.5	482 - j 1.5	171	6.9	6.7
3.0	652 + j 3.2	173	8.2	9.0
4.0	1,864 + j 12.1	173	12.0	25.9
5.0	15,261 - j 19.0	180	16.0	212.0
6.0 and higher	error occurs	-	-	-

It is also worth noting that the resonant frequency is also changed
as the ratio of the radii is increased.
This again, is due to the fact that the antenna geometry is modified
and therefore, so is the electric and magnetic fields spacial
distribution.

The program, however, still gives acceptable values of impedance
for radii ratios of less than 3.0. The exception, of course is the
case where this ratio is 1.5. But for the rest of the values shown
in the table, below 3.0, the program still seems to follow the
theoretical data, within acceptable limits.

The next step was to try a different geometry. The obvious choise
was to increase the wire separation d. As was previously pointed
out, it was suspected that for wire radii that are comparable
in size with the wire separation d, the geometry of the antenna
seems to be excessively changed to give accurate results.

Therefore, the separation d was changed to d = 6.0 cm. and the
antenna impedance was calculated again with MININEC, for several
different radii.
The results , as shown in the following table, are far more accep-
table than the previous.

TABLE 4.10: IMPEDANCE TRANSFORMATION RATIO OF
A FOLDED DIPOLE WITH d = 6.0 cm.

P_2 / P_1	Impedance (Ohms)	Fo (MHz)	$(a + 1)^2$ From [6]	$(a + 1)^2$ MININEC
0.2	212 + $\dot{J}$ 3.4	158	3.0	2.94
0.5	241 - $\dot{J}$ 2.9	158	3.3	3.35
1.0	285 + $\dot{J}$ 5.5	159	4.0	3.96
1.5	314 + $\dot{J}$ 1.4	159	4.5	4.36
2.0	341 - $\dot{J}$ 1.4	159	4.8	4.74
2.5	367 - $\dot{J}$ 3.7	159	5.2	5.10
3.0	391 - $\dot{J}$ 5.5	159	5.6	5.43
3.5	419 + $\dot{J}$ 2.2	159.5	5.9	5.82
4.0	443 + $\dot{J}$ 1.3	159.5	6.2	6.15
5.0	490 + $\dot{J}$ 0.2	159.5	7.0	6.81
6.0	537 - $\dot{J}$ 0.1	159.5	8.1	7.46
7.0	586 + $\dot{J}$ 0.3	159.5	8.8	8.14
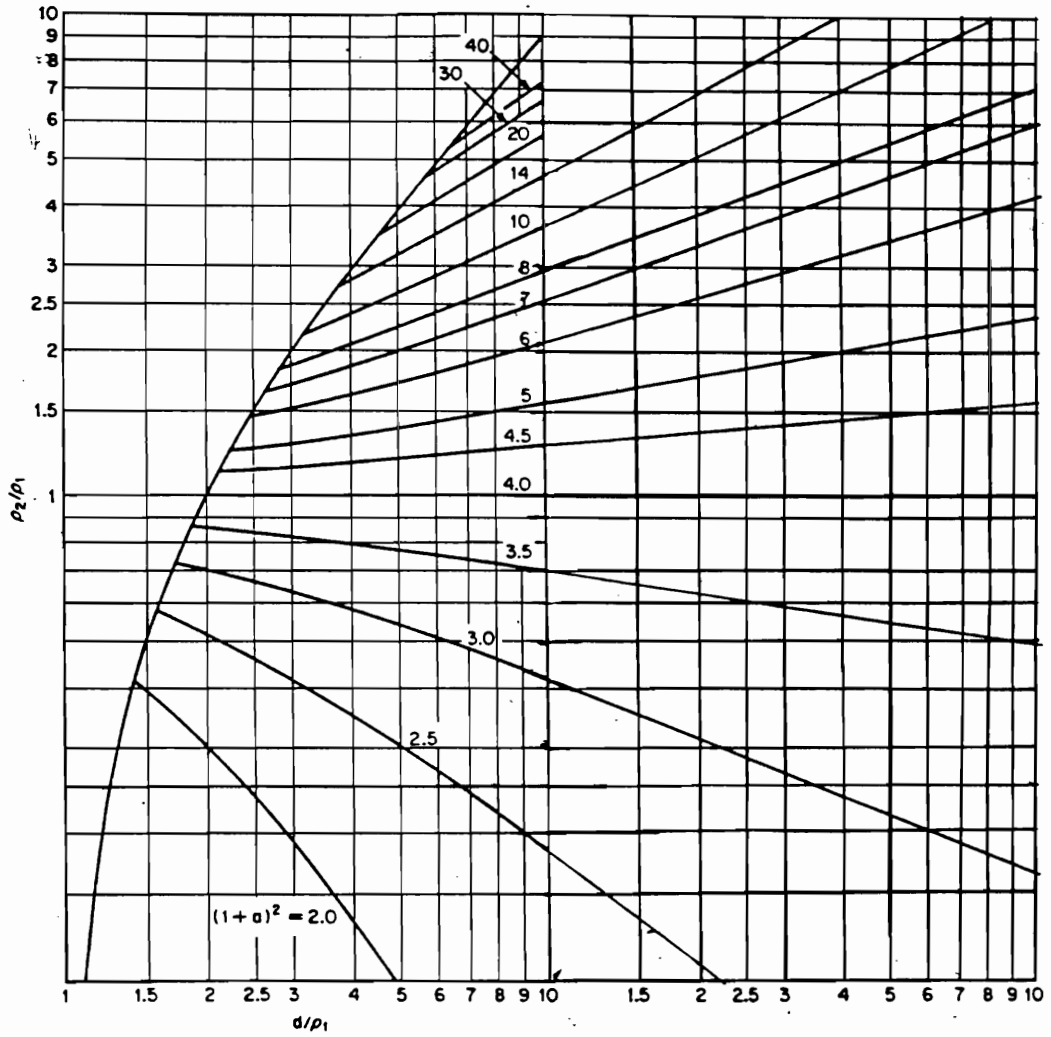
FIGURE 4.18   IMPEDANCE TRANSFORMATION RATIO

EXTRAPOLATED FROM FIGURE 4.12
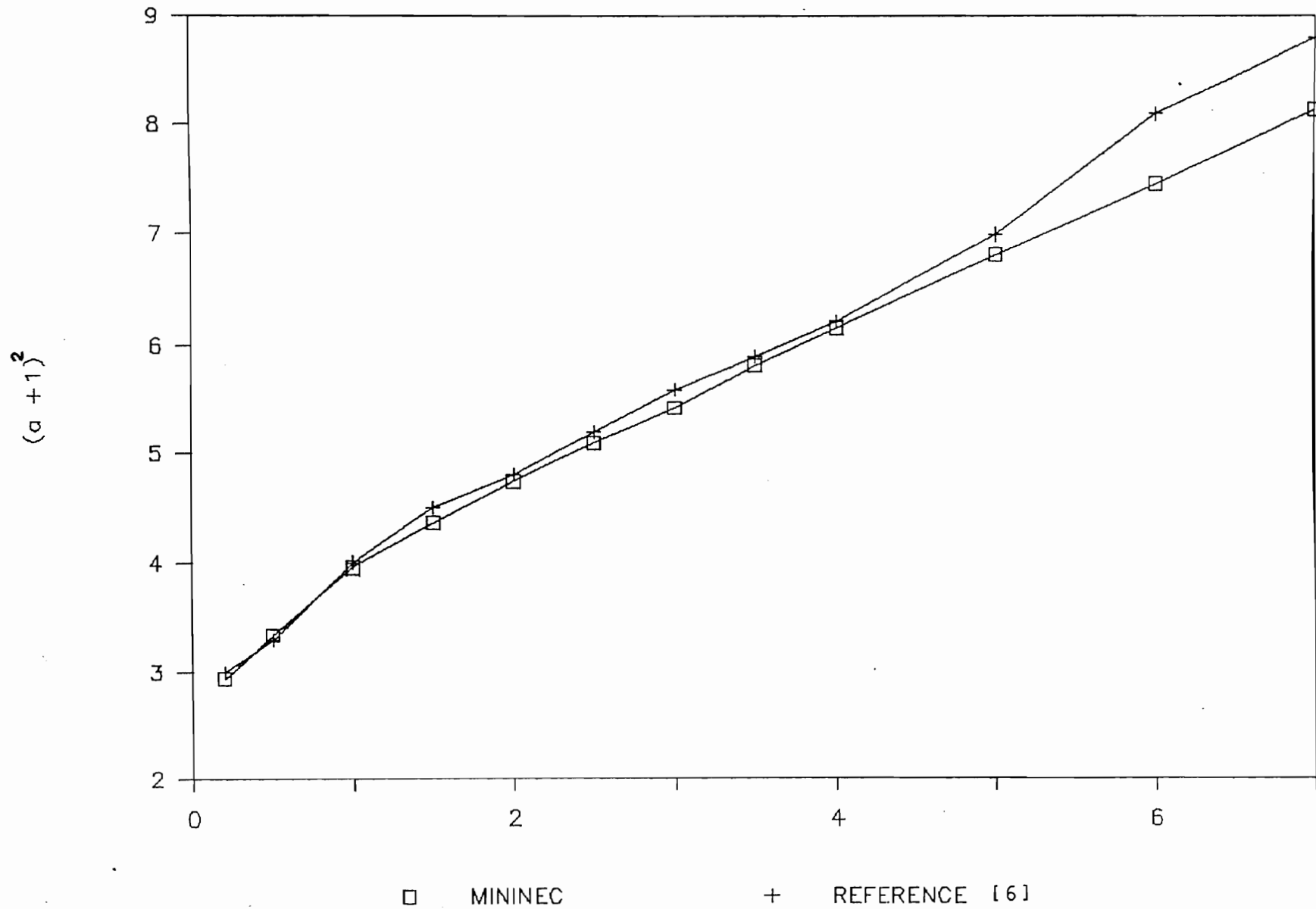
FIGURE 4.19 : IMPEDANCE TRANSFORMATION RATIO
VERSUS RADIUS STEP (FOLDED DIPOLE)

□ MININEC   + REFERENCE [6]

The reference values for the impedance transformation ratio were not readily available from the graphs of figures 4.12 and 4.13. These curves only cover a maximum d/ρ_1 ratio of 10.0. To obtain the required ratio for the antenna being analysed, that presented a wire-radius to separation ratio of 60.0, an extrapolation of the graph of figure 4.12 was done.

Basically, the logarithmic scale of the abcissa was extended, to obtain the required value of 60.0 for the radius-to-separation ratio, and the curves for each value of the impedance transformation (a + 1) were extended using straight lines. This, of course lends itself to some degree of error, but the objective of the analysis with MININEC was only to obtain some degree of confidence in modelling folded dipoles, with stepped wire radius.

The resultant set of curves is shown in figure 4.18

Also, some of the reference values are, of course approximations at best, due to the low resolution attainable with this extrapolated set of curves.

Being that as it may, the MININEC results are amazingly close to the ones used as reference. This is a big contrast with the results obtained for the folded dipole with d = 1.0 cm.

It can be seen that for almost the full range of radii steps , the impedance transformation ratio is very close to the reference value. For larger steps, greater than 5.0, the difference between MININEC and the reference seems to increase. But, in observing figure 4.18, it can be seen that the graph resolution is less for higher values of the step, due to the nature of the logarithmic scale.

The differences therefore, can be due to errors or differences in the extrapolated curves, with the practical values.

Figure 4.19 shows the two sets of values for the impedance transformation ratio. The MININEC values show some divergence from the reference values, for higher values of the abcissa.

4.4.5 FOLDED DIPOLE IMPEDANCE.

An important consideration about the folded dipole, as an antenna geometry, is that its is basically a wire-loop. In that respect, the folded dipole impedance is very much like that of a loop antenna. For very low frequencies (or as the operating frequency approaches zero, or DC) the impedance is basically a short circuit. As the frequency is increased, the loop or folded dipole behaves like one-turn coil, and the impedance becomes more inductive.

Now, we have seen in Figures 4.15 and 4.16 that the folded dipole is resonant for lengths of about half-wavelength. Furthermore, the impedance is capacitive for frequencies below resonance and becomes inductive for frequencies above resonance. This seems to be in disagreement with the impedance behaviour of loop antennas.

The discrepancy can be explained by the fact that what we call "resonance", is not in fact the 1st point of resonance, as is the case of most antennas (e.g. dipoles and monopoles). The folded dipole is always operated at frequencies around the second resonance point, sometimes called anti-resonance.

Resonance is understood here as any point where the antenna reactance becomes equal to zero, with the resistance being a finite number.

The following figure shows a typical folded-dipole impedance curve.
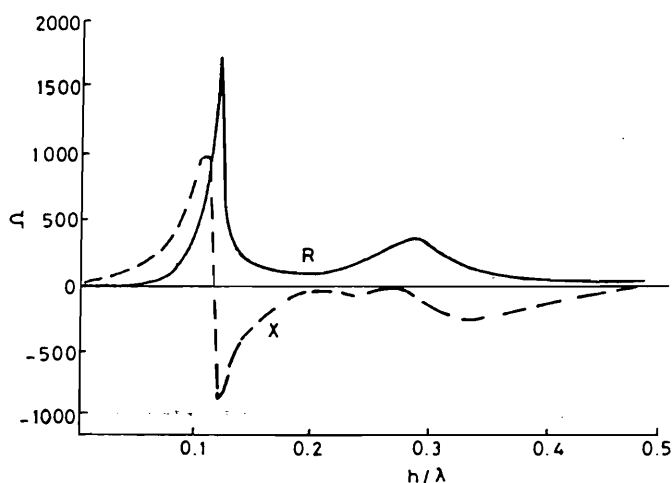
FIGURE 4.20 - IMPEDANCE OF A FOLDED DIPOLE [9]

a

b
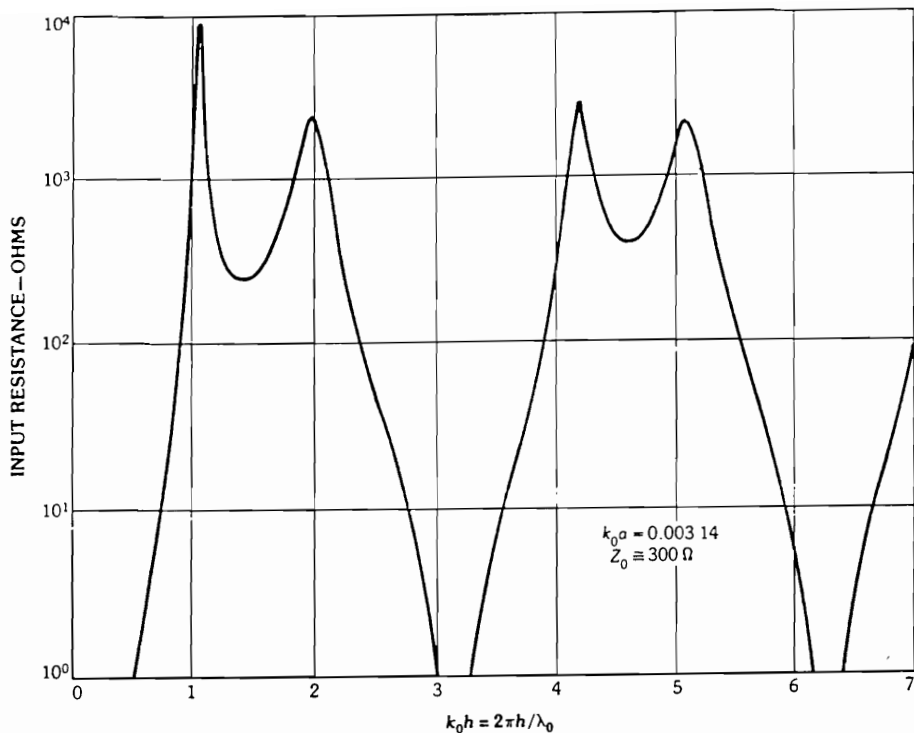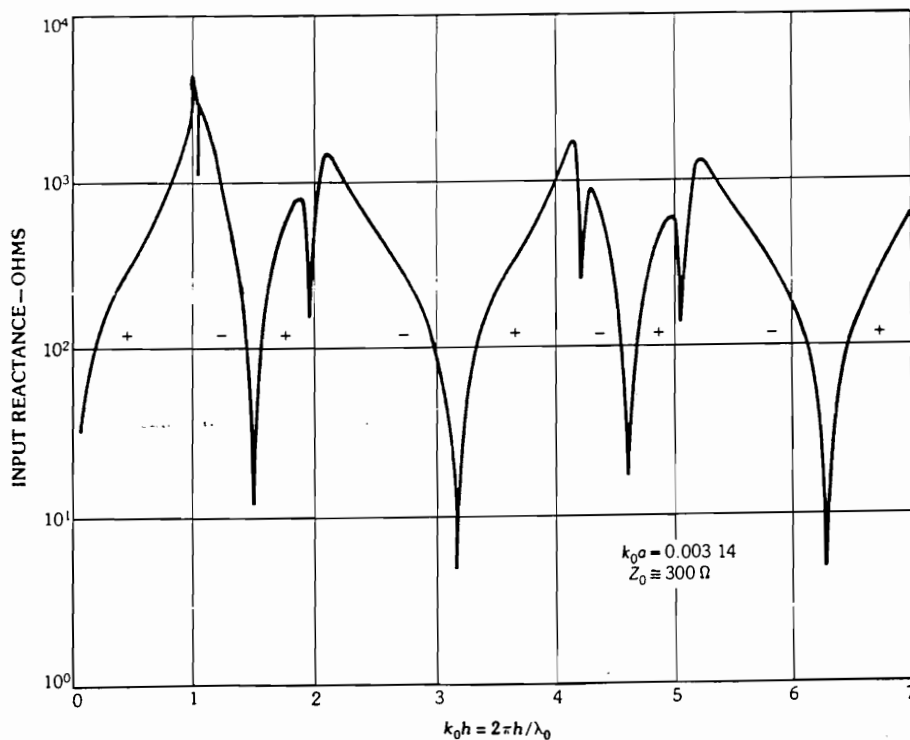
ko a : Electrical radius of both arms

FIGURE 4.21: INPUT IMPEDANCE OF A FOLDED DIPOLE, AS A FUNCTION OF THE ELECTRICAL HALF-LENGTH $k_0 h$, WHERE $h = L/2$ (radians) [9] a) RESISTANCE b) REACTANCE.

The second resonance, or normal operating frequency of the folded
dipole occurs in the curves at the first "valley", where the resis-
tance reaches the known value of 300 ohms.

This point of second resonance occurs at a half-length of aproximate-
ly 1.6 radians. This corresponds to a length of around a half wave-
length.

It can be seen that the reactance also shows a sudden inversion,
indicating a crossing of the zero-reactance value. This inversion,
however is not as sharp as the one for first resonance, thereby
allowing for the operating bandwidths described in the previous
section.

4.4.6 MODELLING FIRST RESONANCE WITH MININEC

Our last step in analysing the folded dipole antenna characteristics
is to find out how MININEC will model the first-resonance impedance
values for this geometry.

The antenna of section 4.4.3 was used for this test.   The separation
of the wires was d = 6.0 cm. and the wire radius was the same for
both arms at a value of 0.1 cm.

Again, the antenna was composed of 4 wires, totalling 34 segments.
The results from MININEC show very good correlation with the data
presented in the previous section.
Naturally, the ohmic values of impedance vary greatly from those
of figure 4.21. This is of course due to the fact that our antenna
has a separation-to-radius ratio of 60.0, and not 12.5 as is the
case of the reference figure.

The results are shown in table 4.11, and also in graphic form
in figures 4.22 (Resistance) and 4.23 (Reactance)

It can be seen that first resonance occurs at a frequency between
94 MHz and 95 MHz., whereas second resonance happens at the expected
frequency of 160 MHz.
At 94 MHz, the antenna has a length of about 0.27 of the wavelength,
which is in accordance with the predicted value of approximately
0.3 wavelengths for the first resonance.
In figure 4.22, the upper limit of the graph has been set to 2000
ohms, in order to appreciate im more detail the lesser values of
input resistance. However, from the table, we can see that the resis-
tance value exceeds by far this upper limit (almost 20 Kohm at 95
Mhz.)

Also, figure 4.23 (reactance) shows the very rapid change from
positive to negative at little below 95 MHz.

In the previous figure, the parameter h is the antenna half-length. Therefore, the folded dipole operating point, would be around the abcissa value of 0.25.

It can be clearly seen that first resonance occurs at apoint well below the half-wavelength point.
This first resonance is characterized by:

1) - A very high value of resistance.

2) - A very sudden change in reactance, from inductive to capaci-
    tive as frequency is increased. Also, the reactance values
    around resonance are very high, in the order of a thousand
    ohms.

These impedance characteristics of the first resonance is what make the use of a folded dipole impractical around this frequency. In particular, the high value of the resistance is a big impediment for practical uses. In addition, the very steep change in reactance makes the possible bandwidth of utilization very small, when compared to that of the second-resonance point.

Figures 4.21a and 4.21b show a more detailed view of the impedance curve of a folded dipole (9). The abcissa gives the value of the electrical half-wavelength, expressed in radians.

The curves correspond to a particular dipole , where the radii a of both conductors is the same, and ko * a = 0.001* π , and their separation remains the same at d = 12.5 * a , thereby yielding a nominal transmission line impedance of Zo = 300 ohms.

Naturally, the actual values of the impedances and frequencies involved, will vary with the wire separation and the raddi of the two antenna arms.

It can be seen from the set of curves of figure 4.21 that the first resonance occurs at a value of the electrical half-wavelength of around 1.1 radians. This corresponds to an antenna length of about 0.3 wavelengths.

The resistance at this point exhibits a sharp peak in value.
The maximum of this peak is in the order of several thousand ohms.

The reactance, on the contrary, shows a sharp inversion point.The impedance below resonance is inductive and increases very rapidly; The actual inversion in reactance is very sharp and is seen in the curves only as a vertical line. Both the inductive and capacitive values of the impedance above and below resonance are of the order of several thousand ohms.

TABLE 4.11: FIRST RESONANCE OF A FOLDED DIPOLE.

Frequency (MHz)	Resistance (ohms)	Reactance (ohms)
30	0.027	289
35	0.068	348
40	0.157	413
45	0.3	488
50	0.72	573
55	1.5	676
60	3.1	801
70	13.7	1180
80	78.25	2015
85	245	3023
88	605	4275
90	1322	5380
92	3791	8692
93	7456	10492
94	15032	9325
95	19388	-1471
100	1981	-4887
105	727	-2605
110	436	-1710
115	323	-1231
120	269	-929
130	228	-544
140	247	-316
150	247	-134
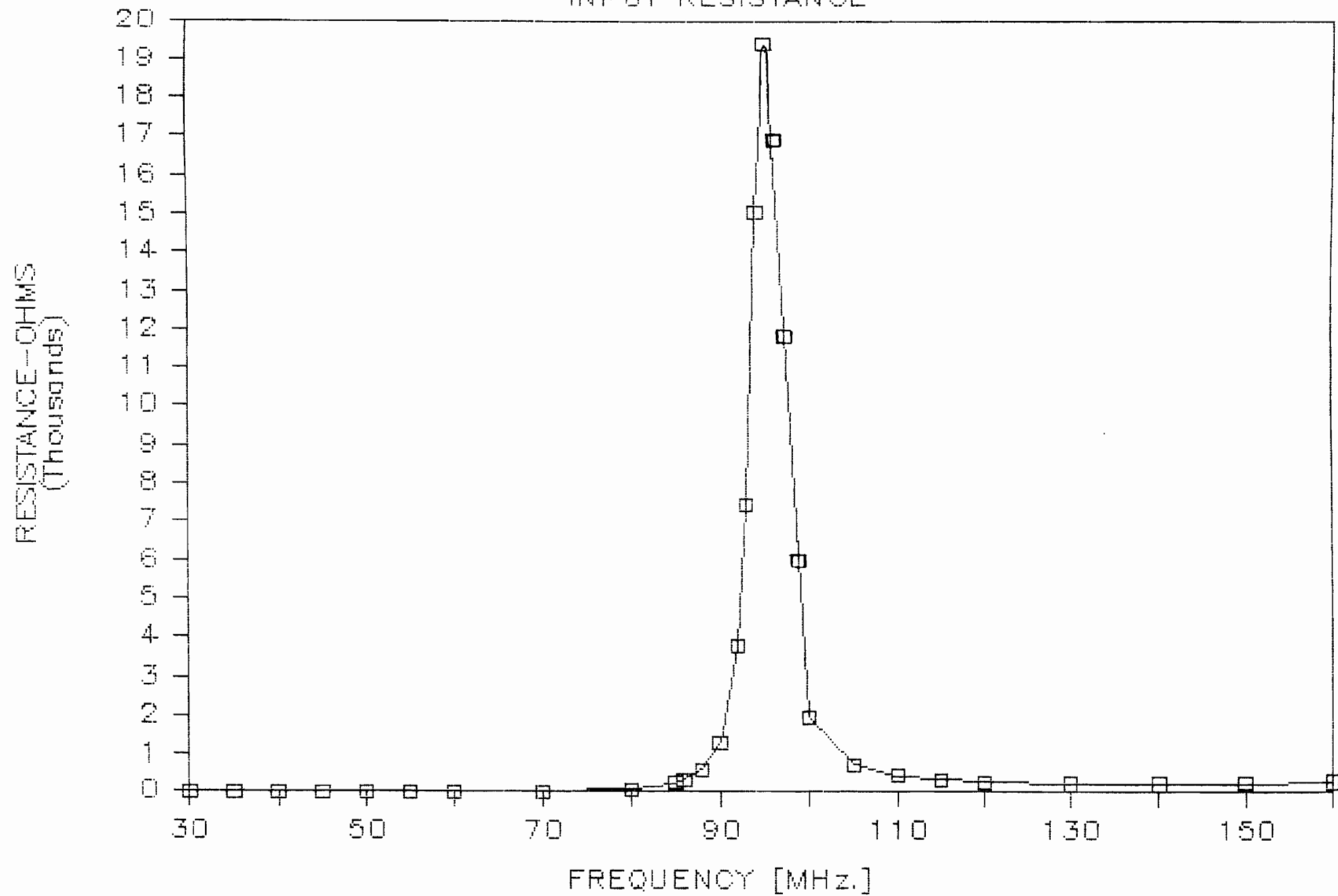
FIGURE 4.22: INPUT RESISTANCE OF A FOLDED DIPOLE, L = 60 cm. AND D = 6 cm. COMPUTED WITH MININEC.
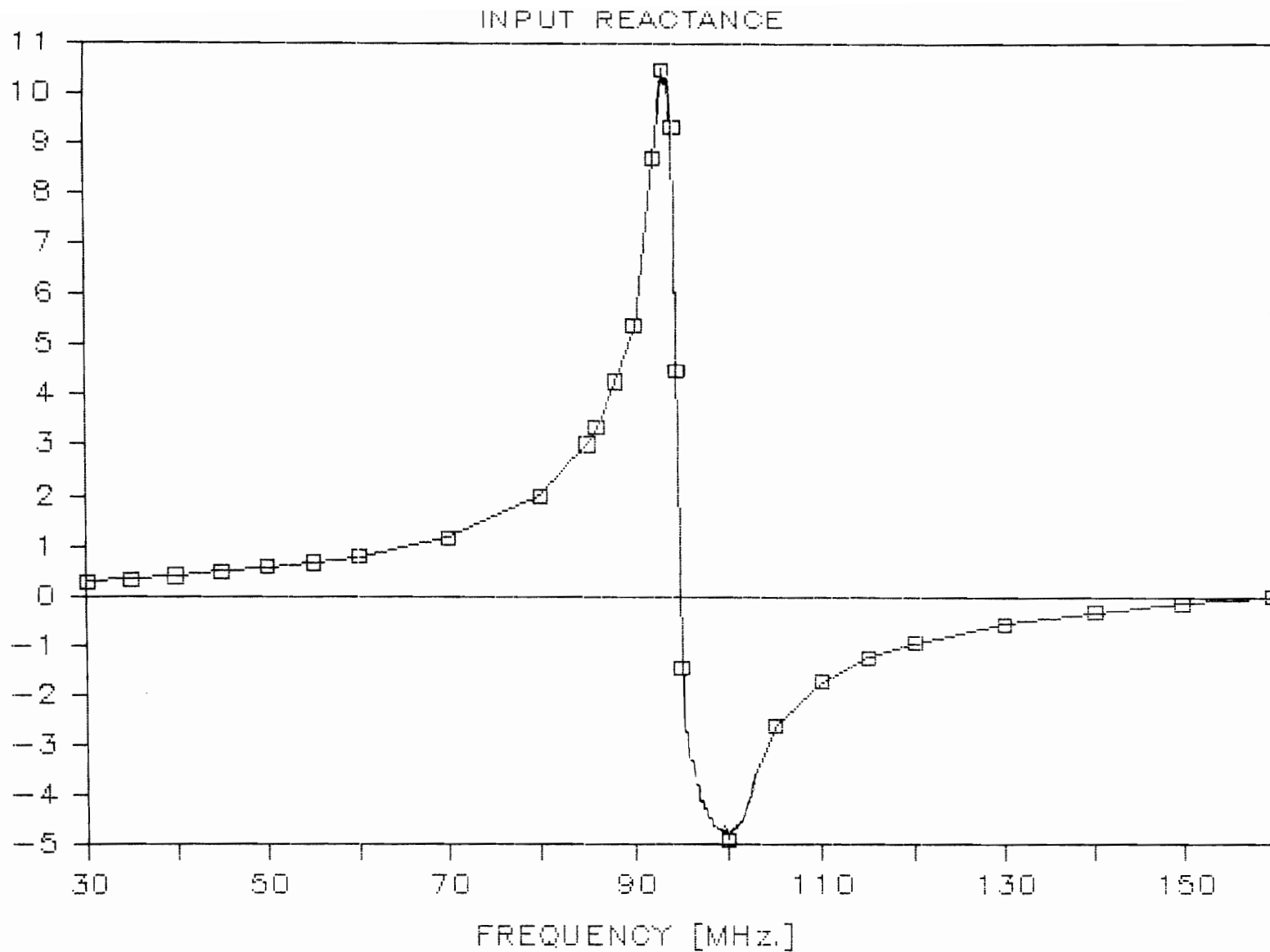
FIGURE 4.23: INPUT REACTANCE OF FOLDED DIPOLE, L = 60 cm. AND D = 6 cm.
COMPUTED WITH MININEC

Note how the reactance tends again to zero as the frequency approa-
ches second resonance. However, the slope of this curve is a lot
smaller than the sharp change encountered for first resonance.
This makes for a moderate bandwidth around second resonance.

4.5   CONCLUSIONS

As a conclusion to this chapter, it can be said that MININEC has
been proven as a valid tool for modelling folded dipoles, and
meander antennas, both of which are the basic components of the
design described in this paper.

For the stepped radii problem, it is obvious that only geometries
where the wire separation is much larger than the excitation-wire
radius, can be used with MININEC. From the experiment described
in this section, it seems that a ratio of P/d equal to 10.0 is
still not large enough to be modelled with MININEC.
For practical geometries, however, where thin wires are used, it
is always possible to obtain ratios of the order of 50 and above.

For the case-study of the folded dipole impedance, MININEC has
been proven to react very well for most of the frequency range of
interest. However, one must keep in mind that most errors in
MININEC are encountered as the frequency is increased, not decreased
because the segment lengths tend to be too big compared to the wave-
length.

In general, enough data was gathered and geometries were studied
as explained in this chapter, to gain sufficient confidence in
the program. This allows to treat the MININEC results obtained
while designing the reduced-size folded dipole as accurate, within
the constraints of the program.

5.0   THE MEANDER FOLDED DIPOLE

5.1 DESIGN OBJECTIVE:

In this chapter, we will describe the design of the reduced-size folded dipole, using only the MININEC program.

The idea of designing a reduced-size folded dipole, was generated while studying the properties of meander antennas. These antennas (3) have been described in previous sections and have been analysed using MININEC. Thus, we have already proved the validity of the program for the design of this type of geometry.

In studying the characteristics of meander antennas, as a means of reducing the size of dipoles and monopoles , it is evident that their low resonant resistance is the one characteristic that can make these antennas less atractive for practical applications. The fact that some sort of matching network or device must be used to adapt the input impedance of the antenna with the relatively higher values of impedance of commercial transmission lines, adds to the cost and the complexity of the antenna system, therefore making it less atractive for real-world applications.

The other characteristic that appears to be somewhat questionable is their narrow bandwidth. However, it is not always desirable to have a wide bandwidth. On the contrary, for some fixed-channel applications, it would be advantageous to have a small bandwidth. This property reduces the effect of adjacent channel interference and in general, adds to the selectivity of the system.

In studying the folded dipole, as covered in previous chapter, it is obvious that this type of antenna provides a means for the designer to choose the antenna input impedance from a wide range of values. This is accomplished, as was explained before, by means of varying the diameter of the wire in the second arm of the folded dipole, or by increasing the separation between arms, or by a combination of both.

Of course, this impedance-adaptability seemed interesting enough to be investigated further and possibly, to be applied to meander antennas. Ideally the objective of the design was to obtain a reduced-size antenna that had an impedance that did not require any matching to common transmission lines.
Of course the common values of commercially available transmission line impedances of 50 , 75 and 300 ohms were a valid goal.

Naturally, other important antenna characteristics had to be maintained, or rather obtained, by the final geometry.

Some of this preliminary design specifications are:

1- Gain had to be comprable to that of a standard folded dipole.
   or about 2.4 dBi.   This refers to the gain of the antenna
   proper, without any parasitic elements.

2- The antenna should be as general-purpose as possible. That is,
   we are interested in designing reduced size common antenna, fit
   to be used in a wide range of frequencies, with proper scaling
   of dimensions. It could be a transmitting or receiving antenna.

3- Radiation pattern should also be comparable to that of a dipole
   or folded dipole. That is, directivity should be moderate.

4- Needless to say, the final geometry, as designed with MININEC,
   had to be phisically feasable. For example, wire radius, bends,
   wire separations and other such dimensions had to be attainable
   in the process of constructing the antenna. Furthermore, wire
   radii should, if at all possible, reflect commercially available
   types of thin-wire.

5- The value of the resonance resistance had to be one of the
   following values of characteristic impedances for common trans-
   mission lines: 50, 75 or 300 ohms. At least, the design should
   be such that the resonant impedance obtained should not have to
   be matched to the transmission line (50, 75 or 300 ohm), for
   a VSWR of less than 3.0.

6- Bandwidth should be as great as poosible.

These were preliminary design objectives, or specificifications.
In addition, although antenna efficiency is not mentioned here as
a design goal, it is a parameter that should always be kept in
mind in any antenna design.

From previous studies (3), we know that efficiency of meander
antennas is comparable to that of the conventional antenna. This
fact gives the designer some reassurance, if not the certainty, that
designs involving meander dipoles or monopoles are likely to have
relatively good values of antenna efficiency.

The design of the subject reduced-size folded dipole with MININEC
met many problems, specially due to the program's inherent limita-
tions. These will be described in detail as we cover some of the
most important aspects of this design.

5.2 ANALYSIS OF THE MEANDER DIPOLE

The meander dipole, will be analysed in this section. This analysis is important, since the meander dipole is the basic component of the folded meander dipole antenna.

The theoretical results obtained with MININEC for this geometry are valuable, since they will serve to understand better the particulars of the folded version. This analysis was not included as part of the preliminary data analysis of chapter 4.0 because there exists no reference data for single folded dipole antennas, to compare the MININEC results with.

However, the results described in chapter 4.2 , for meander monopoles are undoubtly valid for estimating the accuracy of the results for meander dipoles.

The analysis was done as a necessary preamble to the MININEC design of the final antenna, in order to give the designer some guidance on expected results and characteristics for the final configuration. These results, added to the data gathered previously for folded dipole geometries, were of unvaluable use in determining and modeling the folded meander dipole antenna.

In this case, only antennas with N = 2 were analysed (N = number of meander sections per wavelength). The reason for this was that, as was shown in chap. 4.2, antennas with lower N have a greater reduction in size. Of course, the impedance is also smaller for a lower N, but this was not considered to be a major drawback, since it was expected that the impedance-transformation properties of folded dipoles could be used to obtain an appropriate value of input impedance in the final design.

Figure 5.1 shows the geometry for a meander folded dipole with N = 2. The length of the dipole is 60 cm. and it was modelled with MININEC as having 45 segments. The dipole, of course, was center-fed with a voltage source of 1.0 volts. The segmentation chosen provides adequate accuracy of the results for all the frequencies involved.

The wire separation, w, was taken as a variable. Three values of w were tried for the meander dipole with N = 2, and the antenna was subject to the same tests as those performed for the meander monopoles.

The objective was to determine the effect of w on antenna characteristics. We have concentrated our study in two important parameters: the resonant resistance and the antenna bandwidth , for a VSWR value of 2.0. The results are as follows:
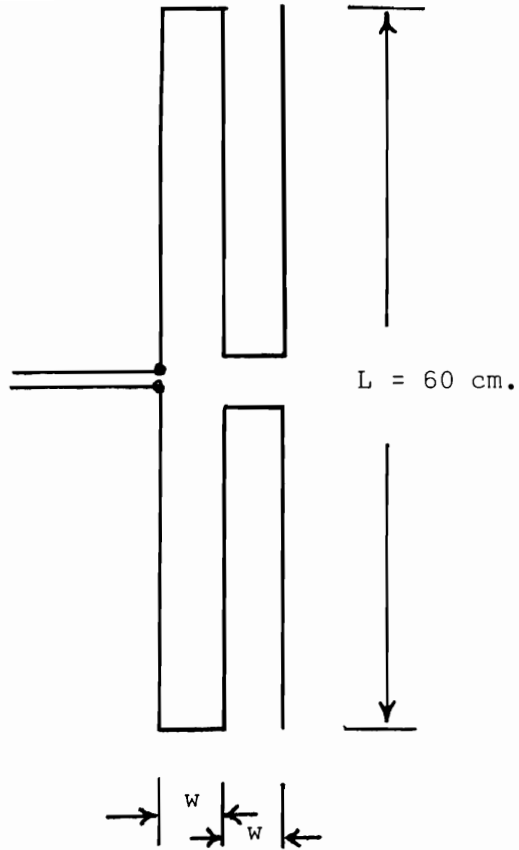
FIGURE 5.1: MEANDER DIPOLE GEOMETRY.(N = 2)

EFFECT OF W (WIRE SEPARATION) IN RESONANT RESISTANCE:

Four values of w were used to model a meander dipole antenna. These are w = 0.5, 1.0, 2.5 and 3.0 cm.

The results are shown in table 5.1, below.

TABLE 5.1: RESONANT RESISTANCE OF A MEANDER DIPOLE.

W (cm.)	Fo (MHz)	Ro (Ohms)	Reduction Factor r
0.5	251	82.4	0.99
1.0	130.2	12.5	0.53
2.5	114.5	10.12	0.46
3.0	109.7	9.2	0.45

The above results reflect what we already know from previous analysis of meander monopoles:

 - The resonant frequency tends to decrease as the wire separation w is increased. This means an increase in size reduction (reduction factor is smaller)

 - The resonant resistance becomes smaller as w increases.

However, MININEC yields some differences that are worth noting.

First, the reduction factor seems to be somewhat smaller than for monopoles over conducting ground. Let us remember that a typical value for the reduction factor r was 0.6 for monopoles. MININEC results for dipoles show factors in the order of 0.4 to 0.5.

In second place, the radiation resistance, although larger than for monopoles, remains at a relatively low value. From comparing meander dipoles with conventional dipoles/monopoles, it was expected that this resistance would be somewhat larger. In any case, the effect of w in the value of this resistance is quite apparent.

For the case, where w = 0.5 cm., we see that the value of the resonant resistance is large, comparable to that of a conventional monopole. Also, the reduction factor is almost 1.0 (no size-reduction) . This no doubt signals an erronous result. This can be attributed to the fact that the wire separation value of w = 0.5 might be too small for the program to yield accurate results.

On the other hand, the smaller the w, the more the antenna ressembles a conventional dipole (the extreme case being w = 0), and we can expect the results to tend to those for a conventional dipole, as w becames increasingly smaller.

The next step is to to determine the effect of changing w, on the antenna bandwidth. The same values of w as shown in the previous table were analysed, and the corresponding geometries were subject to a frequency sweep around their resonant frequencies.
Again, the bandwidth is determined on the basis of a VSWR equal to 2.0.

The results are shown in table 5.2. Also, figures 5.2 and 5.3 show the Smith-Chart representation of the results, for the case where w = 2.5 cm. and w = 3.0 cm.

TABLE 5.2: EFFECT OF W ON MEANDER DIPOLE BANDWIDTH.

w (cm.)	Fo (MHz)	Bandwidth (MHz)	Bandwidth (% of Fo)
0.5	251	20	7.8 %
1.0	130.2	1.0	0.8 %
2.5	114.5	1.8	1.6 %
3.0	109.7	1.6	1.4 %

From these results, we can conclude that meander dipoles follow the expected behaviour already seen in meander monopoles.

We can see that the bandwidth tends to decrease with increasing
w. The value of bandwidth obtained for w = 1.0 might be the result
of a program error due the reasons stated previously (w being too
small compared to the wavelength to yield accurate results)

Although the value in MHz. for the case w = 2.5 cm is greater
than that for w = 3.0 cm., the bandwidth as a percentage of the
resonance frequency is indeed less for the larger value of w.

Figures 5.2 and 5.3 give the Smith Chart representation of the
meander dipole impedance for the case w = 2.5 cm. and w = 3.0 cm.
The actual impedance values for the two cases are given in the fo-
llowing tables 5.3 and 5.4.

TABLE 5.3: MEANDER DIPOLE W = 2.5 cm. IMPEDANCES (MININEC)

Frequency (MHz)	Impedance (Ohms)
70	3.49 - j 446
100	7.53 - j 133
110	9.33 - j 41
112	9.7 - j 22.3
113	9.97 - j 12.9
113.5	10.02 - j 8.2
114	10.2 - j 3.5
114.5	10.2 + j 1.26
114.8	10.28 + j 4.12
115	10.3 + j 6.04
115.2	10.36 + j 7.94
115.5	10.42 + j 10.8
116	10.52 + j 15.6
120	11.4 + j 54.6
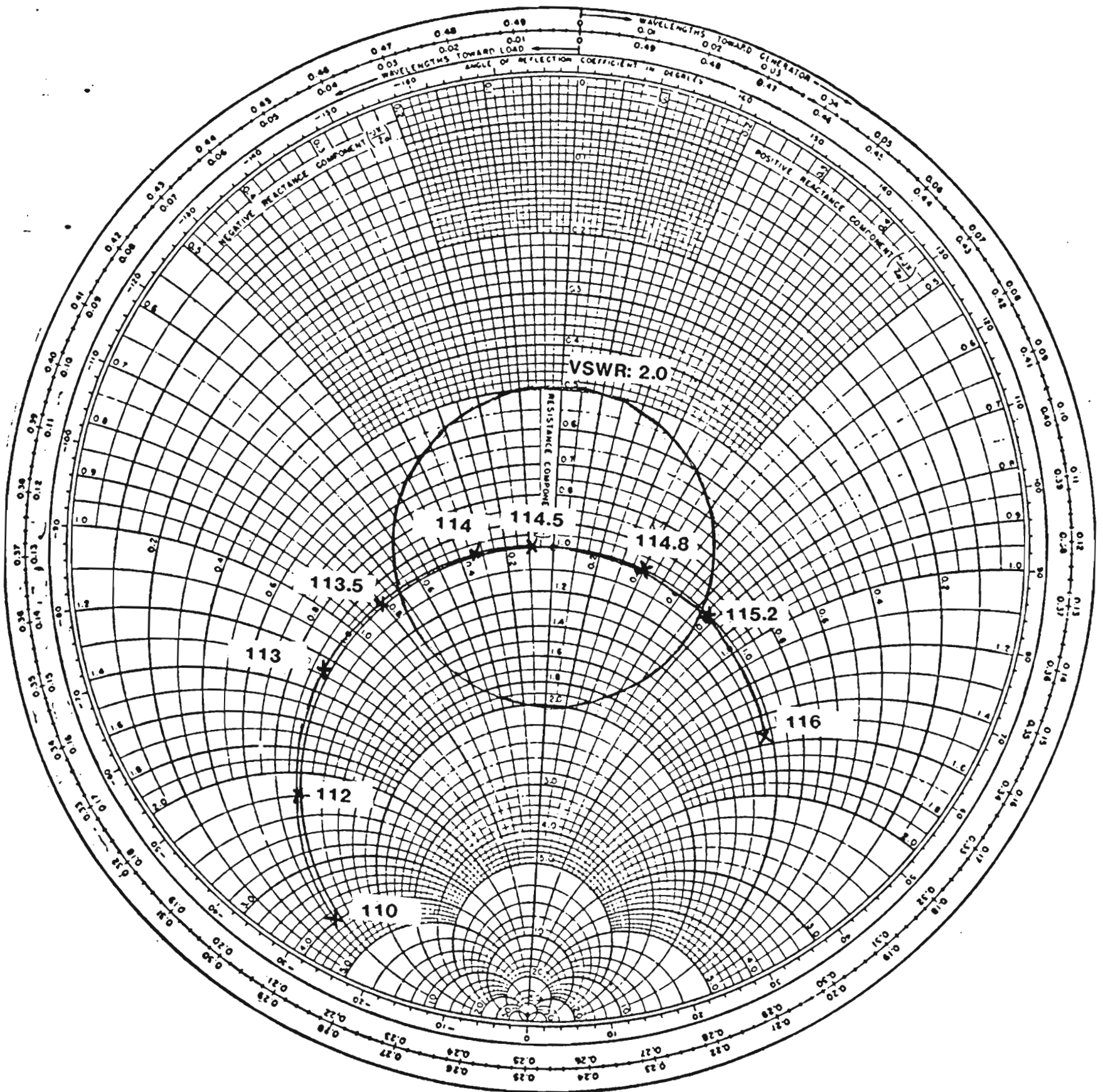
**FIGURE 5.2   MEANDER DIPOLE (w: 2.5 cm.) IMPEDANCE CHART
NORMALIZED TO RESONANT RESISTANCE**
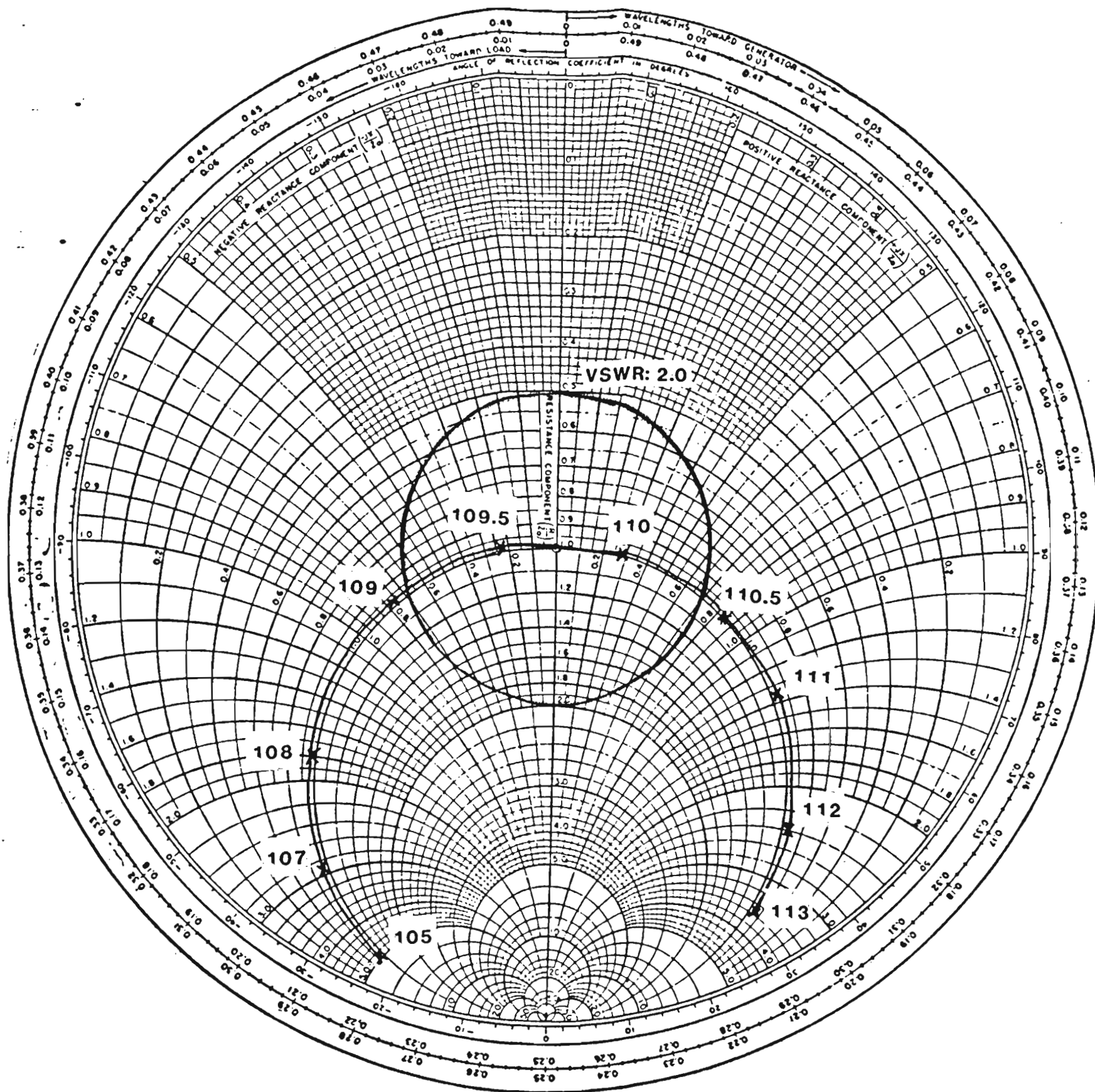
FIGURE 5.3   MEANDER DIPOLE (w: 3.0 cm.) IMPEDANCE CHART
NORMALIZED TO RESONANT RESISTANCE

TABLE 5.4: MEANDER DIPOLE W = 3.0 cm. IMPEDANCE (MININEC)

Frequency (MHz)	Impedance (Ohms)
105	8.27 - $\dot{J}$ 45.1
107	8.63 - $\dot{J}$ 26.1
108	8.8 - $\dot{J}$ 16.55
109	9.0 - $\dot{J}$ 6.96
109.3	9.04 - $\dot{J}$ 4.08
109.5	9.08 - $\dot{J}$ 2.16
109.7	9.12 - $\dot{J}$ 0.22
110	9.17 + $\dot{J}$ 2.67
110.5	9.27 + $\dot{J}$ 7.5
111	9.36 + $\dot{J}$ 12.36
112	9.55 + $\dot{J}$ 22.08
113	9.74 + $\dot{J}$ 31.9
115	10.14 + $\dot{J}$ 51.7

As we can see from these tables, and from the corresponding
Smith Charts, the value of the resistance varies very little
around resonance. The reactance, on the contrary, seems to
dip very sharply at resonance. This, of course explains the
narrow bandwidth that appears to be the predominant characteris-
tic of meander antennas.

Although, as was pointed out, we do not have any experimental
reference to compare these results with, it is obvious that they
are in accordance with those obtained in chapters 3.0 and 4.0,
for meander monopoles.

These results serve as a good starting point, to begin the design
of the folded meander dipole. In doing so, we are to assume that
the properties of folded dipoles will somewhat be maintained by
its meander counterpart, but with the basic characteristics of the
meander dipole, studied in this section.

A point that must be made, is that, in choosing the value of the wire separation w, it was intended to keep the overall "width" of the antenna small. It must be remembered (see fig. 5.1) that this antenna width is equal to twice the value of w.

The main feature of meander antennas is their reduced size. However, the "size" is not only the length L of the dipole. For a meander antenna, the wire separation w must also be considered.

For instance, if a considerable reduction in the length of a dipole was obtained, at the price of making w significantly large compared to the length, then we could not consider the overall size reduction to be very big. In a case like this, we would have to find another parameter, like the antenna aperture, to establish what the real reduction in overall size was.

In this context, the wire separation was kept small compared to the length, in order to have the overall "size" reduction correspond as closely as possible to the reduction in length.
The general criteria adopted for this purpose, was that the total antenna width (equals two times w) was to be not larger than one-tenth of the antenna length. That is:

$$2w < 0.1L$$

$$\text{or} \qquad w < 0.05L$$

This explains the choice of the largest value of w = 3.0 cm. for the meander dipole of length L = 60.0 cm.

Another aspect of meander dipoles that should be noted, is that the value of resonant resistance is somewhat smaller than what could be expected. In fact, the impedances do not vary much from those presented in chapter 3.0 and 4.0 for meander monopoles.

If we compare these results to the case of conventional monopoles and dipoles, the differences are obvious. A conventional half-wave dipole resonant resistance is significantly greater than that of a monopole. This does not seem to be the case for meander dipoles.

Furthermore, the meander monopoles studied in previous chapters, had a length of only 4.5 cm., whereas the values of wire separation studied were basically the same: w = 0.5 or 1.0 cm.
These values of w represent a much greater fraction of the wavelength for the antenna L = 4.5 cm., than for the dipoles studied here.
Nevertheless, the values of resistance do not seem to differ much.

This phenomenon cannot be explained at the moment, since we do not posess experimental data on meander dipoles to serve as reference to our MININEC results.

5.3 CONSIDERATIONS ON SEGMENTATION DENSITY:

In the previous section, we have tried to model various meander dipoles with N = 2 , and have found several results that could be inconsistent with everything we know experimentally about meander antennas. To begin with, let us sum these results:

- Resonant Resistance is comparable, and sometimes less than that of a meander monopole (refer to chap. 4) over conducting ground. This resistance was expected to be larger, if only because the wire is longer for the same resonant frequency. (meaning larger ohmic resistance.)

- Bandwidth is small, but is smaller than the ones found experimentally and with MININEC for meander monopoles.

- Behaviour of the meander dipole, as w is changed, is the same as for meander monopoles. That is, bandwidth decreases with increasing w , and resonant resistance decreases.

- reduction factor is comparable, though somewhat smaller than for a meander monopole.

The geometry analysed in the previous section was composed of 46 segments, which is very near the limit MININEC will accept.
Now, we have found (chap. 3.3.2) that a meander dipole N = 2 can be accurately modelled with a number of segments, that has to be approximately greater than 30.

However, the meander dipole has a physical length of double the one of a meander monopole. A logical conclusion would be that the dipole requires at least 60 segments , for the program to yield accurate results. But we are limited by the maximum number of 50 segments imposed by the program, and thus we may be forced to accept a suboptimal solution.

Therefore, the results obtained with the present segmentation must be treated as valid approximation to the real solutions, but it is doubtful that experimental results will closely match the MININEC results.

We can affirm that the results are indeed valid, because as it has been pointed out, most of the characteristics found in the model of the meander dipole, agree with experimental data [2] for meander monopole antennas. It is only the accuracy of the numerical results such as: resonant resistance, bandwidth, and resonant frequency, that have to be taken as approximations.

To further investigate this point, other segmentations were tried. First, the number of total segments was reduced to 40. Then, the maximum number of segments (50) allowed by MININEC was tried.

In this later case of a 50 segment dipole, segments were added to only the most critical wire, the longest wire where the feed-point is connected (ref. to fig. 5.1). The reason for this is that only 4 extra segments could be added to the original 46-segment geometry, and segments could not be added to every wire in the geometry which has 9 wires in total. Adding 1 or 2 segments to some of the shorter wires would have created an "inbalance" in the antenna, with two symmetrical wires having different segmentation.

For these 3 cases, the resonant frequency and the resonant resistance were found. The results are as follows:

No. of Segments	Res. Freq. (MHz)	Res. Resistance (Ohms)
40	220	59.8
46	130.2	12.6
50	168.5	19.6

Note that for the case of a 50 segment dipole, the resonant resistance has increased over the 46-segment resistance, and the resonant frequency has also increased to 168.5 MHz.
This represents a reduction factor of 0.67, which is perhaps farther from the expected value of 0.5 to 0.6 , than the 0.53 reduction factor obtained previously for the 46 segment segment geometry.
The impedance, by contrast, is maybe closer than the expected value (or higher than a for a monopole), which tells us that at least in this respect the result is closer to the real value.

The case of the 40 segment geometry gives us a higher value of resonant resistance, but the change in resonant frequency yields a reduction factor of 0.88, which is in total disagreement with what we know about meander antennas.

It is worth noting that apparently, the only parameter that presents drastic changes with the segmentation, is the antenna input reactance Thus the change in resonant frequency. The input resitance seemed unchanged by the segmentation. For instance, the resistance at 130 Mhz. for the 40 and 50 segment cases, remained roughly at the 46-segment value of 12.6 Ohms.

The point that must be made, is that probably all of this segmentations are inadequate to predict exact real-life results. Which is why, again, said results are valid only as qualitative, rather than quantitative approximations, due to MININEC limitations.

ANALYSIS OF THE MEANDER FOLDED DIPOLE

In this section, we will try to study the characteristics of the meander folded dipole through a valid MININEC model.

The basic geometry we are modelling is described in figure 5.4. We can see that this is a rather complex geometry. It is formed by two meander dipoles N = 2, connected and separated by a distance equal to d. Or it could also be seen as a meander dipole N = 4 folded over itself.

The antenna is composed of 20 separate wires. The segmentation density , as well as the geometry and the coordinates in space for each wire will be given in detail here.

The antenna was chosen to have a vertical orientation. That is, the length L of the dipole will be along the vertical axis of coordinates (The Z axis.)

The segmentation density used is 50 segments. We must remember that the limit number of segments that MININEC will accept is 50.

However, when we distribute this number of segments over 20 different wires, the segment density per wire tends to be small. This could entail erronous or marginal results, but given the constraints of the program and the complexity of the antenna, we have no other option.
We can say in this respect, that we are forcing the program to its very limits.

Again, in this case, as we are dealing with a new type of antenna, there is no previous experimental data to give us a reference on the accuracy of the results. Nevertheless, we have gathered sufficient data on meander antennas and folded dipoles to be able to determine if the results are correct, or the program is yielding numerically erroneous results.

Again, in trying to keep the dimensions of the antenna, similar to those of a conventional folded dipole, the values of w and the arm separation d, were kept sufficiently small so that the overall width of the antenna was a small fraction of the length L.

We must remember that in the case of a folded meander dipole, the overall antenna width will be:

Width = 4w + d.

In this case, the criteria used was that the width should not be greater than 25% of the antenna length, or

$$4w + d < 0.25L$$
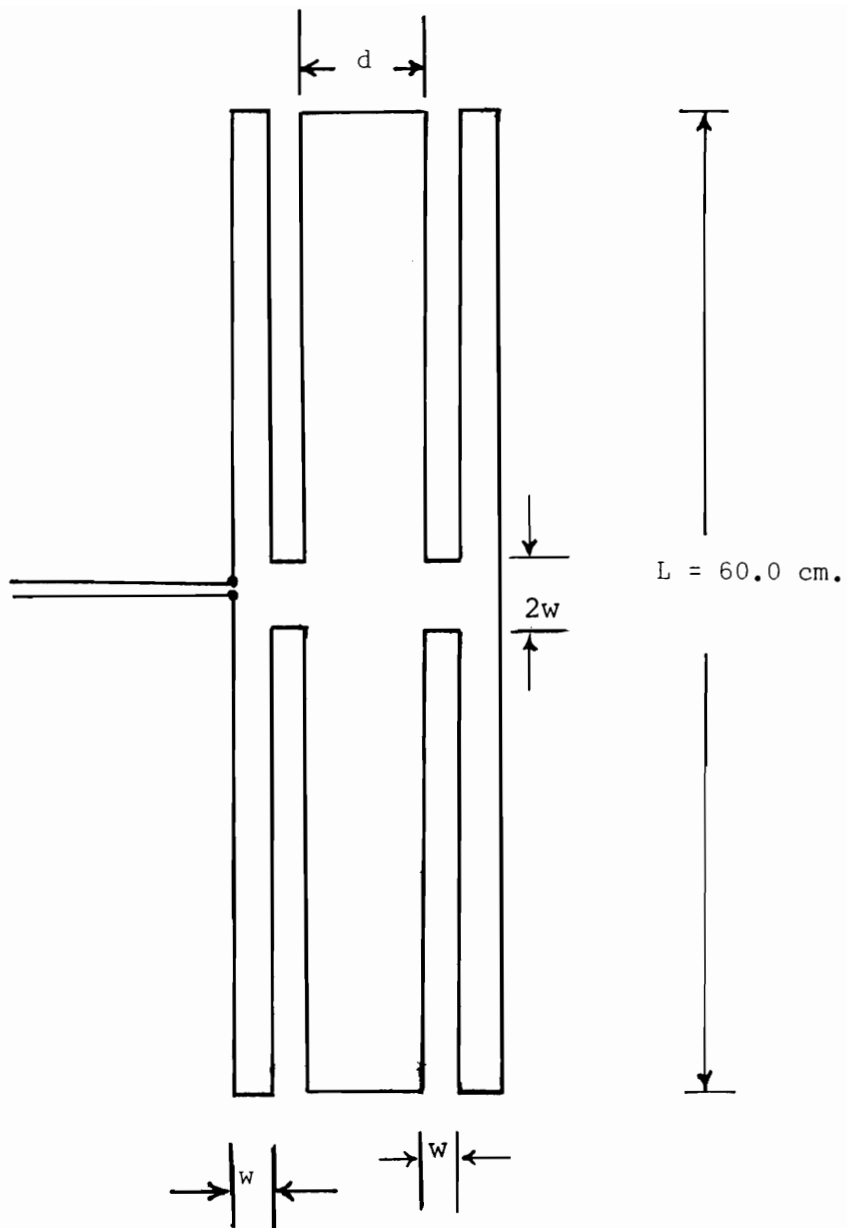
FIGURE 5.4: MEANDER FOLDED DIPOLE GEOMETRY. (N = 2)

The length of the arms was initially set at L = 60 cm., to match the length chosen for the meander dipoles of the previous section.

The following table gives the values of the wire coordinates, as well as the segmentation for each wire, for a meander folded dipole of length L = 60 cm., w = 1.0 cm., and d = 4.0 cm.

TABLE 5.5: FOLDED MEANDER DIPOLE COORDINATES (cm.)

WIRE No.	END 1 COORDINATES			END 2 COORDINATES			SEGMENTS
	X1	Y1	Z1	X2	Y2	Z2	
1	0	0	0	0	0	60	8
2	0	0	60	1	0	60	1
3	1	0	60	1	0	31	3
4	1	0	31	2	0	31	1
5	2	0	31	2	0	60	3
6	2	0	60	6	0	60	1
7	6	0	60	6	0	31	3
8	6	0	31	7	0	31	1
9	7	0	31	7	0	60	3
10	7	0	60	8	0	60	1
11	8	0	60	8	0	0	8
12	8	0	0	7	0	0	1
13	7	0	0	7	0	29	3
14	7	0	29	6	0	29	1
15	6	0	29	6	0	0	3
16	6	0	0	2	0	0	1
17	2	0	0	2	0	29	3
18	2	0	29	1	0	29	1
19	1	0	29	1	0	0	3
20	1	0	0	0	0	0	1

This geometry is far from the ideal one. The most critical wires in this antenna are those containing only 3 segments. For a wave-length of 2 meters (150 MHz), one of these segments will only be 0.048 or 5 % of the wavelength. Although theoretically, this is within the limits of the programs, the results may be inaccurate. In any case, there was no way of knowing if such results were erroneous, until they could be verified with practical laboratory results.

However, we could make some preliminary assumptions about this antenna, that could serve as a basis for determining the validity of the results.:

1- The antenna was expected to have somewhat greater value of impedance at resonance than the meander dipole.

2- The bandwidth, of course, was expected to be at least as narrow as a meander dipole. Furthermore, considering that a folded dipole has a smaller bandwidth that a conventional dipole, it was thought very possible to obtain an even smaller bandwidth for this antenna, than for a meander dipole.

3- The overall impedance change with frequency, should correspond to that of a loop antenna or a folded dipole. This means, the antenna will have a first resonance point characterized by a very high resonant resistance and sharp reactance change.

4- A change in wire diameter in the second "arm" of the antenna, with reference to the feeding-point arm, should somewhat corres-pond to a change in input impedance.

This antenna was subject to basically the same tests with MININEC as those previously accomplished for meander monopoles and dipoles.

A voltage source of 1.0 Volts was applied to the center of wire No. 1, onto segment No. 3.

First, the antenna was subject to a frequency sweep to determine both its second resonance resitance and also to verify the loop antenna characteristics mentioned in our basic assumption No. 3 above.

The results given by MININEC for this first geometry are quite encouraging. In the first place, the input resistance is close to 50 ohms. (one of our target impedances.) at second resonance. Furthermore, the value is roughly 4 times that of a meander dipole with the same values of w and L.

Second, the impedance behaves much like that of a conventional folded dipole. The results are shown in the next page and are also shown in graphical form in figures 5.5 (Resistance) and 5.6 (Reactance). Note the similarity with fig. 4.22 and 4.23
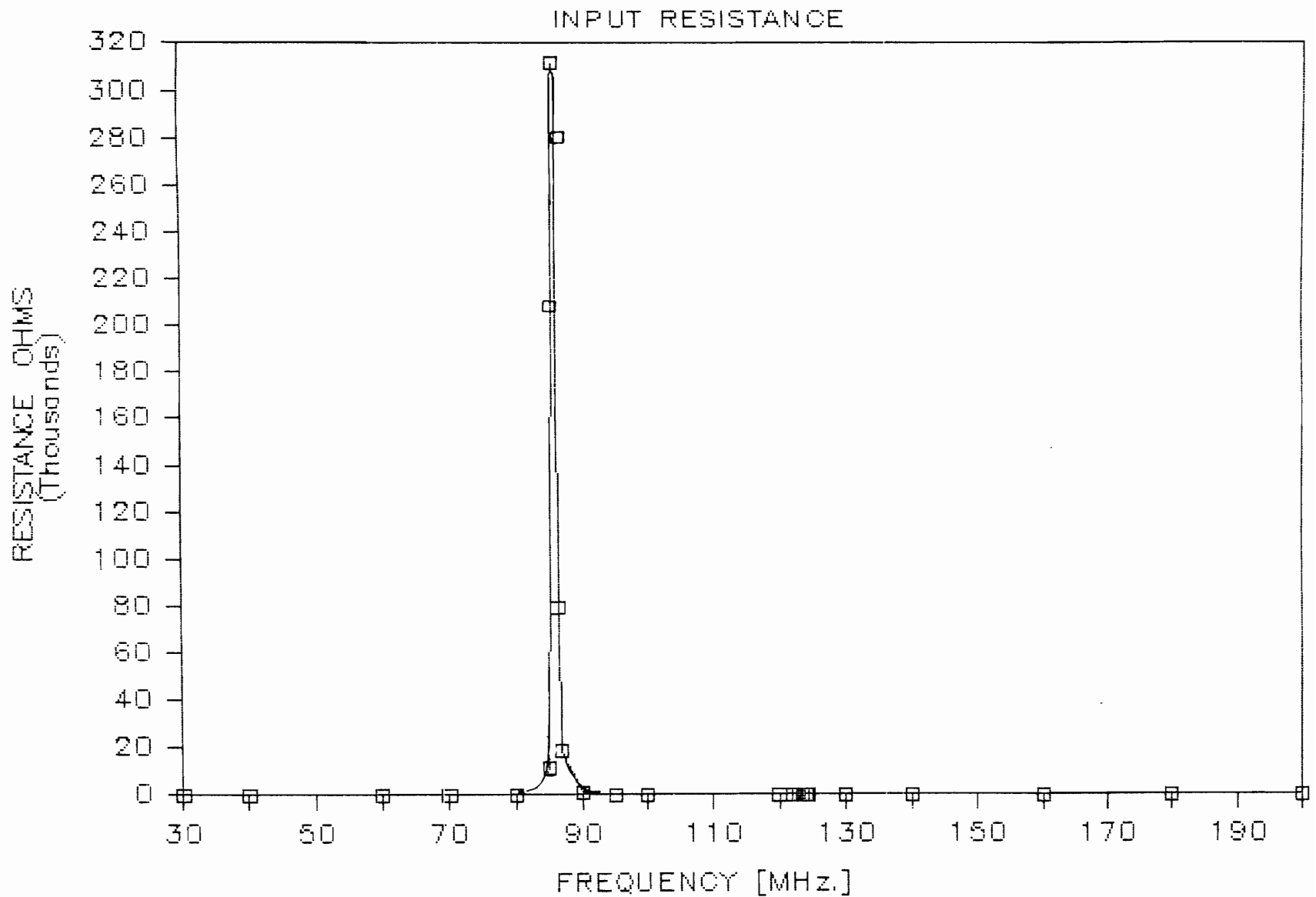
INPUT RESISTANCE

FIGURE 5.5: FOLDED MEANDER DIPOLE INPUT RESISTANCE (w = 1.0 cm.)
VERSUS FREQUENCY.
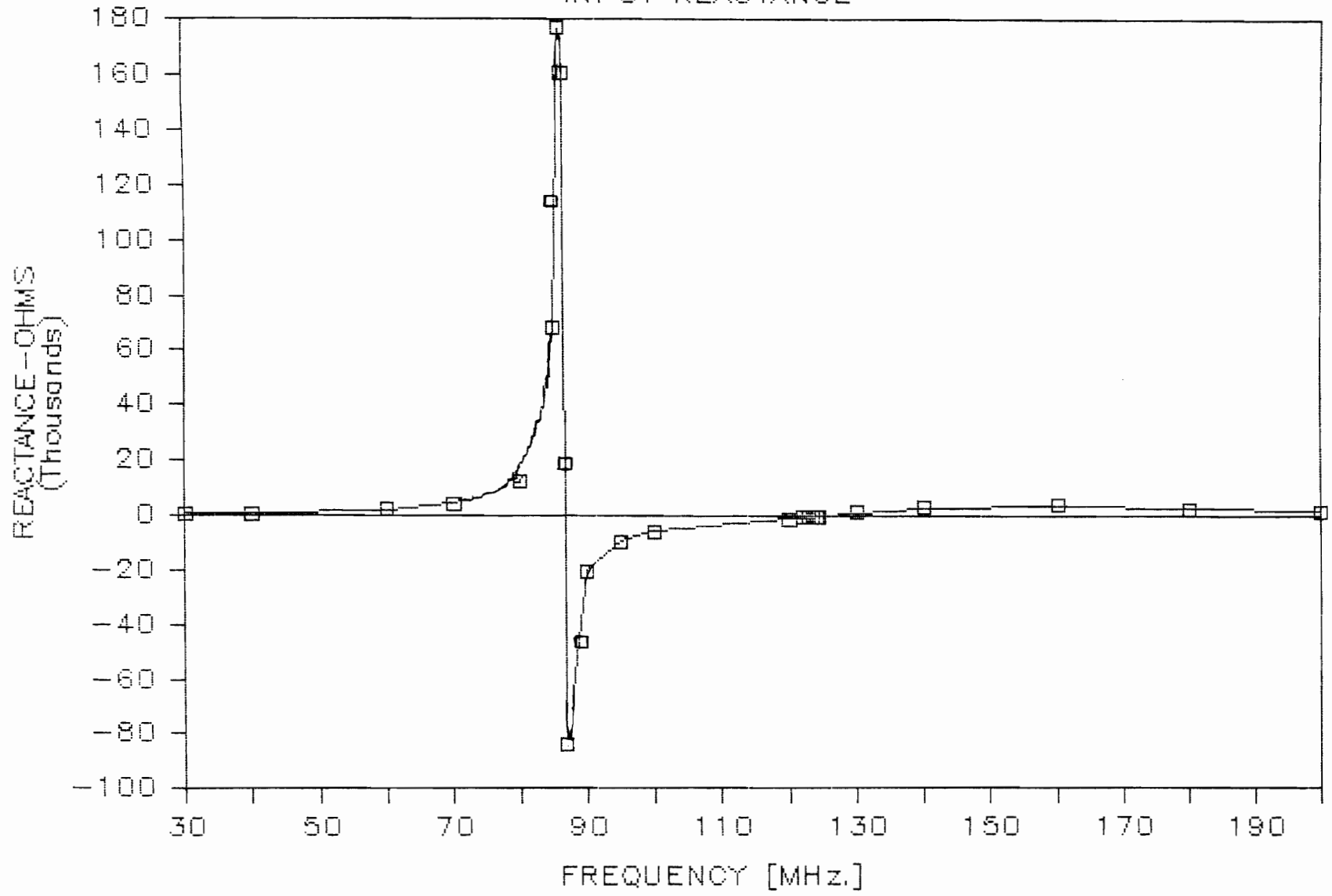
FIGURE 5.6: FOLDED MEANDER DIPOLE INPUT REACTANCE (w = 1.0 cm.) VERSUS FREQUENCY.

TABLE 5.6: MEANDER FOLDED DIPOLE GEOMETRY INPUT IMPEDANCE
50 segment Geometry .   w = 1.0 cm., L = 60 cm.

Frequency (MHz)	Impedance (Ohms)	
30	0.032 + j 626	
40	0.198 + j 959	
60	4.26 + j 2324.5	
70	22.7 + j 4325	
80	287 + j 12225	
85	11136 + j 68204	
86	311489 + j 177000	
87	18656 - j 83890	< 1st. Resonance
90	1189 - j 20371	
95	289 - j 9025	
100	148 - j 5702	
110	75 - j 2804	
120	52.5 - j 825	
122	49 - j 418	
124	46.65 + j 2.1	< 2nd. Resonance
124.5	45.96 + j 109	
130	38 + j 1336	
140	23.1 + j 3399	
160	13 + j 3932	
180	27.35 + j 2806	
200	42.8 + j 1848	

The next step was to analyse the bandwidth of this antenna.
A more fine frequency sweep around the point of second resonance
was accomplished.
The results have been plotted in the Smith chart of figure 5.7
and in the Table 5.7.
Again, the bandwidth is calculated using the resonant resistance
as normalization factor, and a VSWR circle of value 2.0

TABLE 5.7: FOLDED MEANDER DIPOLE IMPEDANCE AROUND 2nd. RESONANCE

FREQUENCY (MHz)	IMPEDANCE (Ohms)
123.0	$48.0 - j\ 209.7$
123.5	$47.4 - j\ 104$
123.7	$47.1 - j\ 61.74$
123.8	$46.9 - j\ 40.5$
123.9	$46.8 - j\ 19.15$
124.0	$46.65 + j\ 2.14$
124.1	$46.52 + j\ 23.5$
124.2	$46.4\ + j\ 44.93$
124.5	$45.96 + j\ 109.1$

It was found that the bandwidth is about 0.25 MHz. This is in accor-
dance with the expected results. A meander dipole with the same
dimensions for w and L , had a bandwidth of roughly 1.0 MHz. The
folded meander dipole seems to present an additional reduction in
bandwidth, just as a folded dipole has a smaller badwidth than the
conventional dipole.

This bandwidth seems too small. However we must remember that it
was defined on the basis of a VSWR equal to 2.0, which is a very
stringent requirement. There are other methods of defining the
bandwidth which will be discussed later.

Also note that the reduction factor (over a conventional folded
dipole) is close to 50%. This represents a small gain in reduction
over the theoretical reduction obtained with MININEC for a meander
dipole in section 5.1.
But we also know that a folded dipole is resonant at a slightly
shorter length than a dipole, so this increase in reduction was
to be expected.
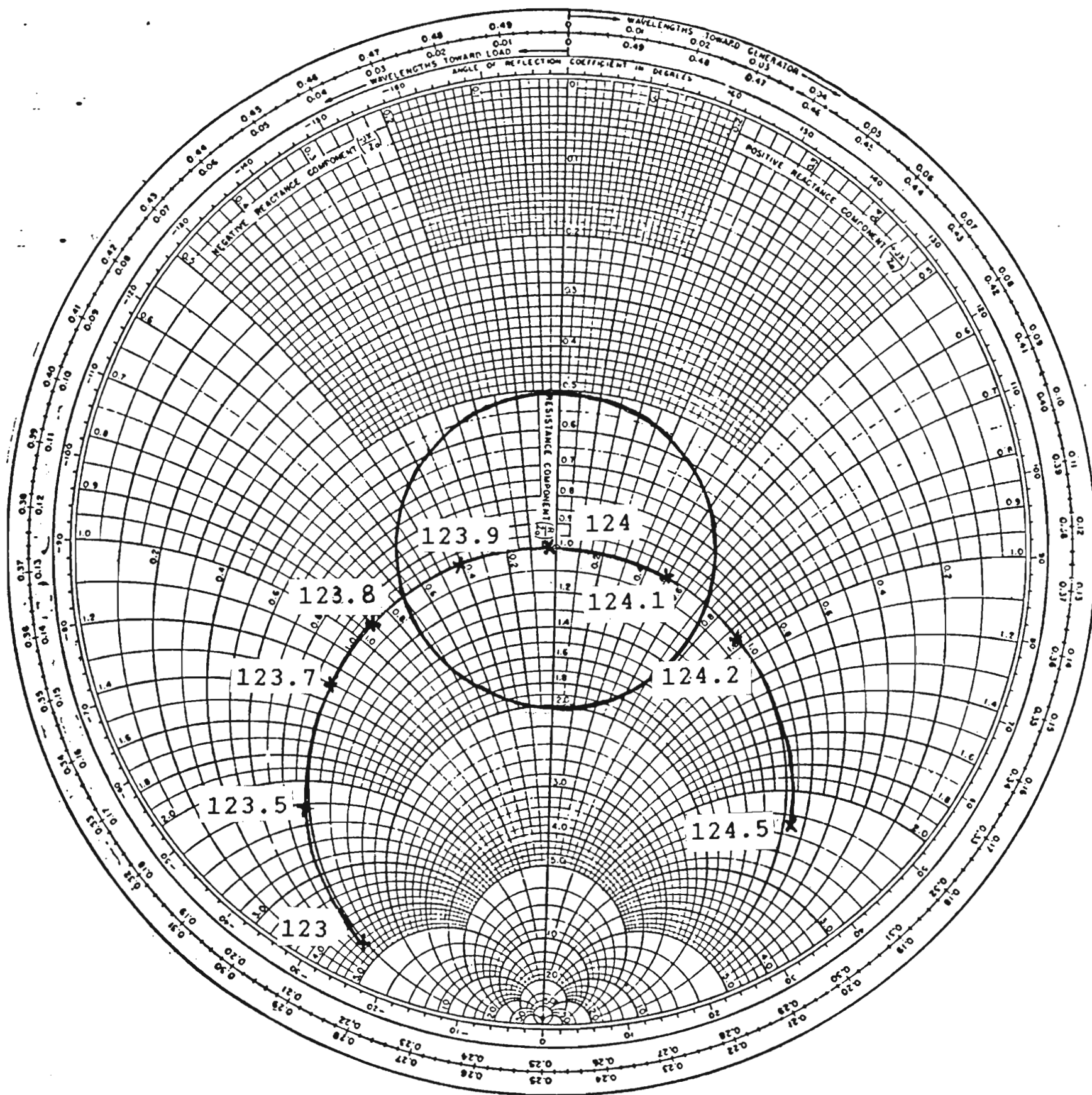
FIGURE 5.7   MEANDER FOLDED DIPOLE (w: 1.0 cm.) IMPEDANCE CHART

NORMALIZED TO RESONANT RESISTANCE

94

5.4.1   EFFECT OF WIRE SEPARATION IN ANTENNA CHARACTERISTICS:

The next test, was to increase the wire separation (w) of the meander arms. The arm separation (d) was kept constant at 4.0 cm. to isolate the effect of varying w.

In choosing the maximum value of w, the criteria for maintaining the overall antenna width within specified limits was considered. Therefore, a maximum value of w = 2.0 cm was taken.

The geometry, and its corresponding wire segmentation was otherwise kept unchanged, as well as the excitation source and feed-point.

The results are shown in Table 5.8

TABLE 5.8: EFFECT OF w IN ANTENNA RESONANT RESISTANCE
         (d = 4.0 cm. , L = 60 cm.)

W (cm.)	Fo (MHz)	Resonant Resist. Ro (Ohms)
0.5	98.2	2.36
1.0	124.0	46.65
1.5	> 200	---- *
2.0	86.6	0.6

* : Freq. of second resonance is greater
    than 200 MHz.

These results do not show any obvious trend. The resonant frequency increases from the value corresponding to w = 0.5 cm. to 124 MHz for w = 1.0 cm. , to a value beyond 200 MHz., and then comes back to 86.6 MHz. for w = 2.0 cm. If anything, the resonant resistance seems to do something similar , starting at 2.36 ohms, increasing to 46 ohms, and then decreasing to 0.6 ohms.

EFFECT OF W ON ANTENNA BANDWIDTH:

Similarly, the effect of wire separation in antenna bandwidth was analysed. From all previous analysis of meander antenna geometries, we know that bandwidth should decrease with increasing w.

The results of the MININEC Analysis are shown in table 5.9.

TABLE 5.9: MEANDER FOLDED DIPOLE BANDWIDTH
(L = 60 cm., d =. 4.0 cm.)

w (cm.)	Fo (MHz)	Bandwidth (MHz)	Bandwidth (% of Fo)
0.5	98.2	0.8	0.81 %
1.0	124.2	0.4	0.32 %
2.0	86.6	0.2	0.23 %

MININEC show two important features:

- The bandwidth shows the expected trend of being smaller with increasing w. Also, the bandwidth is smaller than that of a meander dipole. This is an expected result, since a folded dipole will have a smaller bandwidth than a conventional dipole.

- The resonant frequency, as was pointed out before, does not show the expected results of higher frequency with increasing w (higher reduction factor)

These discrepancies, specially where the resonant frequency, and therefore the resonant resistance are concerned, are again the product of a poor segmentation scheme, that is forced upon the designer by the program's inherent limitations.

We must stress the fact that all these results are to be taken at this point as qualitative approximations of what the antenna real-life behaviour will be. As was shown in section 5.2, the segmentation density is inadequate to yield exact numerical results.

5.4.2 <u>FOLDED MEANDER DIPOLE RADIATION PATTERN.</u>

In previous chapters, radiations patterns of known antennas have been shown, as computed by MININEC. The program accomplishes this by calculating the electromagnetic field components around the antenna, in the far-field region. The theroretical details of this method will not be discussed here, but can be found in reference (1).

The program will let the user select wether the computation is to be done in volts/meter or dBi. If volts/meter is selected, the power level can be changed, and the radial distance of the far field cal-culation must be specified in meters. The zenith or vertical angle (theta) and azimuthal or horizontal angle (phi) are then selected for both the volts/meter and dBi cases.

The results for the dBi calculation are presented in terms of the vertical pattern, horizontal pattern, and total pattern in dB. The total pattern is the vector sum of the two pattern components in dB.

In computing the far field components, the input impedance of the antenna is used to calculate the gain. Therefore, a well converged solution, and hence an accurate impedance result must be used, to obtain accurate gain data.

Now, we have shown that our solutions for the folded meander dipole antenna are most likely not very accurate, due to the poor segmenta-tion density. Therefore, we must assume that the gain, as computed by MININEC will undoubtly introduce some degree of error.

However, we are interested in the qualitative results. That is, it is important to find out if this geometry will yield a pattern that is somewhat practical. Most important, it would be advantageous to find if this antenna has a pattern ressembling that of a conventional folded dipole.

The folded meander dipole having a w = 1.0 cm, L = 60 cm. and d = 4.0 cm. was used for the pattern calculations by MININEC. The 50 segment geometry described previously was used.

MININEC yielded a pattern that is in every way shaped like that of a conventional folded dipole. Figure 5.8 shows the vertical radia-tion pattern. The pattern was calculated at an azimuthal angle of 45 degrees. The zenith angle theta was varied at 10 degrees intervals for a total of 36 angles (360 degrees.). The choise of this number of vertical angles is obvious, since the antenna is suspended in free space.

The pattern, as shown if fig. 5.8 shows the familiar doughnut-shaped radiation pattern, that is the characteristic of dipoles and folded dipoles. Note that the maximum gain, as shown in the listing of re-sults, is roughly 0.6 dBi, for the vertical pattern. However this number cannot be considered valid, since we are assuming that the input impedance is only an approximation.

FIGURE 5.8 FOLDED MEANDER DIPOLE
VERTICAL RADIATION PATTERN
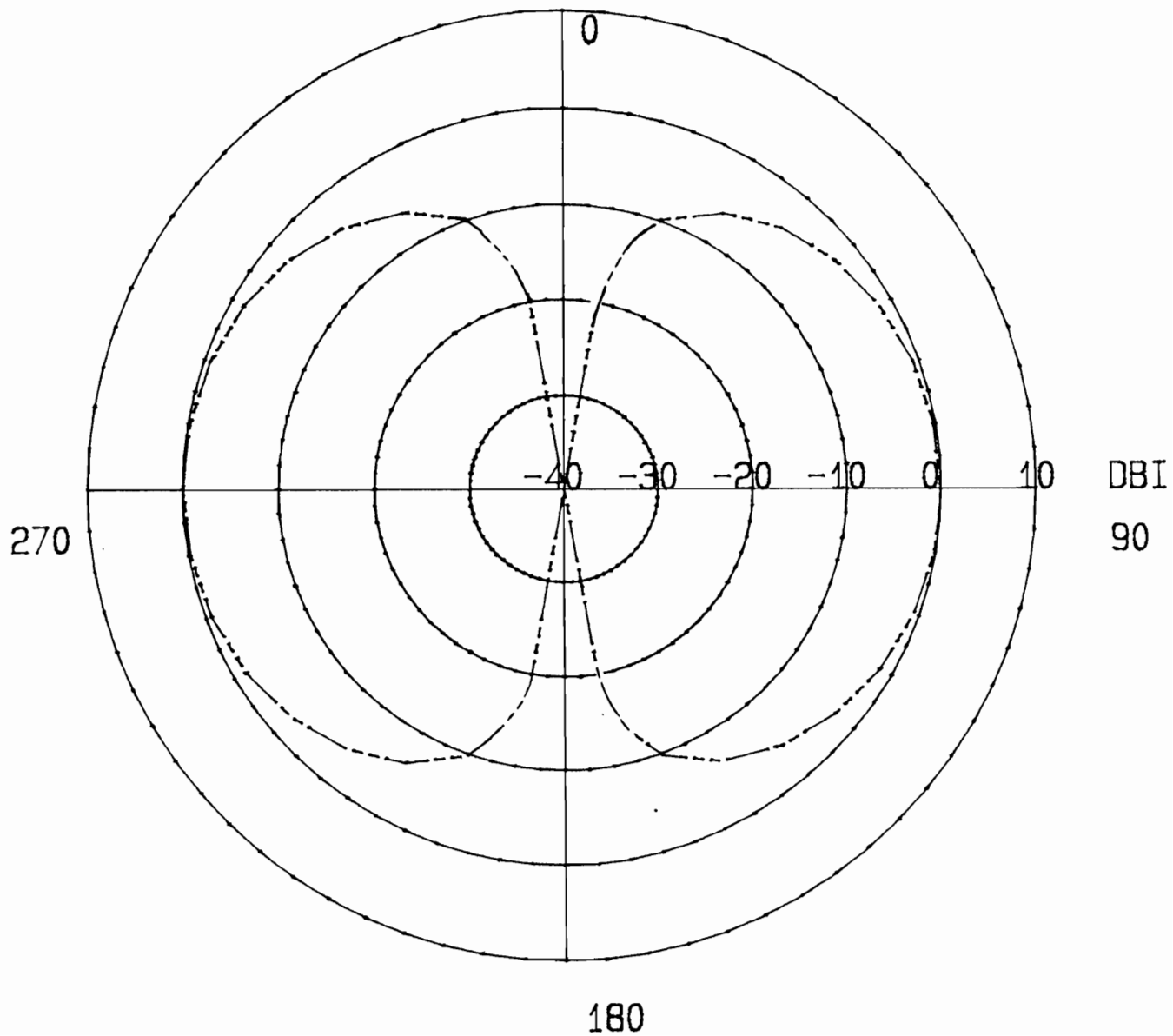
5.3.3 IMPEDANCE TRANSFORMATION RATIO IN A FOLDED MEANDER DIPOLE

One of the most important characteristics of folded dipoles is the impedance transformation ratio. Since one of the reasons for choosing a folded dipole geometry for our meander antenna, was the impedance adaptability, it was necessary to test this feature with MININEC.

To accomplish this test, the wire-radius of one arm of our folded dipole was kept constant at 1.0 mm., while the second arm, the one opposing the feed-point, was changed.

The results, which are shown in Table 5.9, confirm the fact that in a folded meander dipole, the impedance can indeed be adjusted by varying the diameter of the opposing meander arms.

The geometry chosen was the one previously described, with L = 60 cm. w = 1.0 cm. and d = 4.0 cm., and a wire radius of 1.0 mm. This geometry yields an input resonant resistance of 46.6 ohms, for identical wire radius o both arms.

TABLE 5.9: IMPEDANCE TRANSFORMATION RATIO AS A FUNCTION OF CONDUCTOR DIAMETER RATIO.

ρ_2 / ρ_1	Fo [MHz]	Ro [Ohms]	Imp. Transform. $(a + 1)^2$
0.3	121.0	16.9	1.35
0.5	129.1	24.3	1.95
1.0	124.0	46.6	3.73
2.0	124.5	84.6	6.77
4.0	116.9	120.1	9.61

Table 5.9 shows the variation in antenna resonant resistance as the diameter of the second arm is varied. The impedance transfortion ratio was calculated taking as reference the the impedance of the meander dipole described in section 5.2, having a length of 60 cm., w = 1.0 cm., for a resonant resistance of 12.5 Ohms.

We can see that results are constrained to only a narrow range of radius ratios.

The reason for this is that the program will yield erroneous results (such as negative input resistance) for ratios greater than 4.0 or smaller than 0.25. This limits our ability to draw general conclusions about the values of impedance transformation ratio on a folded meander dipole. However, the test proves very well the point that the impedance is, indeed, adjustable in this type of antenna by means of the change in conductor diameter.

It is quite apparent that the impedance of the meander folded dipole does follows the same trend of a conventional folded dipole, when diameter of the arms is varied.

The trend is also similar to that of the conventional folded dipole as seen in chapter 4.0. The impedance transformation ratio on a meander folded dipole increases as the diameter ratio ρ_2 / ρ_1 is is increased.

For diameter ratios smaller than 1.0, the resonant resistance is smaller than the reference resistance of 46 ohms, corresponding to a diameter ratio equal to 1.0.

There are small changes in the resonant frequency, but hese can again be explained by the fact that a change in wire diameter, entails a change in geometry, and therefore the electric and magnetic field distributions are affected.

From this test, there is insufficient data to try to establish any empirical formula for the calculation of the impedance, or its transformation ratio. However, from the limited results given by MININEC, we can at least draw the conclusion that the resonant imprdance can indeed be adjusted by means of varying the diameter of the conductors.

At this point, we must remember that MININEC results for the impedance of this antenna are probably innaccurate. However, we are interested at this point, only in <u>relative</u> changes in the antenna impedance. Within this context, MININEC confirms the impedance-adaptability of the folded meander dipole.

This property, can only be ascertained, of course, within the range of diameter ratios analysed by MININEC: 0.3 to 4.0.

Greater, or smaller diameter ratios would have to be analysed by experimental methods, or using the more powerful NEC program.

Also, as was explained in chapter 4.0, the impedance transformation ratio is also a function of the ratio d/ρ_1 In our case, this ratio was quite large, since our wire radii were in the order of millimeters. The distance d between arms is a parameter that in the case of a folded meander dipole is not clearly defined. For the purpose of this analysis, it was defined as the distance between the innermost conductors of the meander dipoles composing the antenna. However, the distance d could also be defined as the distance between any of the other conductors in both arms.
In any case, however we decide to define d, the ratio d/ρ_1 remains quite large for this particular geometry.

5.4 CONCLUSIONS:

A model of the folded meander dipole has been analysed with MININEC and several valid conclusions can be drawn.

First, the antenna impedance behaves much like that of a conventional folded dipole: it has a point of first resonance characterized by a very high input resistance, and a point of second resonance with a more moderate value of resonant resistance.
Also, the impedance, can be assumed to be higher than for a meander (open) dipole.

The antenna bandwidth, is indeed very small, compared to a conventional dipole, and smaller than a meander dipole. As was said before, this reduction in bandwidth was expected, due to the characteristics of a folded dipole geometry.

The radiation pattern is identical to the folded dipole, or to the meander dipole, for that matter. The gain of the antenna, as given by MININEC, cannot be considered valid, until the impedance values are validated by experimental results.

MININEC has obviously failed to yield numerically accurate results for the impedance of the dipole, as was seen in section 5.3. due to the program's inherent limitations and to the complexity of the model.

Nevertheless, the impedance transformation ratio property seems to be valid for this type of antenna, and it is reasonable to expect that a design can be accomplished with any suitable impedance.

However, sufficient data has been gathered by this analysis, to atempt to validate the results with an experimental model.
The results are encouraging enough to expect that the model will yield a practical reduced-size antenna suitable for narrow bandwidth applications.

6.0   EXPERIMENT

6.1 MEASURING TECHNIQUES AND EQUIPMENT

The experiment described in this chapter, was conducted to
confirm the results previously obtained by MININEC, and most
important, to prove the feasability of the subject design in
real-life conditions. Also, since some of the results given
by the program were suspect of being numerically inaccurate,
the experiment sought to obtain practical data that would
complement the computed results.

The purpose was to build a physical model of the meander folded
dipole antenna, and to test this prototype , in the laboratory.

The test were conducted at F.I.U.'s Communication Laboratory.
The primary test equipment utilized was the Hewlett-Packard
HP4193A Vector Impedance Meter. This instrument measures impe-
dance magnitude and phase. An internal oscillator provides test
signals from 400 KHz to 110.0 MHz. This test signal is a cons-
tant current between 10 µA and 100µA, depending on the range of
the measured impedance.

The instrument measures and displays impedance magnitude
from 10 milliohm to 120 Kilo-ohm. Impedance phase is displayed
from -180 degrees to 180 degrees.

The accuracy of the instrument is as good as 3% of reading,
for the magnitude, and 3.2% for the phase. [12]

Measurements are taken with an RF probe, that can be adapted
several coaxial connectors. For our experiment, the adapter
used was of the BNC type.

One of the major constrainst of this measuring system, is the
fact that it is limited to antennas or components that can be
fed only with a coaxial line.

As is well known, dipoles and folded dipoles, have to be fed by
a balanced transmission line: for instance a 300 Ohm parallel
line.
A balanced transmission-line is defined as one where the currents
on both sides of the line are identical in magnitude , and 180
degrees out of phase. [9]

Coaxial lines, are obviously not balanced lines, since typically the shield, or outer conductor, of the transmission line is grounded. Coaxial transmission lines are very well suited for applications where a ground plane exists, such as in the case of monopoles or whip antennas.

When it becomes necessary to feed a dipole antenna with a coaxial transmission line, it is necessary to use a special kind of impedance transformer. These are known as "Baluns", which stands for "balanced-to-unbalanced" transmission line transformer. These devices typically also adapt the antenna impedance to the coaxial line: for example 50 Ohms to a 300 Ohms input impedance.

However, in our case, where the purpose was to obtain a direct reading of the antenna impedance, it was impractical to distort the readings with the use of any impedance-adapting devices.

This posed a problem, since obviously our antenna required the use of a balanced transmission line.

As a practical solution to this problem, it was decided to make use of an alternate geometry for the meander folded dipole, that would utilize the ground plane, and therefore could be fed by a coaxial line.

It is known that a ground plane will provide an "image" or reflection of the antenna connected to it [4],[6]. Therefore, the geometry of the meander folded dipole described in chapter 5.0 was literally cut in half, with one end being fed by a coaxial adapter and the other was connected to a ground plane.
The ground plane would then, by reflection, provide the other half of the antenna.
This test set-up is described in more detail in section 3.3

The antenna impedance, is slightly changed by this method, but the limitations of the test equipment mandated that one such solution be implemented, in order to obtain useful readings.

The ground plane was composed of two aluminum sheets , 0.3 cm. thick , connected with conducting adhesive foil tape. The total dimensions of the ground plae were 2.08 m. by 1.87 m.

It is necessary to point out that, other than impedance measurements, no other test were to be carried out.
The lack of a reliable means of measuring the radiated electric and magnetic fields around the antenna, precluded us from attempting to measure other antenna characteristics, such as the radiatoion pattern or the antenna efficiency.

However, the impedance measurement would provide us with valuable information about the antenna frequency response and bandwidth.

Furthermore, the laboratory results would indeed confirm, or perhaps invalidate the results obtained with MININEC.

One last consideration was the test equipment frequency range. Since the highest attainable frequency was 110 MHz., all the antenna models tested, had to be resonant at frequencies below this limit.

This did not pose a real problem, but rather provided an advantage. At lower frequencies, all parasitic effects of lead and connector capacitance and inductance are reduced, and it is easier to obtain more accurate readings.

6.2   VALIDATION

6.2.1 TESTING A MONOPOLE OVER CONDUCTING GROUND PLANE

The first step in testing a prototype of the meander folded dipole antenna, was to validate the test set-up.

This was again accomplished by testing a known antenna, in this case a thin wire monopole. This antenna was installed in our test stand and connected to the test equipment through a coaxial panel-mount BNC connector mounted in the aluminum sheet forming the ground   plane.

The purpose was to compare the practical results of this well-known antenna, and compare them to existing theoretical and practical data, as well as to MININEC results.
This would give us some information about the validity of our test set-up and the performance of the test-equipment used.

Figure 6.1 shows the test stand with the monopole antenna connected.
Note that the probe is under the ground plane, therefore not interfering in any way with the antenna radiated field.

The monopole was built of thin 22 AWG tinned-copper wire.
This gage represents a wire radius of approximately 0.32 mm.
The wire was soldered to the center tip of the BNC connector, using standard Tin-Lead electrical solder.
The ground-plane, had the dimensions and characteristics already described in section 6.1.

BNC CONNECTOR

MONOPOLE (L=70 cm.)

2 m. x 1.8 m.
GROUND
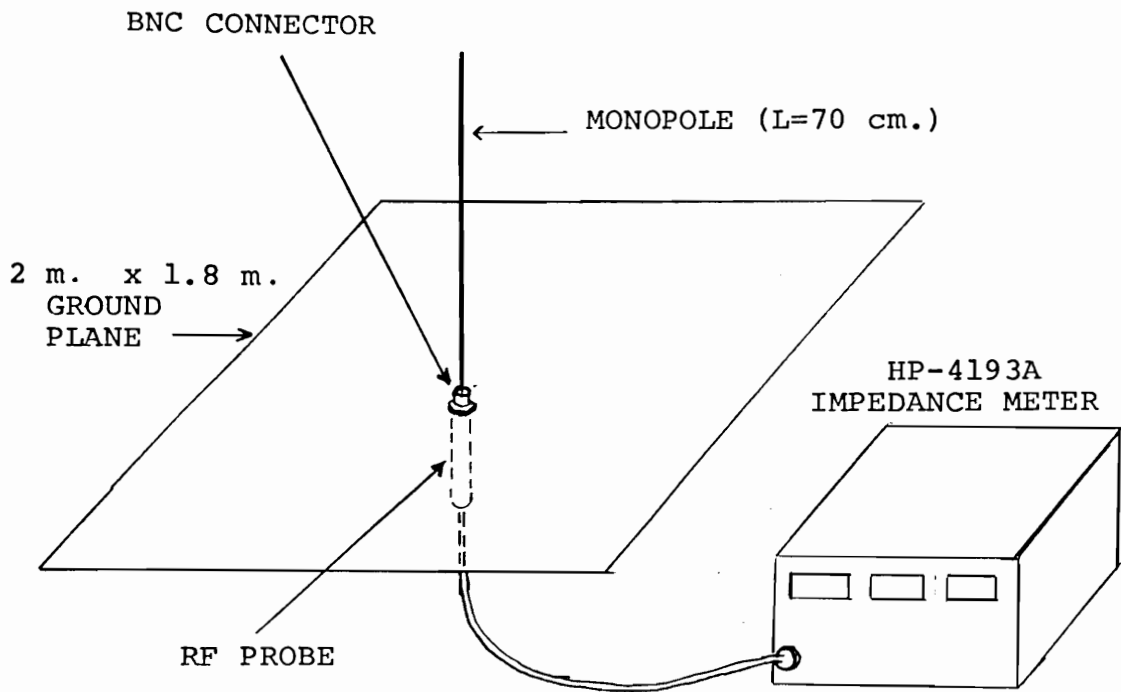PLANE

HP-4193A
IMPEDANCE METER

RF PROBE

FIGURE 6.1 : TEST SET UP FOR MONOPOLE OVER GROUND PLANE.

The antenna was mounted on a piece of styrofoam. This material has an electric permittivity equal to that of air [4]. Therefore, it does not affect the measurement system in any way.

The antenna was attached to the styrofoam with plastic adhesive tape, to held it perpendicular to the ground plane.

The antenna was designed to have a resonant frequency around 100 MHz, due to the operating considerations explained before. Thus, it was cut to a length of exactly 70 cm. This gives a length-to-diameter ratio of over 100,000.

A frequency sweep was conducted from 5 MHz. to the maximum frequency attainable with the tester of 110 MHz.

The results are shown in table 6.1. This table also shows the results obtained with MININEC, for an identical monopole, at the same frequencies.

These results are also shown in graphical form in Figures 6.2 for the resistance, and 6.3 for the reactance of the monopole. Also shown, are the MININEC results, and theoretical data for thin monopoles obtained from [6].

In general, we see good concurrence between the MININEC and data from [6], with the experimental results.
There are, however, some significant differences in the values of resistance and reactance, and also there is about a 3% difference in the resonant frequency.

These differences can be explained by the less-than ideal testing conditions encountered in the laboratory, and they will be discussed in more detail in the section 6.2.2.

6.2.2 CONSIDERATIONS ON THE EXPERIMENTAL RESULTS

The most obvious differences encounterd in the previous validation test with the MININEC results, are:

- Differences in the values of resistance and reactances:
  In general, the reactances and resistances of the experimental results seem to be of a lower numerical value.

- The resonant frequencies differ by about 3 MHz., or 3 %

These differences can be explained by the fact that MININEC assumes ideal conditions such as perfectly straight wires, an infinite ground plane, a constant wire-radius, etc. These conditions can differ significantly from the real-world environment of the laoratory.

TABLE 6. : MEASURED IMPEDANCE OF THIN-WIRE MONOPOLE

F (MHz)	Measured Impedance (Ohms)	MININEC Impedance (Ohms)
5	0 - j 3220	0 - j 5399
10	0 - j 1612	0.2 - j 2684
15	0 - j 1070	0.4 - j 1773
20	0 - j 795	0.8 - j 1312
25	1.1 - j 628	1.3 - j 1031
30	1.0 - j 517	1.9 - j 840
35	0.8 - j 436	2.6 - j 701
40	0.7 - j 369	3.4 - j 593
45	0.8 - j 318	4.4 - j 507
50	1.4 - j 271	5.5 - j 435
55	1.0 - j 231	6.6 - j 386
60	0.7 - j 217	8.4 - j 321
65	0.9 - j 187	10.1 - j 274
70	0.8 - j 158	12.1 - j 232
75	3.0 - j 132	14.5 - j 192
80	4.8 - j 105	17.1 - j 156
85	8.9 - j 80.4	20.1 - j 121
90	14.8 - j 53.8	23.6 - j 87.5
95	22.3 - j 26.0	27.6 - j 55.0
99	29.6 - j 3.8	31.2 - j 29.4
99.6	31.6 + j 0.4	31.8 - j 25.6
103	37.4 + j 31.9	35.4 - j 4.0
105	55.6 + j 51.5	8.7 + j 8.7
110	85.0 + j 61.6	43.9 + j 40.7
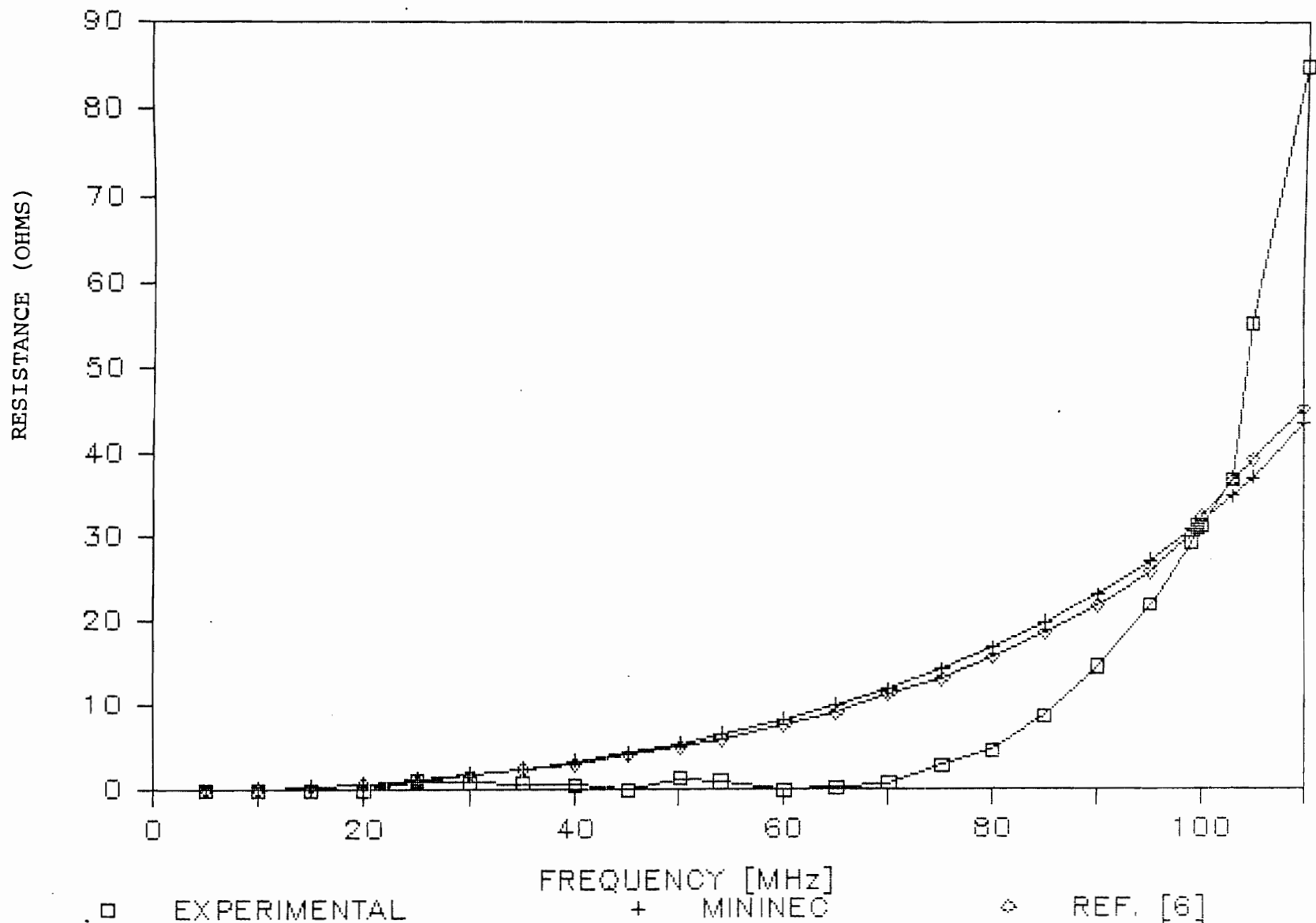
FIGURE 6.2: MEASURED RESISTANCE OF A WIRE MONOPOLE
SHOWING MININEC RESULTS AND DATA FROM [6]
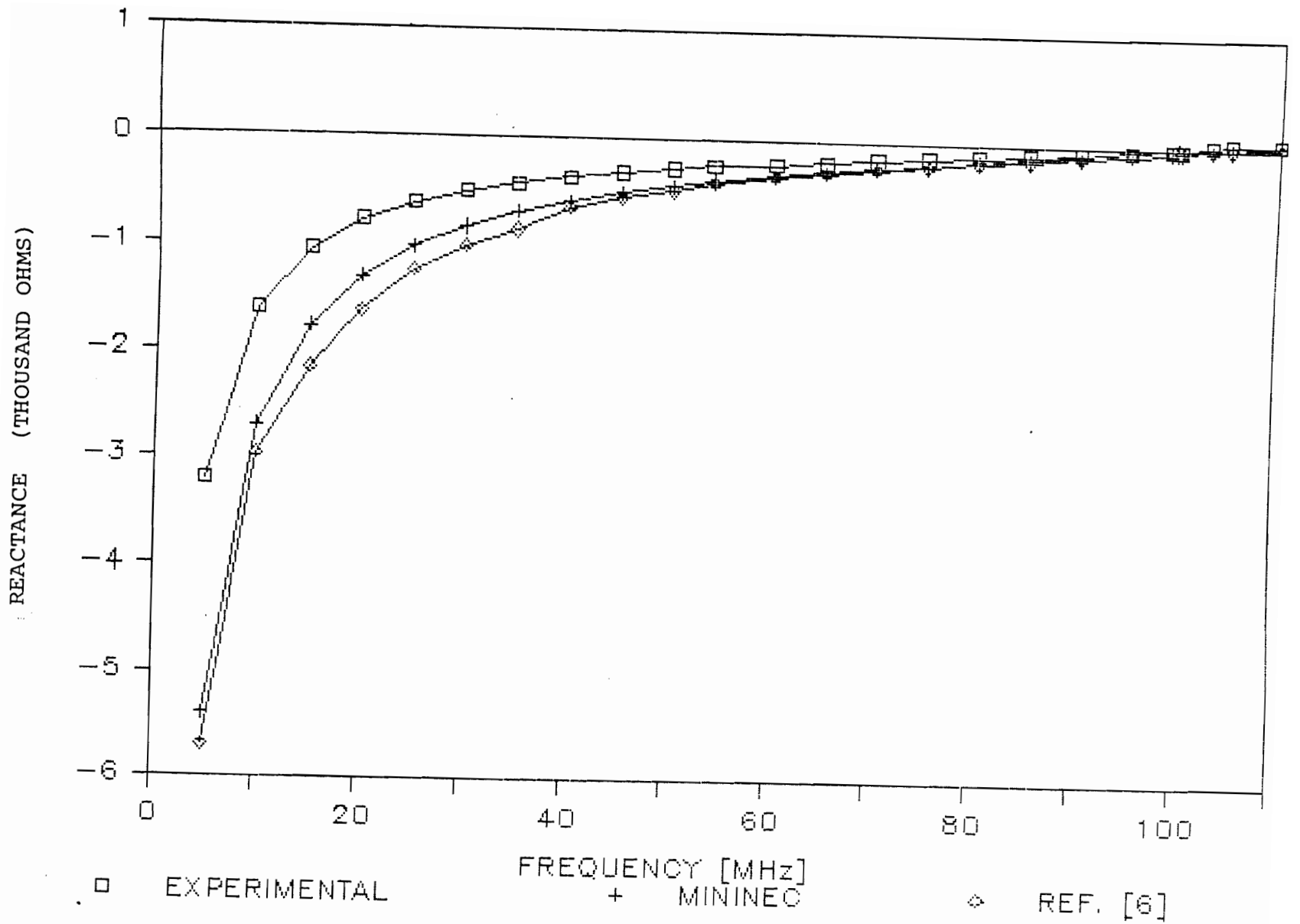
FIGURE 6.3: MEASURED REACTANCE OF A WIRE MONOPOLE
SHOWING MININEC RESULTS AND DATA FROM [6].

The most significant drawbacks of the laboratory environment are:

1- The ground plane: MININEC assumes a perfectly conducting, infinite ground plane. In the laboratory, the ground plane was made of Aluminum, which has a finite resistance, and was far from being infinite.
In fact, at the resonant frequency of around 100 MHz., the wavelength is 3 meters. Our ground plane measured roughly 2 m. x 2 m., a ground plane whose larger linear dimension is less than a wavelength. This in fact , will considerably. alter our results. Unfortunately, a larger ground plane was physically impossible to build in the confined space of the laboratory. Furthermore, a ground plane that would approach the MININEC conditions would have taken several wavelengths in diameter (5 to 10 wavelengths). This amounts to 15 meter in diameter!

2- Parasitic capacitance and Inductances:
These effects tend to increase with higher frequencies.
To quote a few: the HP 4193A tester probe has a specified capacitance of 11 pF.[12]. Also, a BNC coaxial connector will have 1 to 2 pF of capacitance. There is also the inductance of the probe cable. In particular, the parasitic capacitances will tend to make the experimental antenna more capacitive, and it will resonate at a lower frequency.

3- Test equipment limitations:
We must remember that the HP-4193A specifies an accuracy of only 3% for magnitude and 3.2% for the phase. Any error that falls within this range can be assumed to be within the normal operating limits of the instrument.

4- Other factors:
Such as changes in wire radius due to poor manufacturing. small bends in the wire, or the antenna wire not being perfectly perpendicular to ground, all will contribute to make the results differ from those of the computer simulation. Also, there is to consider the effect of soldered connections, poor contact of the probe, ground plane not being perfectly flat, etc. etc.

All of these contribute, in a minor way to make the readings different from the computed results.
However,it is very important to know these differences , and to understand the limitations of the laboratory arrangement. This will be useful in understanding the results obtained while testing a model of the meander folded dipole, and to interpret the experimental results accurately.

6.3 TEST OF A FOLDED MEANDER DIPOLE.

6.3.1 ANTENNA CONSTRUCTION AND TEST SET-UP:

As was explained previously, the characteristics of the instrument used , precluded the test of a full folded meander dipole model, due to the fact that connection to the tester had to be done through a coaxial cable.

It is a well-known fact that antennas above an infinite conducting ground plane behave as if they there was an image-antenna below the ground plane. This is called the Theory of Images, and is discussed in detail in [4], [6], [8] and [13].
The impedance of an antenna over a conducting ground plane, will be half the impedance of an antenna with twice the length, suspended in free space. [4] [6].

This property allowed us to use a model of the Meander Folded that was one-half of the geometry described in chapter 5.0.
One end of this prototype was conected to the ground plane, and the other end was fed the test signal througha BNC coaxial cable.

Figure 6.4 shows the actual prototype antenna geometry, and the image antenna below the ground plane.

Ground Plane

L = 42 cm.
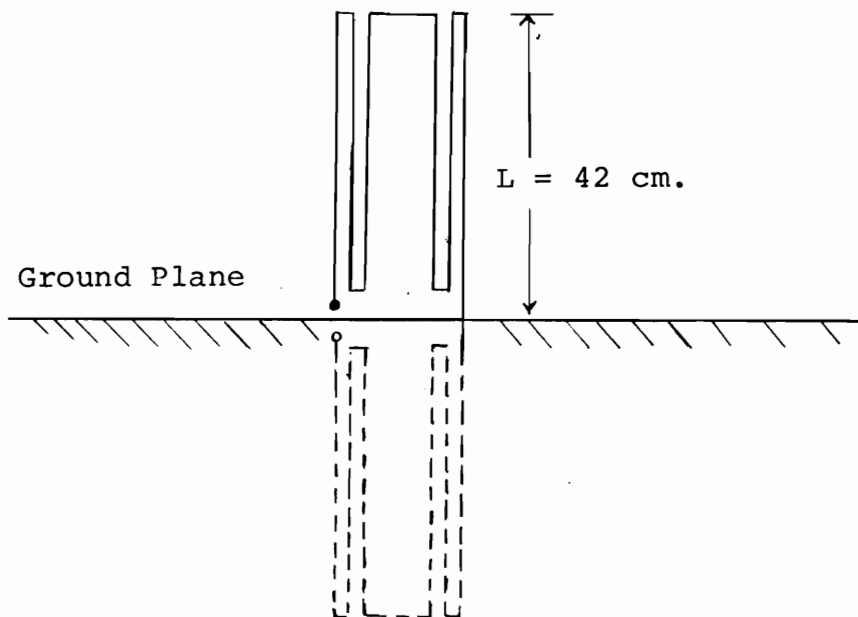
FIGURE 6.4:   GEOMETRY OF THE FOLDED MEANDER DIPOLE
             WITH IMAGE ANTENNA BELOW GROUND PLANE

The antenna was built very much like like the monopole used for validation. In fact, it was desirable to change as little as possible in the test set-up, so as to be able to have a reliable reference when evaluating the test results.

The wire used was the same 22 AWG tinned-copper wire used for the validation test. Also, the ground plane, had the same dimensions as before.

The antenna was also designed to be resonant at around 100 MHz. This frequency was below the maximum frequency attainable with the instrument, and yet was high enough for the dimensions of our prototype antenna to be moderate.

In calculating the heigth of the antenna, we estimated a typical size-reduction factor of 0.55 (See Chaps. 3.0 and 4.0).
At 100 Mhz., the wavelength is 3.0 mts. in free space. Our folded meander dipole antenna would be therefore resonant at a heigth of 0.55 half-wavelengths, or 83 cm.

Since we were dealing with a model that was half-the size of the geometry under study, our model would have a heigth of:

$$L = 83 \text{ cm. } /2 = 41.5 \text{ cm.}$$

This number was actually rounded-up to 42 cm., for ease of construction, and because the reduction factor could easily be as high as 0.6, making it desirable to have a longer antenna to maintain our resonant frequency of 100 Mhz.

The antenna was given a wire separation of w = 1.0 cm., and a distance d between arms (as defined in Fig. 5.4) of 5 cm.

The model was mounted on a piece of styrofoam, which is non-magnetic and has an electric permittivity equal to that of air [4]. This ensures that it would have no effect on the test readings.

The antenna was soldered to the center point of the BNC panel-mount connector installed in the ground plane.
The other end of the antenna was connected to ground with a piece of adhesive foil tape (conducting).
This ground connection involved about 15 cm. of wire connected to the ground plane, with the conducting tape.

Figure 6.5 describes the test set-up for the folded meander dipole antenna.
The instrument's RF probe was connected to the antenna through a male BNC adapter. Since the probe and its cable were under the ground plane, it was assumed that they had minimal effect with the measurement.
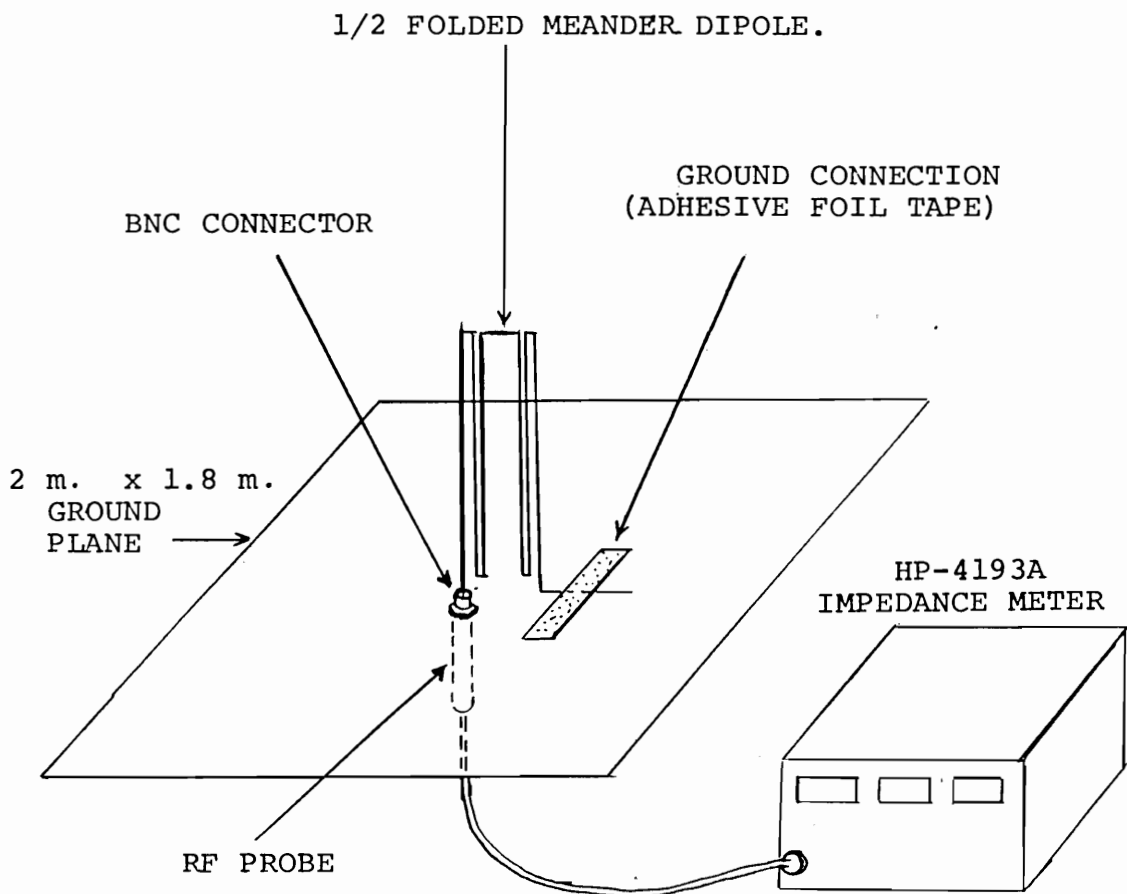
1/2 FOLDED MEANDER DIPOLE.

GROUND CONNECTION
(ADHESIVE FOIL TAPE)

BNC CONNECTOR

2 m. x 1.8 m.
GROUND
PLANE

HP-4193A
IMPEDANCE METER

RF PROBE

FIGURE 6.5: TEST SET-UP FOR FOLDED MEANDER MONOPOLE

.2 IMPEDANCE MEASUREMENT:

A frequency sweep was then done through the operating range of the HP-4193 tester, and impedance measurements were taken.

The results are shown in Table 6.2. They have are also shown in graphical form in Figures 6.6. and 6.7.

The experimental readings were in accordance with the expected values. The resonant frequency was 94.6 MHz., within 5% of the expected value of 100 MHz.(refer to 6.3.1)
At 94.6 Mhz, the approximate resonant length L of a monopole over conducting ground is calculated by:

$$L(monopole) = 0.25 \text{ x } 300/94.6 \text{ x } 0.95 = 75.3 \text{ cm.}$$

where 0.95 is the size factor described in 4.3.2.

Therefore, the measured size-reduction factor r of our antenna is the ratio of the length L(meander) of our prototype antenna, to the length L(monopole) calculated above.
(Both antennas are resonant to 94.6 MHz.)

$$r = L \text{ (meander) } / L \text{ (monopole) } = 42 \text{ cm.}/73.5 \text{ cm.}$$

$$\text{or } r = 0.557$$

This value is within 2% to the assumed factor of 0.55, used for designing the antenna.

The resistance and reactance behave very much as predicted by MININEC for this type of antenna (Refer to Figures 5.5 and 5.6)

The impedance is characterized by a point of first resonance with a very sharp change in reactance and a very high resistance. The second resonance also shows a somewhat rapid change in reactance and a more moderate resistance value.

The value of resonant resistance is 32.5 ohms. This is somewhat larger value than expected. This result represents half the value of a meander folded dipole impedance in free space.
Which means that the meander folded dipole should have a resonant resistance of :

$$Ro = 2 \text{ x } 32.5 \text{ Ohms} = 65 \text{ Ohms.}$$

The rapid change in reactance is indicative of a narrow bandwidth around second resonance. This will be discussed in the next section.

TABLE 6.2: MEASURED FOLDED MEANDER MONOPOLE IMPEDANCE.

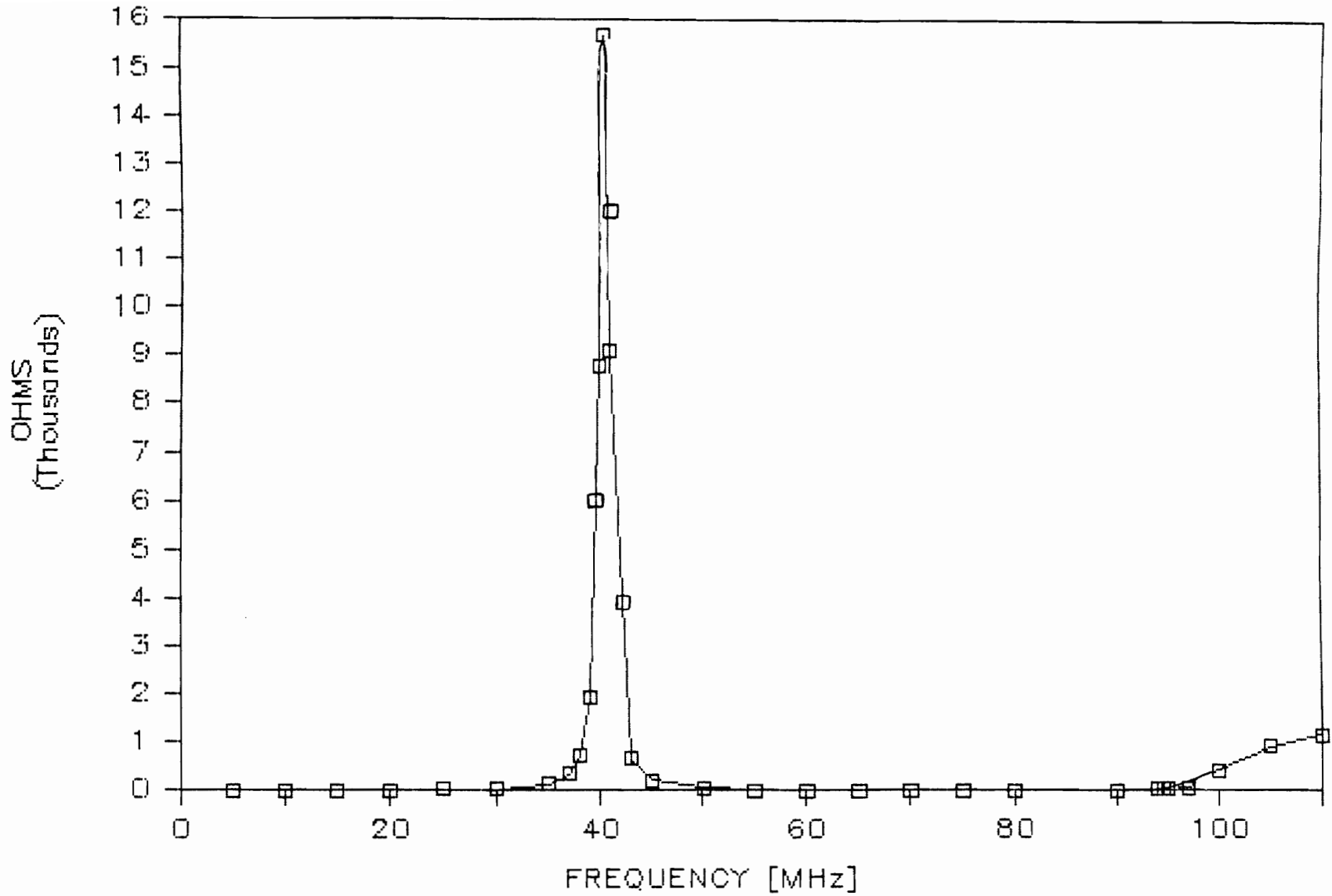| Frequency (MHz)	Impedance (Ohms)
5	8.2 + j 59.5
10	9.6 + j 124.2
15	11.9 + j 200.6
20	15.9 + j 303.6
25	25.0 + j 461.3
30	48.9 + j 755.4
35	154.7 + j 1550
37	359.4 + j 2494
38	709.7 + j 3488
39	1944 + j 5091
40	8803 + j 7706
40.5	15670 + j 136 <-- 1st. Resonance
41	9091 - j 7709
43	659 - j 3427
45	204 - j 1979
50	60.5 - j 863
55	21.9 - j 661
60	11.1 - j 490
65	9.3 - j 380
70	7.4 - j 304
75	7.6 - j 243
80	11.3 - j 190
90	14.0 - j 140

FIGURE 6.6 : MEASURED RESISTANCE OF A FOLDED MEANDER MONOPOLE
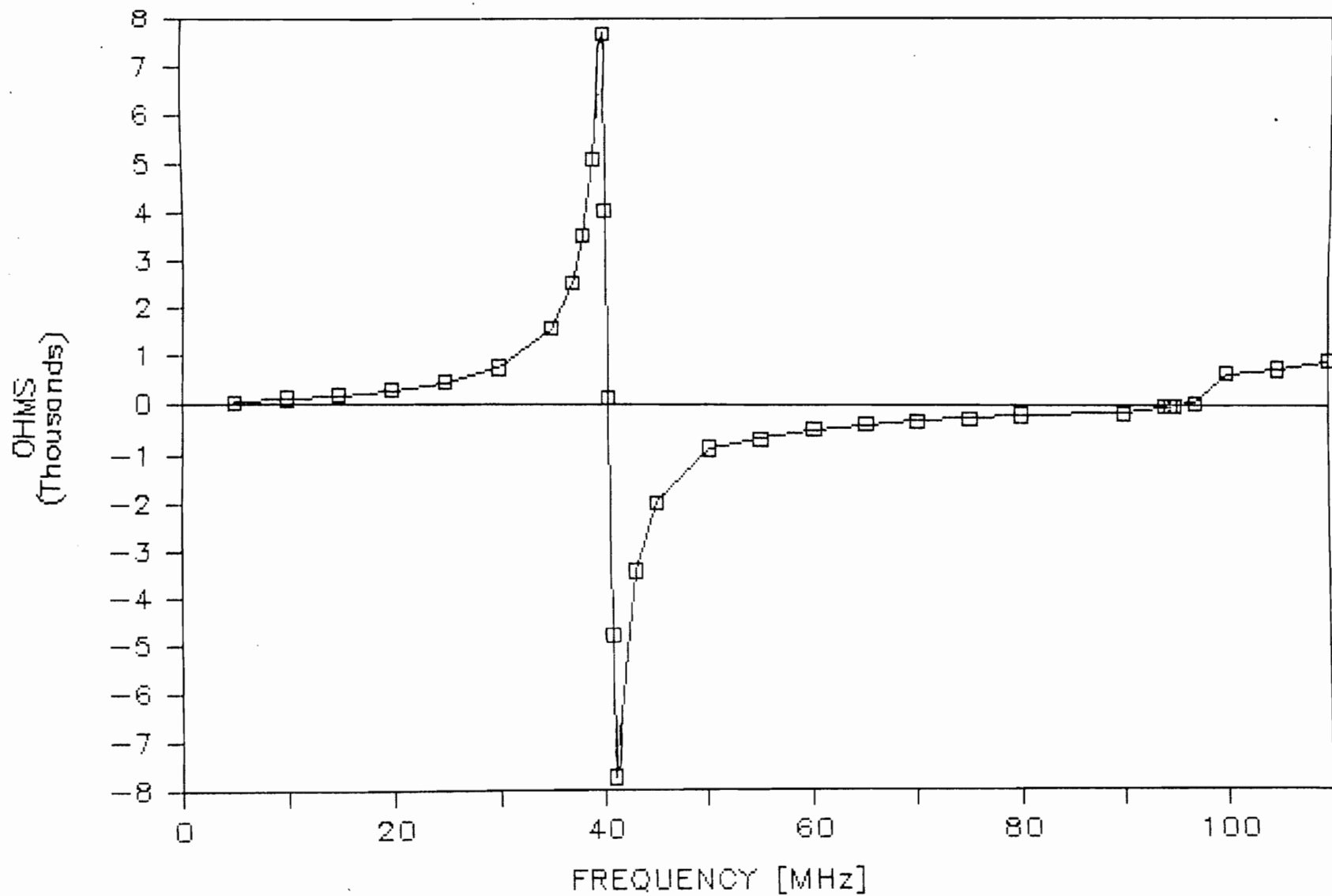
FIGURE 6.7: MEASURED REACTANCE OF A FOLDED MEANDER MONOPOLE.

TABLE 6.2 (CONTINUED): MEASURED IMPEDANCE OF A MEANDER
                            FOLDED MONOPOLE.

Frequency (MHz)	Impedance (Ohms)
94	29.6 - j 15.8
94.6	32.5 - j 0.5 <-- 2nd. Resonance
95	34.5 + j 6.0
97	51.0 + j 60.0
100	424 + j 656
105	927 + j 572
110	1161 + j 937

It must be noted that the impedances of table 6.2 are not
the direct readings from the experiment, since the instrument
only gives magnitude and phase of the impedance. But with these
two parameters, resistance and reactance can be easily
calculated.

6.3.3. BANDWIDTH OF FOLDED MEANDER DIPOLE

The next part of the experiment consisted in measuring the
operational bandwidth of the antenna. This was accomplished
by taking a new set of reading, around the second resonant
frequency. This time, the frequency steps would be smaller
in order to obtain a higher frequency resolution.

The antenna tested, was of course,the some one described in
the previous section.

The results are shown in Table 6.3 and are also presented in
graphical form in the Smith-Chart of Figure 6.8.

Note that the results of Table 6.3 differ slightly from those
of Table 6.2. The differences are due to the accuracy of the
instrument, which was used in another frequency scale, and to
numerical approximations when calculating the impedance values
from the Magnitude and phase numbers given by the tester.

TABLE 6.3: MEASURED IMPEDANCE OF FOLDED MEANDER MONOPOLE
AROUND 2nd. RESONANCE.

Frequency (MHz)	Impedance (Ohms)
93.2	25.8 - j 31.3
93.4	26.6 - j 27.5
93.6	27.0 - j 23.7
93.8	28.3 - j 19.7
94.0	29.7 - j 15.8
94.1	29.8 - j 12.6
94.3	30.8 - j 8.7
94.6	31.9 - j 5.0
94.9	33.0 + j 0.96
95.1	35.1 + j 8.1
95.6	37.6 + j 18.0
95.8	38.8 + j 21.0
96.0	40.4 + j 28.2
97.0	51.1 + j 59.8

These results have been presented in graphical form in the
Impedance Chart of Figure 6.8. The Smith Chart shown in this
Figure also serves to estimate the antenna bandwidth.

So far, we have defined The antenna bandwidth on the basis of
a VSWR of 2.0. This is a very stringent requirement, and very
few commercially available antennas can meet this specification
through their entire operation range.

A more practical way of defining the bandwidth would be on the
basis of a VSWR of 3.0 or higher.
Figure 6.8 shows two VSWR circles, which specify different
operating bandwidths for the antenna.
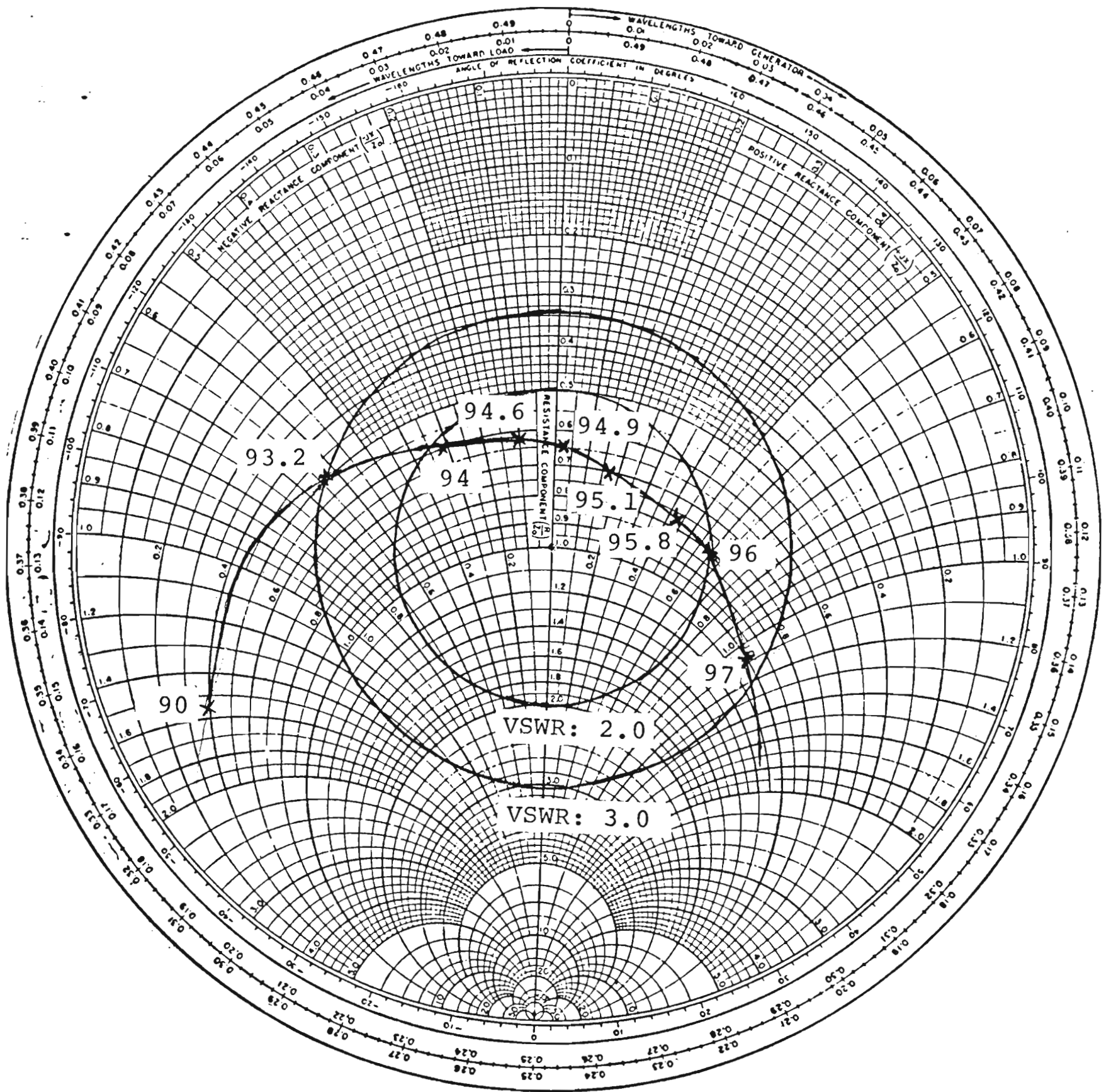
FIGURE 6.8 : IMPEDANCE OF FOLDED MEANDER DIPOLE
NORMALIZED TO 50 OHMS.

We can see that for a VSWR of 2.0, the bandwidth is approximately 2.0 MHz. or 2.1 % of the resonant frequency.

For a VSWR of 3.0, the bandwidth is approximately 4.0 MHz, or 4.2 % of the resonant frequency.

These numbers are higher than those predicted by MININEC in section 5.4.1, where the bandwidth given by the program for different wire separations were all under 1.0 % of the resonant frequency. These practical results tell us our antenna is actually better than predicted by the program, since a wider bandwidth is always desirable.

6.3.4   EFFECT OF WIRE SEPARATION ON ANTENNA CHARACTERISTICS:

The wire separation was changed in the antenna used for the previous tests. We have seen in chapter 5.0 that changes in w will somewhat affect the antenna characteristics. The most important effects with increasing w are:

  - Resonant Resistance is reduced.
  - Bandwidth is reduced.
  - Reduction factor is reduced.

The antenna tested previously was modified to have different wire separations of w = 1.0 ,2.0 and 3.0 .The separation between arms was kept constant at 5 cm.

Again, a frequency sweep was accomplished around the point of second resonance, for each antenna.
The results are shown in Table 6.4.

TABLE 6.4: EFFECT OF WIRE SEPARATION ON EXPERIMENTAL ANTENNA
           CHARACTERISTICS.
           (Bandwidth measured for VSWR = 2.0)

W (cm.)	Ro (ohms)	Fo (MHz)	Bandwidth (MHz)
1.0	32.5	94.6	2.0
2.0	27.6	88.4	1.6
3.0	23.5	85.2	1.1

Note that the bandwidth was estimated on the basis of a
VSWR = 2.0

From the results of Table 6.4, we see that the known behaviour
of meander antennas as the wire separation is changed [2], is
also valid for our experimental model of a folded meander
dipole. Note that a wire separation of w = 2.0 cm. would be
best suited for working with a 50 Ohm transmission line.
For w = 2.0 cm., our full-sized meander dipole in free space,
would theoretically have a resonant resistance of twice that of
the test antenna or Ro = 27.6 x 2 = 55.2 Ohm.

The experimental results confirm the trend of a lower resonant
resistance,and a smaller bandwidth as w is increased. Also,
the lowering of the resonant frequency is indicative of a lower
reduction factor (more size reduction).

6.3.5   IMPEDANCE TRANSFORMATION WITH CHANGES IN WIRE DIAMETER.

The last test accomplished with our experimental antenna was t'
impedance adaptability property, through changes in conductor
diameter in both arms.

Let us remember that our basic antenna was built with a conductor
of radius = 0.32 mm..
The first step consisted of changing one arm of our folded
monopole with 18 AWG copper wire, which has radius of approxi-
mately 0.66 mm.
By connecting the excitation source to one arm and grounding the
opposite arm of this antenna alternately, two sets of readings
were taken. One corresponds to a radius ratio of:

$$\rho_2 / \rho_1 \quad = \quad 0.32 \text{ mm} / 0.66 \text{ mm.} = 0.485$$

and the other corresponding to a ratio:

$$\rho_2 / \rho_1 \quad = 0.66 \text{ mm./ } 0.32 \text{ mm.} = 2.06$$

Impedance readings were then taken from this new antenna, using
the same test set-up described previously.

The next step was to replace the 22 AWG wire (radius = 0.32 mm.)
with a thinner 28 AWG wire, that has a radius of 0.25 mm.

Again, by alternately connecting the instrument to one end of
this antenna, and grounding the other, two sets of readings were
taken for diameter ratios ρ_2 / ρ_1 = 2.64 and 0.38.

The results are presented in Table 6.5:

TABLE 6.5: EFFECT OF CHANGES IN CONDUCTOR DIAMETER ON ANTENNA IMPEDANCE.

P_2 / P_1	Fo (MHz.)	Ro (Ohms)
0.380	89.7	21.1
0.485	91.6	21.5
1.0	94.6	32.5
2.06	92.1	33.6
2.64	89.9	40.2

As we can see from the results shown in Table 6.5 , there are indeed changes in the resonant resistance as the conductor diameter is changed. The trend corresponds to that predicted by MININEC, and also to the behaviour expected of conventional folded dipoles.

The changes in resistance are however, quite moderate. We see that the impedance does not increase as drastically as predicted by MININEC in Table 5.9.

We can also point out that the increase in wire diameters were limited to those allowed by existing type of wires. For higher diameter ratios, copper tubing would have to be utilized. This presents the problem that if the radius of a conductor is comparable to the wire separation, then the geometry of the antenna is altered excessively.
The obvious solution is to build a larger antenna, with a wire separation w that would be much greater than the copper tubing diameter. At this point, as was explained before, we would need a much larger ground plane. This was impractical, if not impossible, due to the dimensions of the laboratory.

Also note that there are changes in the resonant resistance. This is due to minor differences introduced in the test antennas, during their manual fabrication, and to the fact that the antenna geometry is also slightly altered when the wire diameter is changed.

6.4 DISCUSSION OF EXPERIMENTAL RESULTS.

We have built a model of the Folded Meander Dipole and tested it under laboratory conditions.
The results, as presented here are quite encouraging. The antenna has an impedance that can be adapted to several transmission lines. (50 Ohms, 75 Ohm transmission lines)

The antenna has a working bandwidth of 4 % of the resonant frequency, for a VSWR of 3.0. This bandwidth is very much in the same range as many commercially available antennas.

Furthermore, we have investigated two ways by which the antenna impedance could be adapted to other transmission lines:

- By changing the wire separation w (This will reduce Bandwidth)
- By changing the wire diameters ratio.

Also, the laboratory experiment has shown that this type of antenna could be built as a full dipole, or, as in the test model, as a monopole with one end grounded.
This last geometry is probably more attractive, since it can be fed with a conventional coaxial transmission line.

The experimental results for the resonant frequency and reduction factor are close to the ones predicted by MININEC within 2 to 3%.

Although the impedance values varied with reference with MININEC, the general behaviour of the antenna was adequately predicted by the program. Let us remember that the resonant resistance value given by the program, in chapter 5.0 was not considered an accurate result, due to the program's limitations.

Although there were no means available in the laboratory to measure other important characteristics, such as efficiency and radiation pattern, the results obtained give us the confidence that MININEC predictions in refrence to these characteristics will not be significantly different than the real ones for this antenna.

7.0 CONCLUSIONS

7.1 BASIC THEORY OF MEANDER ANTENNAS:

Meander antennas exhibit many of the basic characteristics of conventional dipoles and monopoles. We have seen in previous chapters that their radiation pattern is similar to the pattern of these conventional antennas, and we know from [2] that the efficiency is comparable, if somewhat smaller.

The most obvious disadvantage of meander antennas is their low input impedance at resonance, as was seen in Chapter 4.0.

The following sections will attempt to explain some of these characteristics, based upon known antenna theory.

7.1.1 SELF AND MUTUAL IMPEDANCE OF ANTENNAS

Antennas such as dipoles suspended in free space, have an input impedance, that under ideal conditions is not affected by any surrounding structure or nearby conductors.

This ideal input impedance is generally known as the antenna self-impedance. This is the input impedance of the antenna, when its current distribution and radiated field are not affected by any surrounding conducting structures.

In an array of antennas, the driving point impedance of an individual element may differ considerably from its self impedance because of the effect of mutual coupling with other elements of the array [6].

In a multielement array, the relations between the currents and voltages are given by:

$$V_1 = I_1 Z_{11} + I_2 Z_{12} + \ldots + I_n Z_{1n} \qquad (7.1)$$

$$V_2 = I_1 Z_{12} + I_2 Z_{22} + \ldots + I_n Z_{2n}$$

$$\vdots \qquad \vdots \qquad \vdots \qquad \qquad \vdots$$

$$V_n = I_n Z_{1n} + I_2 Z_{2n} + \ldots + I_n Z_{nn}$$

Where: Vn = Impressed voltage at nth. element
        In = Current flowing in nth. element
       Znn = Self Impedance of nth. element
 Zmn = Znm = mutual impedance between mth and nth element.

The driving point impedance for elementh 1, for instance, is found from the ratio of the impressed voltage to the current, and is obtained from the above equations as follows [6]:

$$Z_1(input) = V_1 / I_1 = Z_{11} + (I_2/I_1)Z_{12} + \ldots + (I_n/I_1)Z_{1n} \qquad (7.2)$$

It is readily seen that the input impedance or the driving point impedance of a particular element is not only a function of its own self impedance but also a function of:

    -The the relative current flowing in the other elements and

    -The mutual impedance between elements.

Several authors have treated the subject of estimating the value of the mutual impedance between elements [4], [6], [13] In particular, C. Balanis [13] gives simple mathematical relations for estimating the mutual impedance of wires positioned for mutual coupling.

Refering to figure 7.1, showing two wires suspended in space and parallel to each other, the induced voltage at antenna 2, referred to its current at the input terminal, due to radiation from antenna 1, is given by:

$$V_{21} = -\frac{1}{I_{2i}} \int_{-l_2/2}^{l_2/2} E_{z21}(z) I_2(z)\, dz \qquad (7.3)$$

where Ez_{21} is the E-field component radiated by antenna 1 which is parallel to antenna 2. It would be calculated as if antenna 2 were absent. $I_2(z)$ represents the current distribution along antenna 2. This basic relation is used to develop a formula for the mutual impedance between antennas 1 and 2, using known relations for the E-field and assuming a sinusoidal current distribution in the dipoles. [13]
(7.3) can rewritten as:

$$V_{21} = j\frac{\eta I_{1m} I_{2m}}{4\pi I_{2i}} \int_{-l_2/2}^{+l_2/2} \sin\left[k\left(\frac{l_2}{2} - |z|\right)\right]$$
$$\times \left[\frac{e^{-jkR_1}}{R_1} + \frac{e^{-jkR_2}}{R_2} - 2\cos\left(\frac{kl_1}{2}\right)\frac{e^{-jkr}}{r}\right] dz \qquad (7.4)$$
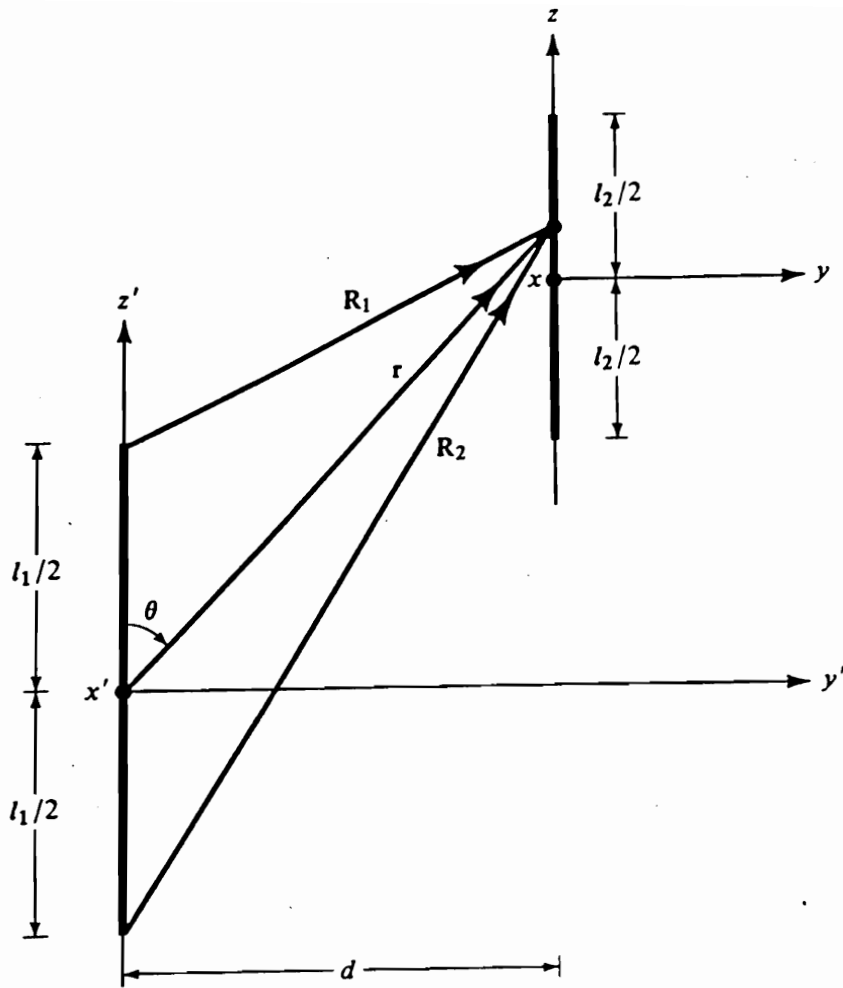
FIGURE 7.1: DIPOLE POSITIONING FOR MUTUAL COUPLING [13]

And the mutual impedance of (7.2) , referred to the input current I_{1i} of antenna 1, can be written as [13]:

$$
Z_{21i} = \frac{V_{21}}{I_{1i}} = j\frac{\eta I_{1m} I_{2m}}{4\pi I_{1i} I_{2i}} \int_{-l_2/2}^{l_2/2} \sin\left[k\left(\frac{l_2}{2} - |z|\right)\right]
$$

$$
\times \left[\frac{e^{-jkR_1}}{R_1} + \frac{e^{-jkR_2}}{R_2} - 2\cos\left(k\frac{l_1}{2}\right)\frac{e^{-jkr}}{r}\right] dz
$$

(7.5)

where R_1 , R_2 and r are the distances of figure 7.1

and $\quad k^2 = \omega^2 \mu \varepsilon$

$\quad \eta \quad =$ intrinsic impedance of the medium $= \sqrt{\mu / \varepsilon}$
$\quad$ I m , I m = maximum currents of antennas 1 and 2
$\quad$ I i , I i = Input currents of antennas 1 and 2

The mutual impedance ,as given by (7.5) is referred to the current at the input terminals and can be translated to the current maxima by [13]:

$$Z_{21m} = Z_{21i} \frac{I_{1i} I_{2i}}{I_{1m} I_{2m}} \tag{7.6}$$

or $\quad$
$$Z_{21m} = j \frac{\eta}{4\pi} \int_{-l_2/2}^{l_2/2} \sin\left[k\left(\frac{l_2}{2} - |z| \right) \right]$$
$$\times \left[\frac{e^{-jkR_1}}{R_1} + \frac{e^{-jkR_2}}{R_2} - 2\cos\left(k\frac{l_1}{2} \right) \frac{e^{-jkr}}{r} \right] dz \tag{7.7}$$

For two identical antennas (each of length $1 = n\lambda/2$, n= 1,2,3..) (7.7) can be written in a simplified form. For the case where the two dipoles are side-by-side as shown in Figure 7.2, (7.7) reduces to:

$$R_{21m} = \frac{\eta}{4\pi} \left[2C_i(u_0) - C_i(u_1) - C_i(u_2) \right] \tag{7.8a}$$

$$X_{21m} = -\frac{\eta}{4\pi} \left[2S_i(u_0) - S_i(u_1) - S_i(u_2) \right] \tag{7.8b}$$

$$u_0 = kd \tag{7.8c}$$

$$u_1 = k\left(\sqrt{d^2 + l^2} + l \right) \tag{7.8d}$$

$$u_2 = k\left(\sqrt{d^2 + l^2} - l \right) \tag{7.8e}$$

where Ci(x) and Si(x) are the sine and cosine integrals:

$$S_i(x) = \int_0^x \frac{\sin y}{y} \, dy \qquad\qquad (7.9a)$$

and

$$C_i(x) = -\int_x^\infty \frac{\cos y}{y} \, dy = \int_\infty^x \frac{\cos y}{y} \, dy \qquad (7.9b)$$

The impedance of (7.7) can be referred to the input terminal by:

$$Z_{21i} = Z_{21m} \left(\frac{I_{1m}}{I_{1i}} \right) \left(\frac{I_{2m}}{I_{2i}} \right) = Z_{21m} \left[\frac{1}{\sin(kl_1/2)} \right] \left[\frac{1}{\sin(kl_2/2)} \right] \qquad (7.10)$$

For identical lengths of both antennas $l_1 = l_2$ (7.10) reduces to:

$$R_{21i} = \frac{R_{21m}}{\sin^2(kl/2)} \qquad\qquad (7.11a)$$

$$X_{21i} = \frac{X_{21m}}{\sin^2(kl/2)} \qquad\qquad (7.11b)$$

The mutual impedance, referred to the current maximum and given by (7.7) of a side-by-side arrangement of two half-wave dipoles has been plotted [13] and is shown in Figure 7.2.

The side by side arrangement of dipoles exhibits a large mutual impedance, as compared with other arrangements (for instance, a collinear arrangement) Since the antennas are placed in the direction of maximum radiation.

Also, the mutual impedance increases as the size of both side-by-side dipoles is increased, for a given wire separation.
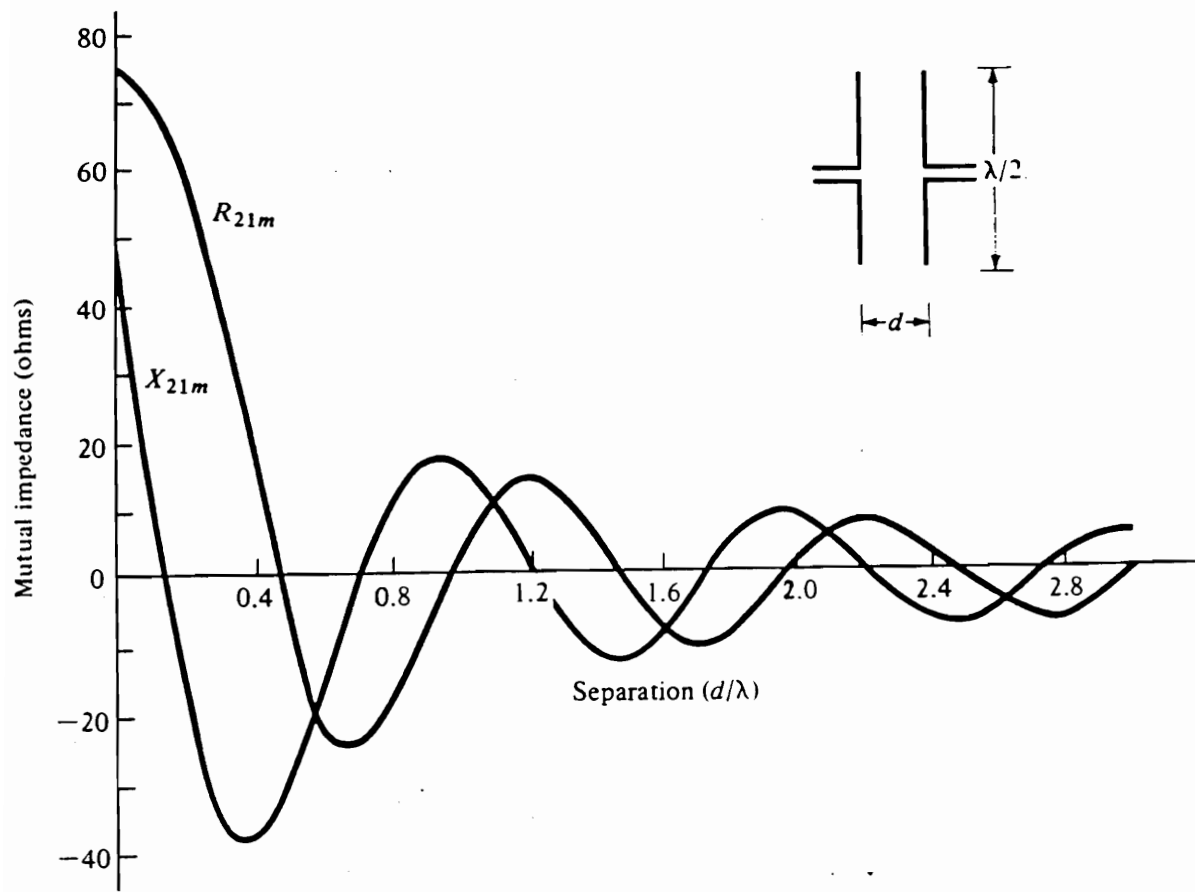
FIGURE 7.2: MUTUAL IMPEDANCE OF A SIDE-BY-SIDE ARRANGEMENT OF HALF-WAVELENGTH DIPOLES   (FROM [13])

7.1.2 IMPEDANCE OF A MEANDER DIPOLE

The low resonant resistance of a meander dipole can be explained on the basis of the mutual impedance between its parallel arms.

It is obvious, when analysing the geometry of meander antennas, that they are composed of several parallel arms , all of which contribute to the radiated field. These arms must interact between each other somehow, to vary the input impedance of the antenna.

Refering to Figure 7.3, we can model a meander dipole with N = 2, the simplest form of meander antenna, as being composed of three independent parallel wires, each having a length somewhat shorter than a half-wavelength.

In fact, for a dipole having a reduction factor of 0.6, the length of each parallel section is:

$$l = 0.6(\lambda_0/2)$$

or $$l = 0.3 \lambda_0 \qquad (7.12)$$

Since we can assume that the wire separation w is much smaller than the wavelength, we will disregard the effect on the impedance of the small horizontal sections. These will not have a significant effect in the radiated field of the antenna, provided that $w \ll \lambda_0$

We can see from Figure 7.3 that the dipoles can be considered as having their own independent excitation.

However, from 4.2.4 , we have learned that a meander dipole has a current distribution which magnitude is close to a sinusoidal distribution along the wire, and which phase remains more or less constant along the wire.
We can assign to each wire an input current, that on the average, will be :

$$I_1 > I_2 > I_3$$

Since I_1 and I_2 will flow in opposite directions in space, they will be considered as being 180 deg. out of phase.
By contrast, since I_1 and I_3 are flowing in the same direction in space at the same time, the will be assumed as being in phase.

The input impedance of the antenna is given by (7.2):
for a meander dipole N = 2:

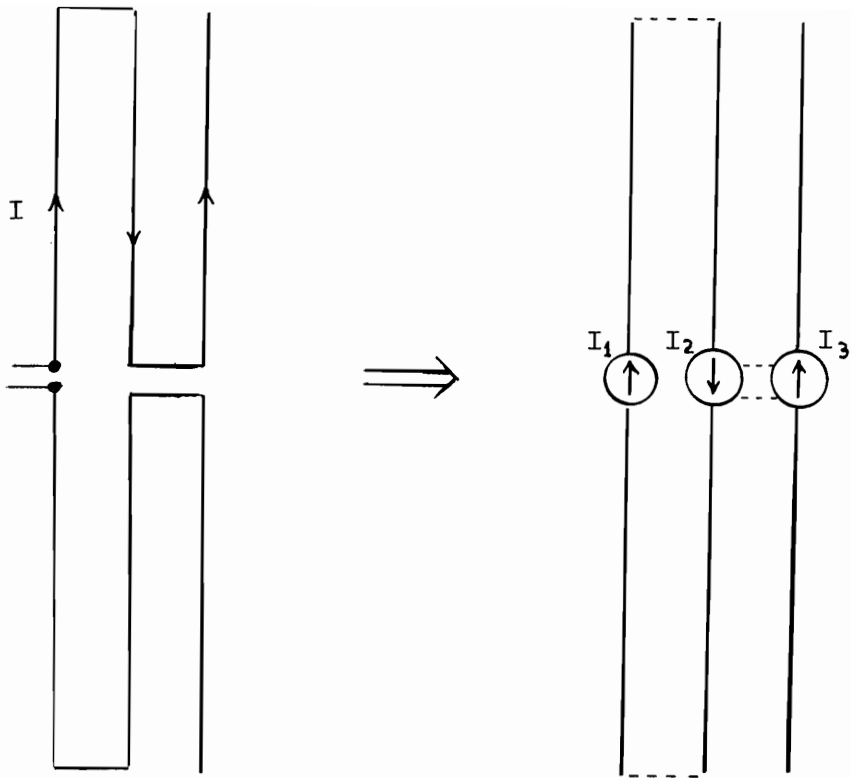$$Z(input) = Z_{11} + (I_2/I_1)Z_{12} + (I_3/I_1)Z_{13} \qquad (7.13)$$

FIGURE 7.3: EQUIVALENT REPRESENTATION OF A MEANDER DIPOLE.
(The dimension of wire separation w has been
exagerated.)

Z_{11} is the input impedance of the first antenna with length
$l = 0.3$

Z_{12} is the mutual impedance between antenna 1 and 2

Z_{13} is the mutual impedance between antenna 1 and 3

Now, we know from Figure 7.2 that the mutual impedance, for
dipoles placed very close to each other (at d = w, for meander
antennas) will be   inductive and of a higher magnitude.

We have also said that I_1 and I_2 can be considered 180 deg. out of
phase and I_1 and I_3 are in phase.
Thus, (7.13) can be rewritten as:

$$Z(input) = Z_{11} - |I_2/I_1| \cdot Z_{12} + |I_3/I_1| \cdot Z_{13} \qquad (7.14)$$

where the terms $|I_2/I_1|$ and $|I_3/I_1|$ are less than 1.0 in
magnitude.

The mutual impedances Z_{12} and Z_{13} being inductive, they will
make the input impedance of the antenna more inductive, (or
less capacitive) This will have the effect of decreasing the
resonant frequency of the antenna, which explains the size-
reduction properties of meander antennas.

7.1.3 RADIATED FIELD OF A MEANDER DIPOLE

The radiated fields of meander antennas can be explained
on the basis of the Array Theory. [4]

Refering to Figure 7.4, we have two isotropic sources separated
by a distance d. If the two sources are identical in amplitude
and of the same phase, and assuming they have the same
polarization, the far field is given by:

$$E = E_1 + E_2 e^{j\psi} \qquad (7.15)$$

where:
E_1 = far electric field at a distance r due to source 1
E_2 = far electric field at a distance r due to source 2
$\psi = (2\pi d/\lambda)\cos \theta$

The quantity ψ is the phase-angle difference between the fields
of the two sources measured along the radius-vector line at the
angle θ

It has been proven that a meander antenna such as the one designed in this thesis is feasable and can be used in many practical applications.

The antenna can be used as a Folded Meander Dipole, or as a Folded Meander Monopole, as was done in the laboratory construction of chapter 6.0.

Let us sum up the characteristics of the Meander Folded Dipole, as they compare with other conventional antennas, and with other meander geometries.

RESONANT RESISTANCE:
The resonant resistance of our prototype antenna has met the design specification stated in chapter 5.0: it is of a higher value than other meander antennas, and can be fed with a 50 ohm line, while maintaining an acceptable value of VSWR.
For, the case of a full dipole configuration, the resonant resistance can be expected to be twice the value of our experimental model, in the range of 60 to 70 ohms. Depending on the value, a 50 or 75 ohm coaxial line could be used in practice to feed this antenna.
In the case of a full Meander Folded Dipole in free space, a balun (balanced-to-balanced line transformer) would be necessary at the feed point, to connect the coaxial line. This is not a major disadvantage, since most dipole antennas that use coaxial lines, need this type of matching device.

ANTENNA BANDWIDTH:
The experimental bandwidth is higher than the one initially predicted by MININEC. We have seen that for a VSWR of 3.0, our prototype antenna shows a bandwidth of about 4% of the resonant frequency. Although this bandwidth can be considered small when compared to those of conventional antennas, it is still quite adequate for many applications. Furthermore, the bandwidth is comparable that of meander monopoles [3] and of dipoles, as shown in chapter 5.0.
It should be noted that a narrow bandwidth can be useful and desirable for many applications, since it adds to the selectivity of a receiving system.

IMPEDANCE ADAPTABILITY:
This is a very important feature. We have seen that the input impedance can be varied by two methods:

In (7.15) the reference for the phase for the two sources was taken at source 1.

We see from (7.15), that in the case of a meander dipole the quantity ψ would be very small since $d/\lambda = w/\lambda \ll 1.0$

Therefore, the resultant far field will be equal to the sum of the contributions of each parallel arm of the meander dipole. The antenna behaves, if viewed from the far field, as one single dipole.
This explains the fact that meander antennas have a radiation pattern very similar to the one for a conventional dipole.
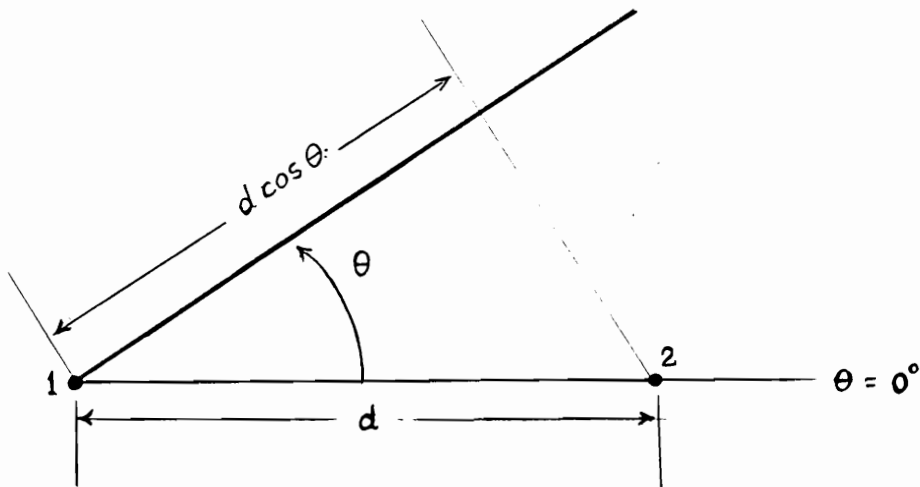

FIGURE 7.4: TWO ISOTROPIC POINT SOURCES SEPARATED BY A DISTANCE d.

- Changing the wire radius, on both arms of the dipole

- Changing the wire separation w.

The wire radius method was not extensively proven in the labora-
tory due to practical limitations of space and equipment. However
it was shown that some changes in the value of the input resis-
tance occur as the wire-radius is changed.

The second method, is a known property of meander antennas [3]
but it entails a change in bandwidth, as was seen in the experi-
ment and in the computer simulation (refer to Chap. 5.0).

Therefore, for the case of a thin-wire Folded Meander Dipole,
these methods can be used to "fine-tune" the antenna impedance,
rather than to obtain drastic changes in this parameter.

SIZE REDUCTION:
The major reason for this design was of course to obtain a reduc-
tion in size over a conventional geometry.
We have obtained a size-reduction for our experimental antenna,
of approximately 45%. This is comparable, if not greater, than
the size reduction obtained for meander monopoles [3].
Our major goal has been accomplished: to obtain a practical an-
tenna that would have about half-the-size of its conventional
counterpart.

These characteristics of the design, are an obvious advantage
over the more simpler geometries described in [3].

MININEC has been proven to be a most useful tool in the design
of wire antennas. Even with complicated wire-geometries, as
was the case with the Folded Meander Dipole Antenna, where the
program was stretched to the limit of its capabilities, the
results were reasonably close to the practical results.
In spite of the numerical errors made by the program in calcula-
ting the antenna impedances, MININEC presented us with a good
overall description of the antenna characteristics.

It is obvious however, that a great amount of time and practice
with the program is necessary, in order to entertain designs
that are complex in nature. It is important to know the pro-
gram's limitations and to acquire a "feel" for the accuracy
of the program's results.

The antenna designed in this thesis, was subject to nearly all the tests that MININEC could accomplish, that were useful for our purposes.

Later, in the laboratory, the prototype antenna was also subject to as many tests were possible, within the constraints of available equipment, time and physical space.

There remains to be accomplished a practical measurement of the radiation pattern of this antenna and of its radiation efficiency.

In particular the radiation efficiency, which cannot be estimated with MININEC and requires a physical measurement, is of great importance in establishing the usefulness of this antenna.

It is my hope that this design will someday be perfected and its characterization completed by future generations of better-equipped researchers.

REFERENCES

1. A.J. Julian,, J.C. Logan, J.W. Rockway, "MININEC: A Mini-Numerical Electromagnetics Code.", NOSC TD 516, September 1982.

2. J.W. Rockway, J.C. Logan, D.W.S. Tam, Shing T. Li, "The Mininec System: A Microcomputer Analysis of Wire Antennas". Artech House, 1985.

3. Jalil Rashed and Chen-To Tai, "A new Class of Wire Antennas", IEEE/AP-S Symposium, May 24-28, 1982.

4. John D. Kraus, "Antennas". McGraw-Hill, 1984.

5. R.W.P. King, "Tables of Antenna Characteristics." I.F.I./Plenum Corporation, 1971.

6. R. Johnson and H. Jasik, "Antenna Engineering Handbook." McGraw-Hill 1984.

7. G. Brown and O. Woodward Jr., "Experimentally Determined Impedance Characteristics of Cylindrical Antennas." . IRE Proceedings, Vol. 33, 1945, p 257-262.

8. S. Uda and Y. Mushiake, "Yagi-Uda Antenna" Maruzen Co. Ltd. Tokyo 1954, p. 19

9. Y.T. Lo and S.W. Lee, " Antenna Handbook" Van Nostrand Reinhold Co., N.Y. 1988

10. A.W. RUDGE, K. Milne, A.D. Oliver, P. Knight, "Handbook of Antenna Design." IEEE Electromagnetic Waves Series. 1984

11. G. J. Burke and A.J. Poggio, "Numerical Electromagnetic Code (NEC) - Method of Moments." NOSC TD 116, Jan. 1981

12. Hewlett-Packard HP-4193A Vector Impedance Meter Operation Manual.

13. C. Balanis, " Antenna Theory". Harper and Row Publishers. 1982.

14. R.P. Owens, "Microstrip Antenna feeds" , Handbook of Microstrip Antennas, Vol. 2, p. 846-848. J.R. James and P.S. Hall, 1989.

15. H. Nakano, H. Tagami, A. Yoshizawa, J. Yamauchi, " Shortening Ratios of Modified Dipole Antennas." IEEE Transactions on Antennas and Propagation. Vol. AP-32 No.4, April 1984, pp.385-386.

16. J. Wong and H. King, "Height-Reduced Zigzag Meander Monopoles with Broadband Characteristics." IEEE Transactions on Antennas and Propagation. Vol. AP-34, May 1986, pp. 716-717.